FACULTY OF SCIENCE AND TECHNOLOGY

MASTER'S THESIS

Study programme / specialisation: Petroleum Engineering / Production and Process Technologies	The *autumn semester*, *2022* Open / ~~Confidential~~
Author: Mikela Albriktsen	
Supervisor at UiS: A. H. Rabenjafimanantsoa Co-supervisor: Rune W. Time External supervisor(s): -	
Thesis title: Oscillating Flow and Pressure Drop in Horizontal Pipes	
Credits (ECTS): 30	
Keywords: Pressure oscillations, Pressure drop, Rheology, Viscoelasticity, Polyanionic cellulose (PAC)	Pages: 109 + appendix: 20 Stavanger, 15.12.*2022*

Oscillating Flows and Pressure Drop in Horizontal Pipes

Supervisors: A. H. Rabenjafimanantsoa & Rune W. Time

by

Mikela Albriktsen

A thesis submitted

in Partial Fulfilment of the Requirements

for the Degree of

Master of Science

in

Petroleum Engineering

Process and Production Technologies

University of Stavanger

[15.December 2022]

ACKNOWLEDGEMENT

First and foremost, I would like to express my most profound appreciation to my supervisors: A. H. Rabenjafimanantsoa and Rune Wiggo Time , for their motivational support, helpful contributions, and valuable advice.

I very much appreciate Kim André Vorland's guidance on using the Anton Paar MCR 302 Rheometer.

I also wish to thank my family and friends for their support throughout the study time and thesis writing.

Finally, I would also like to thank the University of Stavanger for allowing me to write this thesis and providing facilities to accomplish experimental work.

Mikela Albriktsen

15.December 2022

ABSTRACT

Name of the student: **Mikela Albriktsen** Department: **IEP**

Thesis title: **Oscillating flow and pressure drop in horizontal pipes**

Degree for which submitted: **M.Sc.**

Thesis supervisor: **A. H. Rabenjafimanantsoa & Rune W. Time**

Month and year of thesis submission: **December 15, 2022**

The study's main aim is to evaluate oscillating flow and pressure drop in horizontal pipes. First, the equipment is calibrated to ensure the correct flow rate. Calibration is done with three methods. These are, Calibration under a constant flow rate, Calibration under continuous pressure (height), and calibration under variable pressure and flow rate. Proceeding from calibration, water is treated with two polyanionic cellulose polymer concentrations. The concentrations are 1% and 2% PAC, respectively, 5g PAC and 10g PAC added to 5l water. Test performed are Oscillatory tests using PASCO, Amplitude sweep, Fast Fourier transform, and hysteresis test.

Keywords:

Pressure oscillations, Pressure drop, Rheology, Viscoelasticity,Polyanionic cellulose (PAC)

Contents

List of Figures

List of Tables

Nomenclature

$cos\beta$	Pipe incline relative to vertical direction
η_B	Bingham viscosity
γ	Shear rate
$\gamma_{min/max}$	Maximum/minimum shear rate
μ	Newtonian viscosity
μ	Viscosity
μ_0	Effective Casson high share rate viscosity
ρ	Fluid / liquid density
τ	Shear stress
τ_0	Effective Casson yield stress
τ_B	Bingham yield point

τ_{HB}	Herchel-Buckley yield point
CP	Cone/Plate
D	Pipe diameter
f	Fanning factor
FFT	Fast Fourrier Transformation
G''	Loss modulus
G'	Storage modulus
g	gravity
$H-B$	Herchel-Buckley
K	Consistency index
K_{HB}	Herchel-Buckley consistency factor
LVE	Linear viscoelastic region
n	Constant flow behavior
PAC	PolyAnionic cellulose
PV	Plastic viscosity
rpm	Rotations per minute
UiS	University of Stavanger
v	average velocity

YP	Yield point
YS	Yield stress

1

Introduction

This introductory chapter provides relevant background knowledge for the study and experiments performed. In brief, this chapter concludes with a background, problem formulation, and research method used.

1.1 Background

Drilling fluids are essential for production and drilling operations. Fluid travel from the steel tank to the mud pump, from the pump to the drill string, and down through the drill bit. From the drill bit nozzle, the drilling fluids flow upwards through the annulus and to the equipment removing contaminants and sediments before the fluids are back in the steel tank. The drilling fluids have multiple vital functions through this circulation process and undergo vibrations and oscillations from the well to stable control operation. The main functions of drilling fluids are to lubricate and cool the drill bit, reduce friction and fluid loss to the formation, and transport sediments and off-cuttings back to the ground [1], [2].

Particle structure impacts the rheological characteristics. Viscosity and elasticity are some of the properties underlying the term rheology. Viscous properties such as shear rates are needed to forecast annular frictional pressure loss during drilling, filter loss, and displacement efficiency. Pressure controls are essential in horizontal wells. Horizontal wells are more exposed to differential sticking. This mechanism results from the drill string being unmoved and laying on the lower wall of the borehole during drilling [3], [4].

Regulation of valves and the pump can affect the flow and cause an unsteady flow, pressure relates to the flow, and as an impact from unsteady flow, it can result in transient pressure. Transient pressure has several driving factors and can depend on the fluid compressibility, flow rate, and pipe system. Unsteady flow characterizes many engineering problems and is determined by the pulsating flow in the system. Rotating or popped valves can generate oscillatory motion, but information about pulsating turbulent flow physics still needs to be provided despite its broad relevance.

Oscillatory motions are complex as a result of the component motion. However, studies on pulsating flow show that low-frequency oscillatory flow is a slightly more stable flow for axisymmetric disturbance when compared to a steady flow. In addition, investigation on pulsatile pipe flow indicates that amplitude and frequency increase Reynolds number when reversal flow does not occur. Therefore, in slow and large amplitude, the oscillating flow will suppress turbulence in a downstream disturbance [5], [6].

1.2 Problem formulation

This thesis aims to study pressure and oscillating flow relation and compare Newtonian with non-Newtonian fluids in the pipe. Polyanionic Cellulose, PAC, is used as a component to make viscoelastic properties of the fluids. Understanding this relationship between pressure and oscillations can be used in the oil and gas industries. It also can be implemented in hemodynamics experiments, where liquid can mimic blood in veins. Pulsatile flows are used in the medical research field.

In this experiment, the flow and pressure drop relation in non-steady oscillatory flows alongside the velocity profiles from peristaltic pumps using different fluids is studied. Fluids were pumped through both elastic and rigid tubes, and the behavior of the differential pressure was studied.

1.3 Research method

The experiments were done on a small scale to make it possible to perform the study by a single person. An experimental setup on a larger scale would need at least two people to stand on different sides of the testing section. Pasco sensors from Capstone were used to record the pressure difference between the inlet and outlet of the tube, as well as the mass flow rate. The effect of oscillating flow and pressure drop in a horizontal pipe test section was investigated through laboratory experiments, at the Multiphase flow lab at the University of Stavanger. Before starting the experiments, calibration tests of equipment are performed with the use of water. Equipment calibration includes Ohaus mass balance weight, calibration under constant height, and calibration under continuous pressure. Calibrations are performed to determine a basis for further testing with polymers. Flow rate is recorded using a weighing scale connected to the Pasco interface. The lab setup contains a pressure sensor, peristaltic pump, rigid and elastic pipes, a custom-made pipe holder, and a computer with PASCO software. After calibrations, two distilled water and PAC concentrations are used for further testing. The concentrations are 5g PAC in 5l water and 10g PAC in 5l water. PAC amount corresponds to 1% and 2% PAC by weight, respectively. Oscillatory flow is connected to the rheology of the fluid. Therefore, tests of rheology are conducted. Figure 1.1 shows this thesis' outline and central parts.

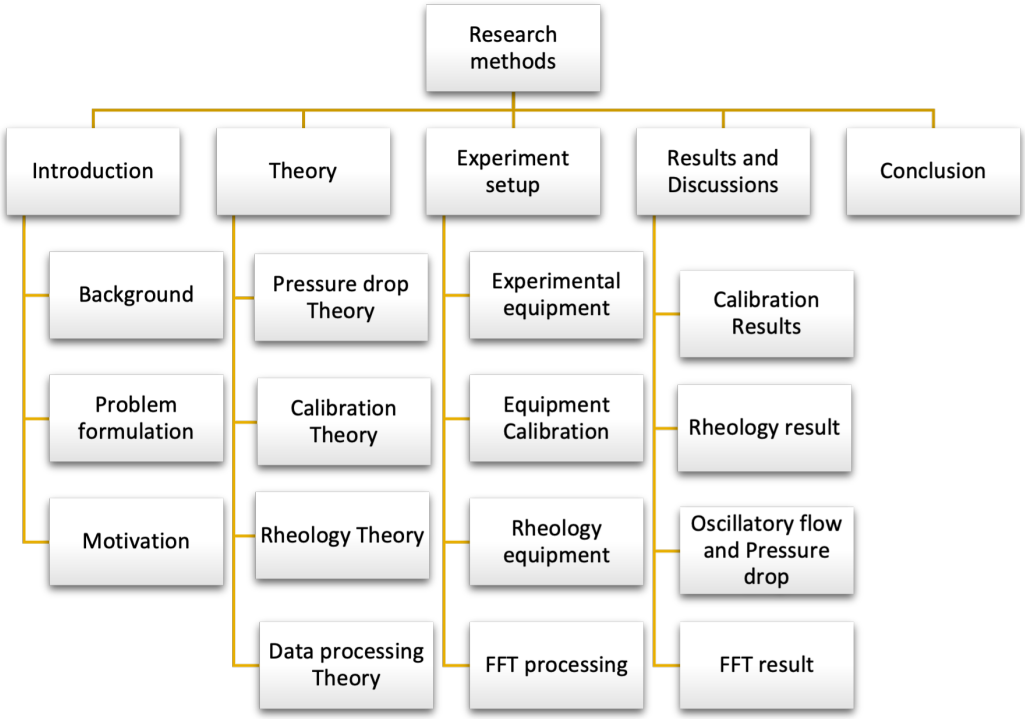

Figure 1.1: Thesis research illustration

1.4 Motivation

Expanding knowledge of pressure oscillations and pressure drops in horizontal pipes can be used in several industries. For example, there are several engineering problems with the unsteady flow in the petroleum industry, and a deeper understanding of the topic can improve the industry. Another field of use is hemodynamic experiments, where the liquid can mimic blood in veins. Nevertheless, a wide range of application grounds for the experiment and a laboratory experiment is an intriguing way to evaluate the impact of pressure oscillations, pressure drop, and polymer impact.

2

Theoretical

This chapter deals with the related theory and serves as a basis for the experiments.

2.1 Pressure drop

The pressure drop in pipe flow depends on pipe diameter, viscosity, density, and flow velocity. In addition, the pipe wall roughness and pipe inclination are essential. The total pressure gradient in a pipe is the sum of frictional, hydrostatic, and acceleration pressure gradients. Frictional pressure drop for laminar single phase flow can be determined with constant flow velocity and pipe diameter, from the following equation

$$(\frac{dp}{dx})_f = \frac{4}{D} * \frac{16}{R_e}\frac{1}{2}\rho U^2 \tag{2.1}$$

Laminar friction factor R_e corresponds to Fanning friction factor , $f = \frac{16}{R_e}$

Hydrostatic pressure gradient are defined as

$$(\frac{dp}{dx})_h = \rho g cos\beta \tag{2.2}$$

where,

g= *gravity*

ρ= fluid density

$cos\beta$= pipe incline relative to vertical direction.

Acceleration pressure gradient in one dimensions is given by

$$(\frac{dp}{dx})_a = -\rho U * \frac{dU}{dx} \tag{2.3}$$

For acceleration pressure gradient, total energy will not change with change in pressure.

Combining the three components provides the pressure drop equation for a single phase flow[7]

$$\frac{dp}{dx} = (\frac{dp}{dx})_f + (\frac{dp}{dx})_h + (\frac{dp}{dx})_a \tag{2.4}$$

Pressure drop are only depending on frictional component for the horizontal test tube, the hydrostatic and acceleration pressure component will equal zero for this thesis experiment.

With oscillations, the effective gravity of fluid makes a rise in periodic pressure fluctuations. This effect can further induce flow instability in the system. To better understand the effect and measures pressure drop, it is essential to know the connection between flow and pressure drop. Pressure drop has, in multiple studies, been evaluated for turbulent and laminar flow in pipes. Due to the oscillating flow in pipes, more pressure drop measurements still need to be done. From a study on vertical oscillations and pressure drop, the results show the magnitude of flow rate oscillations is reduced with increased Reynolds number[8].

2.2 Reynolds number

In pipes, Reynolds number defines the flow as turbulent or laminar. Turbulent flows are associated with high values of the Reynolds number. The internal force is proportional to the fluid density, and the viscous forces need to be more vital to prevent rapid fluctuations from occurring in the fluid. On the other hand, the laminar flow has larger viscous forces and can prevent fluctuations from occurring. The flow will then perform in a line for all the small to moderate Reynolds numbers [9][10].

$$Re = \frac{\rho * v * D}{\mu} \tag{2.5}$$

where :

v = average velocity

D = pipe diameter or characteristic length for the flow system

ρ = density of the liquid

μ = viscosity of the liquid

Reynolds numbers for turbulent flow are often called the critical Reynolds number and are given with $Re_{cri} = 2300$. The critical number can differ with geometry and flow conditions. However, all values of Re$\geq$ 4000 will give turbulent flow. For most flows in circular pipes, the following Reynolds numbers give: Laminar flow $\rightarrow R_e \leq$ 2000. Transitional flow $\rightarrow$ 2000<Re<4000. Turbulent Re>4000. The transitional flow will switch between the laminar and turbulent flow. Depending factors on flow are also geometry, surface roughness, flow velocity, surface temperature, and fluid type.[10][9]

2.3 Calibration

Calibrations are performed for all laboratory equipment used in the thesis. Calibration of equipment gives a standard and scale used to compare further studies. Variations in conditions can impact test results, and a finalized standard gives grounds for retesting and provides an association between measurements to minimize measurement uncertainty. Are often performed on weights/scales and pressure measurement equipment[11], [12].

In this thesis, three calibration methods are used. Calibration with constant flow rate, section:3.2.2 , calibration with constant pressure, section 3.2.3 and calibration with variable pressure and flow rate in the section 3.2.4. The flow rate of using the pump under variation of rpm and correlation between flow rate and pressure would give an expression of Q versus pressure and will further be used for flow rate values. Equivalent to constant pressure, the evaluation is made by pumping liquid through the pipe at a constant pressure. Calibration under variable pressure and flow rate are calculated from measured values in calibration under constant pressure.

2.4 Rheology

Rheology is studying the deformation of all matter. The relationship between flow rate and flow pressure is of primary interest and has two fundamental relationships, Laminar and Turbulent flow regime [3].

2.4.1 Shear thinning effect, shear stress and shear velocity

The shear thinning effect occurs when decreasing velocity while increasing shear stress. The synonym used is pseudoplastic flow behavior. Decreasing viscosity values at higher shear stress will, for a polymer solution, result in shear thinning flow behavior. When polymers are at rest, the edges of molecule chains become entangled, and the filamentary molecules form balls. The entangled balls are deformed with applied shear, and individual molecules are less flow resistant than the entangled balls, thus, resulting in a shear-thinning effect.

Shear stress is calculated from software; records used in determining share stress are share force and shear area. Shear forces are recorded from the torque used at each measuring point, or shear force can be determined from rotational speed, taken from the flow resistance force of the sample. Shear areas are given by the measuring system used. The following equation defines shear stress.

$$\tau = \frac{F}{A} \tag{2.6}$$

Shear rates are calculated from velocity and shear gap size. Velocity is recorded from the rotational speed at each measuring point, and rotational speed can be either preset or determined from the flow velocity of the sample if the shear force is the preset value.

$$\dot{\gamma} = \frac{V}{h} \tag{2.7}$$

Combining shear stress, shear rate, and Newton's law, the term law of viscosity is defined.

$$\eta = \frac{\tau}{\dot{\gamma}} \tag{2.8}$$

Yield points are defined as the lowest shear value the material can have above fluid behavior and below for a material behavior corresponding to solid matter. The yield point and Bingham model correspond with the following equation :

$$\tau = \tau_B + \eta_B \dot{\gamma} \tag{2.9}$$

Where,

τ_B = Bingham yield point

η_B = Bingham viscosity

whereas, τ_B are a axis intercept and η_B are derived from the slope of the curve [13]

2.4.2 Rheology models

There exist five different rheological models. A brief introduction is provided for all the models. Rheological models are divided into Newtonian and non-Newtonian fluids. Non-Newtonian fluids do not conform to Newton's laws, and the relationship between share rate and shear stress depends on the type and concentration of the chemical composition of the blended fluid system. Rheological models describe a mathematical expression of the viscous forces present in a fluid and flow behavior. Flow behavior expresses the shear rate and shear stress relationship [3].

Herschel-Buckley

Herschel-Buckley model is modified from the power law model, and the model can encompass both yield behavior of non-Newtonian fluids and allows shear thinning. When shear stress and shear strain are zero, the power law model is valid[14].

Herschel-Buckley model is expressed by the following relation :

$$\tau = \tau_{HB} + K_{HB}\gamma^n \tag{2.10}$$

Where,

τ_{HB} = Herschel-Buckley yield point

K_{HB} = Herschel-Buckley consistency factor

n = Herschel-Buckley flow behavior index

Curve fitting determines the consistency index and flow index, while, yield point are calculated from the expression[14]:

$$\tau_{HB} = \frac{\tau^{*2} - \tau_{min} * \tau_{max}}{2\tau^* - \tau_{min} - \tau_{max}} \tag{2.11}$$

And, τ^* are determined by interpolation of the corresponding shear strain given as[14]:

$$\gamma^* = \sqrt{\gamma_{min}\gamma_{max}} \tag{2.12}$$

Where,

γ_{min}= Minimum shear rate

γ_{max}= Maximum shear rate

Newtonian model

The Newtonian model characterizes the fluid by viscosity and is fluids like water, gas, and high-gravity oils. Relationships for a Newtonian model are defined with the following equation :

$$\mu = \frac{\tau}{\gamma} \tag{2.13}$$

Where,

τ = shear stress

μ= Newtonian viscosity

γ= shear rate

For Newtonian fluids, the rheological curve will be a straight line passing through the origin. Newtonian viscosity will not change with share rate, and the only parameter needed is μ [2].

Bingham plastic

Bingham plastic model is defined from plastic viscosity and yield stress and needs finite stress for flow to be initiated. Therefore, Bingham plastic curves are defined in the following equation:

$$\tau = YS + PV\gamma \tag{2.14}$$

Where,

τ = shear stress

PV= Plastic Viscosity

YS= Yield stress

γ= shear rate

Plastic viscosity is defined as the shear stress and yield strength needed to give shear rate. In the petroleum industry, Fann35 viscometers are used. From measured

viscometer data, the plastic velocity can be determined with the following expression:

$$PV[cP] = \theta_{600} - \theta_{300} \tag{2.15}$$

where,

θ_{600}= Fann viscometer reading at 600 rpm

θ_{300}= Fann viscometer reading at 300 rpm

Yield stress is the shear stress needed to create flow. With Fann viscometer readings, yield stress can be expressed with the following equation [2].

$$YS[\frac{lbf}{100ft^2}] = \theta_{300} - PV \tag{2.16}$$

Power law

Power law describes the flow model for pseudoplastic flow. Pseudoplastic fluids have a non-linear curve, and viscosity will decrease while increasing the shear rate. Suspension of long-chain polymers is typical pseudoplastic. Power laws are given with the following expression:

$$\tau = K\gamma^n \tag{2.17}$$

Where,

K = Consistency index

n = Constant flow behavior

K and n can be derived from the following expressions using Fann35 viscometer :

$$n = 3.32log\frac{\theta_{600}}{\theta_{300}} \tag{2.18}$$

$$K = \frac{\theta_{300}}{511^n} \tag{2.19}$$

Power law can give inaccurate results with low shear rates due to an absence of yield stress. Power laws are dependent on the constant flow behavior, n, and for different values of,n, the three models can be defined[2][3].

- n $<$ 1 Pseudoplastic - Viscosity will decrease with shear rate
- n = 1 Newtonian - Viscosity will not change with shear rate
- n $<$ 1 Dilatant - Viscosity will increase with shear rate

Casson model

Casson model is a hybrid model between Bingham and Power law model, as the Casson model allows both yield behavior and shear-thinning. The model is defined by [14]:

$$\tau^{\frac{1}{2}} = \tau_0^{\frac{1}{2}} + \mu_0^{\frac{1}{2}}\gamma^{\frac{1}{2}} \tag{2.20}$$

Where,

τ_0= Effective Casson yield stress

μ_0= Effective Casson high share rate viscosity

2.4.3 Viscoelastisity

Fluids under applied force will be deformed, and the ability of the liquid to show viscous and elastic behavior is referred to as viscoelasticity. From an evaluation of the fluids viscoelastic properties of a fluid, the gel strength and structure, barite sag, and solid suspension can be determined. Viscoelastic properties are determined by two types of oscillatory tests, amplitude sweep test, and frequency sweep test. Amplitude sweep test is used in this study and is described in 3.1.7.

Viscoelasticity is defined through two parameters: G' represents elastic behavior and G" represents viscous behavior. With deformation, there will be a loss of energy and storage of energy. Therefore, the stored energy is measured with G', and the energy lost by deformation is given with G' [15] [16][17][18].

Transient shear stress and shear rate are expressed with the following equations:

$$\gamma(t) = \gamma sin(\omega t) \tag{2.21}$$

$$\tau(t) = \tau_0 sin(\omega t + \delta) \tag{2.22}$$

Expansion of the formulas give :

$$\tau(t) = \tau_0[(sin(\omega t) * cos(\delta)) + (cos(\omega t) * sin(\delta))] \tag{2.23}$$

$$\tau(t) = \gamma_0[((\frac{\tau_0}{\gamma_0})cos(\delta) * sin(\omega t)) + ((\frac{\tau_0}{\gamma_0})sin(\gamma)cos(\delta t))] \tag{2.24}$$

$$\tau(t) = [G' sin(\omega t) + G'' cos(\omega t)] \tag{2.25}$$

Elastic and Viscous modulus :

$$G' = \frac{\tau_0}{\gamma_0} cos\delta \tag{2.26}$$

$$G'' = \frac{\tau_0}{\gamma_0} sin\delta \tag{2.27}$$

Phase angle, elastic- and viscous moduli impact the viscoelastic behavior. Table 2.1 defines how damping angles affect viscoelastic behavior. The liquid will be perfectly elastic at a zero-degree angle and perfectly viscous at a ninety-degree angle. Forty-five-degree angles give a perfect viscoelastic phase as the ratio of elastic and viscous are 50/50 [18].

Ideal-viscous flow behavior	Behavior of a viscoelastic liquid	Viscoelastic behavior showing 50/50 ratio of the viscous and elastic portions	Behavior of a viscoelastic gel or solid	Ideal-elastic deformation behavior
δ=90^o	$90^o \succ \delta \succ 45^o$	δ=45	$45^o \succ \delta \succ 0^o$	δ=0^o
tan $\delta \rightarrow \infty$	tan $\delta \succ 1$	tan δ =1	tan $\delta \prec 1$	tan $\delta \rightarrow 0$
(G'$\rightarrow$0)	G" $\succ$ G'	G'=G"	G'$\succ$ G"	(G"$\rightarrow$0)

Table 2.1: Angles and viscoelastic behavior [15]

2.5 Oscillatory test

Oscillatory tests use the CP concept from the amplitude sweep test; samples are placed between two cone/plates. The top plate moves back and forth parallel to the lower stationary plate. With a constant rotation speed, the test correspondingly has a constant oscillating frequency. The upper plate sensor detects the deflection path, while the lower plate sensor gives strain or deflection after rheological evaluation [18].

2.5.1 Amplitude sweep test

Viscoelasticity can be determined with an amplitude sweep test, performed by varying the amplitude of shear stress while keeping a constant frequency. When G' and G" is constant for small deformation values and the curve provides constant plateau values, the phenomenon is called linear viscoelastic range (LVE). With more significant deformation, the G' and G" change, and the lines should interact at some point for the sample to show viscoelastic behavior. The point of interaction is called the flow point. Flow points occur when the system is equally viscous and elastic. Storage modulus, G', will deviate from the horizontal line, referred to as the Yield point. Amplitude sweep test results are illustrated in figure 2.1. The illustration displays storage modulus, G', loss modulus, G", as a function of shear rate. The illustrated range where G' > G" is in the LVE range, and the fluid will be in a gel-like character. Right figure 2.1 are liquid character and G" > G'[18].

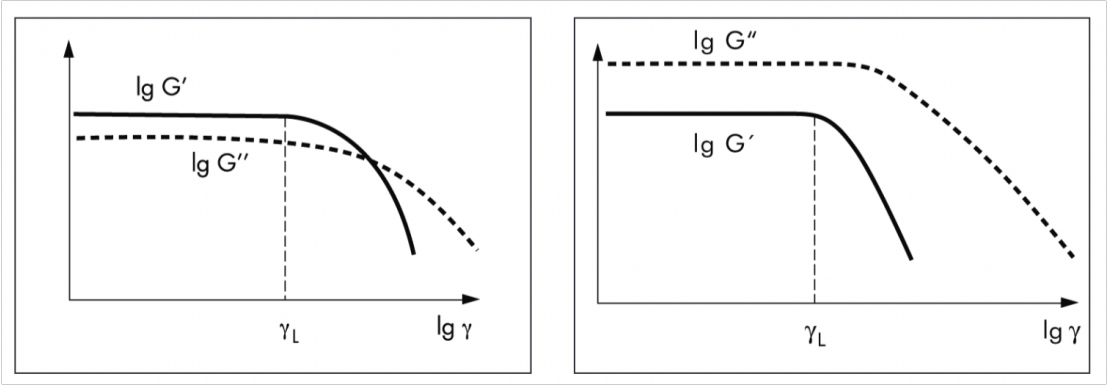

Figure 2.1: Amplitude sweep test G' and G" vs deformation, [18]

Linear viscoelastic regions (LVE) are determined from the amplitude sweep test. The test is a plot between G' and G" on the y-axis and strain, or shear stress is plotted on the x-axis. LVE defines the range a sample can handle without destroying the structure of the sample [13].

2.6 Polymer

PolyAnionic Cellulose (PAC) has a high purity and is a demi-natural additive, thickening agent, and filtrate reducer. PAC is a white powder that dissolves immediately in water and is an indispensable product for drilling mud. Making drilling mud with PAC is also essential for confecting well liquid and is a suitable filtrate controller, rheology controller, stabilizer and can increase viscosity [19].

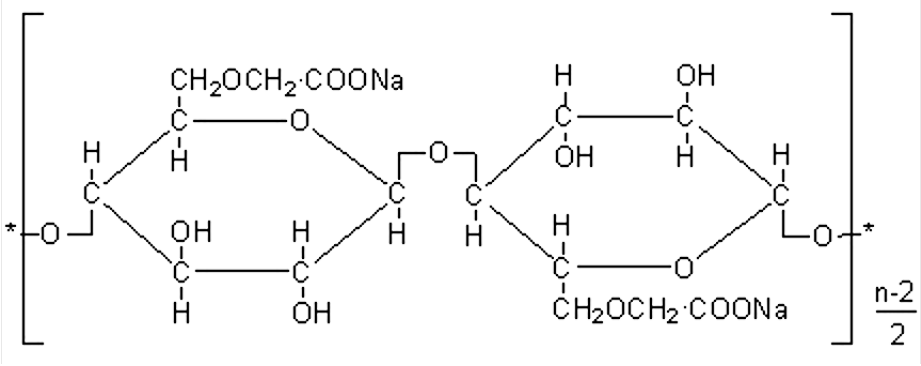

Figure 2.2: Structural formula of PAC[19]

Experimental use of PAC is often associated with investigation in cuttings transport in drilling fluid model systems. PAC are assumed to behave purely viscous in laboratory experiments. However, it found that PAC are not purely viscous. Tests have shown that on time scales of 0.01 to $1s_1$, the average stress difference gives a viscoelastic behavior from the polymeric microstructure [20].

2.7 Data processing

2.7.1 Fast Fourrier Transformation

FFT converts measured time-dependent pressure drop signals into individual frequency components. The components are a single sinusoidal oscillation at different frequencies and have explicit amplitudes and phases. Signals must be repeated periodically and contain a whole number of periods to be transformed into time vs. frequency graphs. The graph indicates how often an analog signal is scanned [21].

2.7.2 Hysteresis

Hysteresis measurements are determined from displacement between measurements. The process of the hysteresis test is to deform the sample from minor stress to more significant stress and back to minor stress again. For the same measuring point, the increasing stress and decreasing stress can correspond to the same value or at a lower value on the Y axis. If the measuring point doesn't overlap, the test indicates hysteresis.

3

Experiment setup

Experimental studies are performed with an oscillating pump pumping water through a non-flexible horizontal pipe at the test section. Water is stored in a tank under the test section and will be taken up through the peristaltic pump. Test sections are defined as horizontal non-elastic tubes. Pressure sensors are placed at the start and end of the horizontal test tube and measure the pressure drop, and analysis is directly displayed on the computer using PASCO software. rpm is manually changed

on the peristaltic pump, affecting the pressure drop measurement. Water exiting the test section is stored in a small tank and weighed with an Ohaus scale. Logged weights are automatically registered in PASCO software with the use of Bluetooth. Mass flow and pressure drop are plotted with time on each period logged.

The equipment used is highly sensitive, the test is performed with care, and a custom-made table is made to ensure the test section tube is stable for all tests at the intended height. Tubes from the test section and to the differential pressure sensor are loosely placed and can be affected by tube vibrations during testing. Figure 3.1 illustrates the equipment setup, photo illustrations are given in Appendix E.

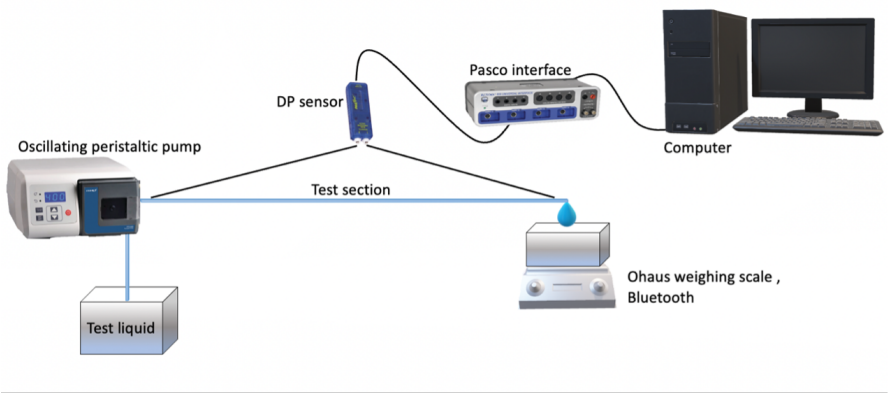

Figure 3.1: Illustration of the experimental setup

3.1 Experimental equipment

Setup of experimental test: Water is pumped from a tank of water and transported with flexible hoses through the oscillatory pump. From the pump, there is a shift from flexible to nonflexible tubes, and at the end of the tube, water will be collected

in a new tank and weighted with Ohaus material balance weight. Weight is connected to the computer through Bluetooth.

Pasco DP sensor has one measuring point at the start of the tube where the pump is stationed and a second measuring point at the end of the tube. The DP sensor combines the two measures, and the computer evaluates the pressure drop. PASCO is used to plot the flow of water against pressure drop for different pump rpm. The sampling rate can be changed in the program. The maximum sampling rate for the DP sensor is 1KHz, while for Ohaus mass scale, the maximum sampling rate is 20Hz.

3.1.1 Peristaltic pump

Inside the pump, there is an elastic pipe containing the fluid flow, the pipe is squeezed and relaxed in a circle sequence from three rotating arms. Rotating motion causes high-stress values on the pipe, providing high deformation on the pipe and affecting liquid transport.

Usually, the pump is used in the medical and pharmaceutical industries. The pump controls dosage and repeatability where there is a need for precise dosage and repeatability due to the constant calibrated flow.

Fluid flow is strongly related to the tube's deformation, and changing the pipes on the inlet and outlet can cause a difference in the results. The pump can change flow direction and flow speed with increasing and decreasing rpm values.

Oscillating flow is made from the peristaltic pump, which has a cylindrical rotor that squeezes and relaxes the pipe. The elastic pipe in the pump will be exposed to

Figure 3.2: Photo of Peristaltic pump, [24]

high-stress values from the pipe deformation, the pipe deformation affects the liquid transport [22], [23].

3.1.2 Pressure sensor

The dual pressure sensor is connected at the start outlet from the peristaltic pump, and one sensor is at the end of the test section tube. The sensor is capable of reading two absolute pressure or one gauge pressure and one differential pressure. For this setup, the pressure sensor is used to read differential pressure. Transient and steady-state flow studies are possible for sample rates up to 1KHz; pressure units are given in kPa, N/m^2, or psi. In this thesis, the pressure units are given in kPa.

Pressure over the test section and horizontal tube determines the differential pressure. The differential pressure is positive when port 1 has a higher pressure than Port 2. When sampling, the sensor uses dynamic variable over-sampling, providing smoother data with noise reduction and improving resolution for measurements[25].

Figure 3.3: Photo of DP sensor [25]

3.1.3 Ohaus mass balance

Ohaus mass balance scale sends measures directly to the PASCO software with Bluetooth, providing an easy sampling graph at the computer. The mass balance weight is highly sensitive and needs to be used with consideration and care not to interface with the measured weight. A small bump in the weigh table may cause some impact on the measured outcome. The maximum sampling rate for the scale is 20 Hz. Therefore, samplings that rely most on weight are performed with regard to the maximum sampling rate.

Ohaus weight with model nr., SKX422, is used for the tests in this thesis. The maximum capacity for this weight is 420 g. Starting tests, an Ohaus weight with a maximum capacity of 630g was used; due to Bluetooth sending error, this mass balance weight was not further used.

3.1.4 PASCO 850 universal interface

PASCO universal inter-phase is the connecting component between the sensor and the computer. With PASCO software on the computer, the sensor-measured data are displayed and analyzed on the software.

The interface has an unmatched rapid sampling rate and is the most used lab interface in laboratory education today. The standard unit generates 500 Milliewatts, and one power output generates 15 watts. The sampling rate is high-speed and has a rate of 10 MHz for two channels and 1 MHz for the rest of the channels[26].

Figure 3.4: Photo of the Pasco interphase [26]

3.1.5 Anton Paar - Density meter

Measured density with four-digit precision, measuring results are based on oscillation characteristic knowledge. Density is measured from a u-tube inside the machine, and the tube is shown on the screen for correct filling and has a bubble detector. The machine can use multiple fluids with dirt, shock, and spilling withstanding tubes. Densities can range from 0 g/cm3 to 3 g/cm3. [27]

3.1.6 Silverson

Silverson machines are heavy-duty laboratory mixer emulsifiers. The ones used for this experiment are of the model L2R and serial number L2R5756. Ensuring the working head is fully immersed in liquid at all times is vital to avoid damage to the machine. Therefore, all test fluids from distilled water and polymers are mixed with the Silverson machine. The working head has two bolts that can be removed for thoroughly cleaning equipment before starting new mixing [28].

3.1.7 Anton Paar - Viscosity, MCR 302

Anton Paar MCR 302 and complementing software are used for conducting Viscosity testing. Viscoelastic performance in a fluid determines the ability of the fluid to be viscous, elastic, or both. The amplitude sweep test determines storage modulus, loss modulus, shear stress, and damping factor, and all measuring points are plotted by the computer software - Anton Paar RheoCompass 1.30.

Amplitude sweep tests are performed with a cone and plate measuring system called Cone/plate (CP). Starting the Rheometer program, the gap needs to be set to zero gap. Then, a sample can be added, and the test needs to be correct to not over - or under-fill the plate; the correct amount of filling is when the sample is aligned with the end of the cone/plate. Trimming the sample is an effective way to get the right sample amount; trimming is performed with a spatula after the sample is overfilled and lowered to a zero-gap position. The sample is correctly trimmed when the upper diameter of the upper plate and the sample corresponds, and a slight bulge will be formed at the edge [13].

The following parameters are used when conducting the test :

Angular Frequency	Strain angular Amplitude interval	Temperature
10 Rad/s	0.01 % - 1000 %	22 $°C$
10 Rad/s	0.00001 Pa - 1 Pa	22 $°C$

Table 3.1: Anton Paar Measurement input

3.2 Equipment calibration

3.2.1 Ohaus mass balance weight

The mass balance weight are calibrated using PASCO software and Bluetooth. Kern check weights are placed on the scale and compared to Ohaus mass balance measured weight. Check weight and measured weight are plotted to evaluate the trend line and compliance between both weights. Results in section 4.1.2 the kern check weight is commented as set weight and the measured weight is set to the actual weight.

3.2.2 Calibration under constant height

Calibrating with constant height is performed to calibrate the equipment and make a pre-study before comparing it to the thesis scope test. Density is constant for all the calibration tests. The first test has 500 ml test fluid; as the weight where the defect, the estimation of 500 ml is performed with eye measurement. This is a non-effective and inaccurate measuring scheme to perform alone. The weight is therefore switched after the first test. For the continuing tests with the new weight, the amount of water used in the test is lowered from 500ml to 250ml; Ohaus weight has a maximum limit, and for the limit to not be exceeded, the test amount needed to be lower. The first test with new weight is with weight on the table under the test section pipe. To ensure correct measurements, the 2nd test is with the weight and test section in a straight line.

Elastic tubes are used in the beginning, and pressure drop was measured. Rigid tubes are only used in the test section for the first set of analysis tests.

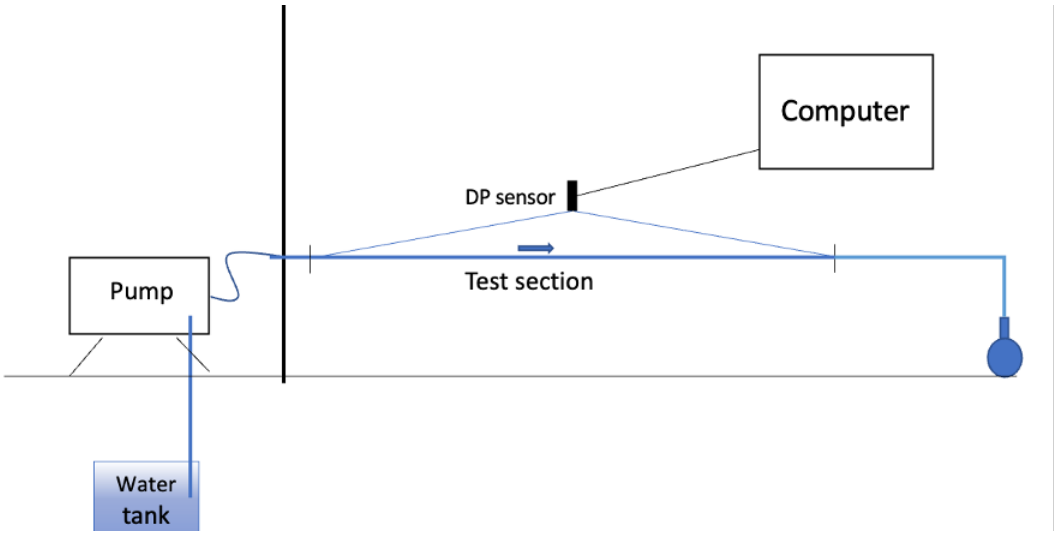

(a) Ohaus weight and test section at same level

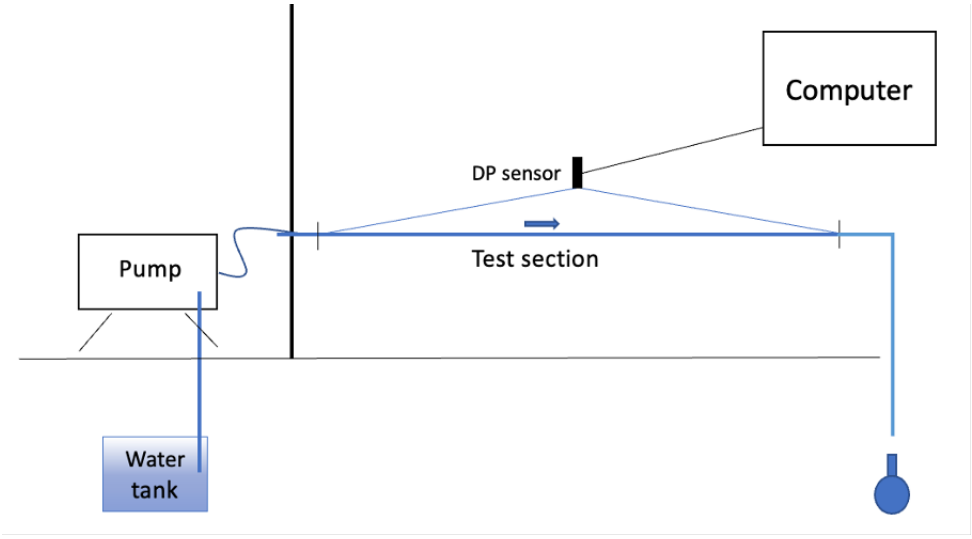

(b) Ohaus weight under test section height

Figure 3.5: Illustration of ohaus weight placement

Calculating Q:

$$Q = V\rho = (mass/time)/\rho \tag{3.1}$$

3.2.3 Calibrating under constant pressure

Tube diameter in the test section can be measured and calculated. Ensuring the correct diameter of the tube, the calculated diameter from this test will be evaluated against the measured diameter. Measuring diameter is performed with calipers, and all results are given in section 4.1.4.

Figure 3.6 shows a schematic drawing of the test. Water is stored in a tank under the pump, and the pump provides water in the hanging tank, which can be raised and lowered to the desired height. There are in total: 5 heights evaluated in this test. Height-regulated tanks have constant water flow in and out. Thus, the water height is at all times the same. Water in the tank must be at the same point for a correct height measure. Height is estimated with a thumb stick from the height of the test section tube and up to the middle part of the piping, providing water flow to the test section. The outlet section of the test tube has a volumetric flask for water management. Water flowing through the system is measured at 1 liter and time is noted. Flow rates are calculated and plotted with height.

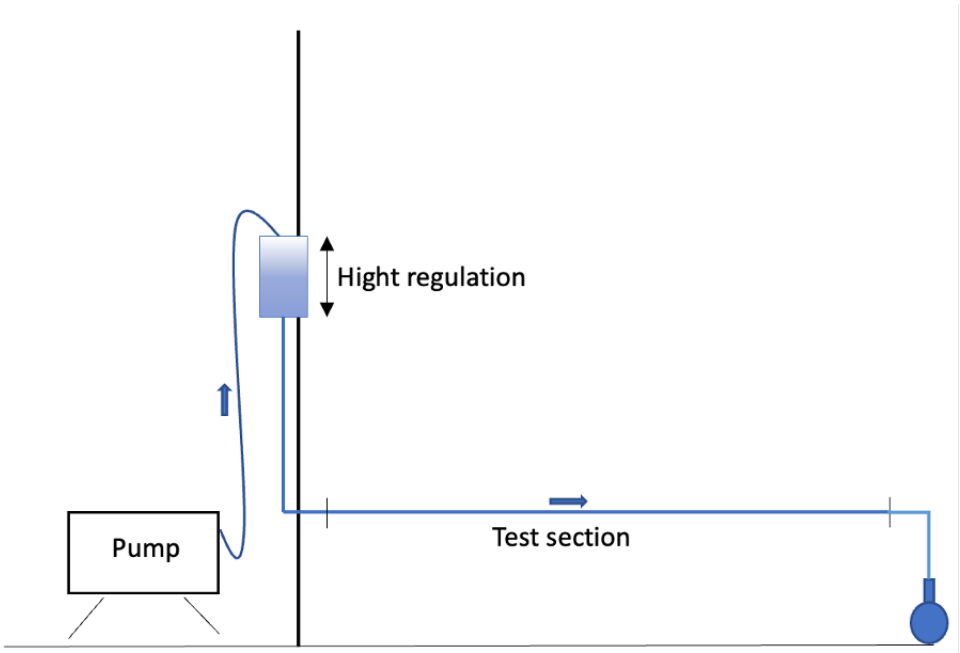

Figure 3.6: Test section calibration

3.2.4 Calibrating under variable pressure and flow rate

Calibration under variable pressure and flow rate is calculated from results in calibration under constant pressure. Section 3.2.3 describes calibration method and results is given in table 4.4.

3.3 Analysis

Pressure drop is one of the main scopes of this thesis and after calibrating the equipment used, the scope experiment can be executed.

3.3.1 Mass rate

Mass rates are evaluated by pumping water through the test section and filling 250 ml, time will be taken to calculate the mass rate.

3.3.2 Pressure drop

Pressure drop analysis in PASCO software has many options, and for calibration, the sampling rate is chosen to 20 Hz to align with the maximum sampling rate possible for Ohaus mass scale. Although differential pressure samples alone have a maximum sampling rate of one kHz, the sampling speed of twenty Hz gives noisy sampling and difficulties in observing the trend for pressure drop at different RPMs.

The pump pushes the tube and water as described in the theory part, the movement should be possible to observe in pressure drop analysis.

Three rates are chosen to illustrate the pump's impact on differential pressure over time. Results are given in section 4.2.1

3.3.3 FFT

FFT is evaluated in two sections. FFT for calibration analysis is given in 4.2.2, and FFT results for polymer solution are given in section 4.4.4. Fast Fourier transformation turns a number series into a graph and sin waves. PASCO software has a feature to make an FFT graph from differential pressure and time measurements. This is automatic for the series chosen, and the graph needs to be fitted to the right intent and analyzed. In section 4.2.2, FFT is executed for three cases with a sampling rate of 1 kHz and one comparison graph contained from a 20Hz sampling rate. Four rpm speeds were chosen for the pump at frequencies 4, 13, 81, and 125.

3.3.4 Hysteresis

Hysteresis test uses Anton Paar MCR 302 machine and associated software. A test batch of distillate water and PAC are placed between two parallel plates, as described in section 3.1.7 . When the sample is trimmed, the test is ready to be executed. The hysteresis test is evaluated from - to - and provides information on viscosity to the first and last point of the test, regression area, and hysteresis area. Hysteresis has a measuring area from 5 to 130 γ^* and takes 120 measuring points in the selected area. When 120 points are provided between 5 to 130 γ^*, the test sample is stationary on a γ^* equal to 131 for 50 measuring points, which takes about 3.6 seconds. The last part of the test from 130 to 5 γ^* is performed similarly from 5 to 130 γ^*. Test temperatures are kept constant at 22 $^\circ C$.

3.4 Procedure of mixing polymer

Starting mixer at high speed containing approximately 2,5 l water. Distillate water is mixed with PAC powder by adding small amounts. Adding too much simultaneously causes the PAC powder to form lumps of powder and not fully disperse with the water. When all PAC powder is mixed with 2,5 l water, the rest of the water is added, and the final amount of water is 5l. Ensuring thoroughly mixing the two components, the Silverson mixer is left for 5 minutes after all the powder is mixed into water and before shutting it down. The mixer is cleaned, and the bucket with the mixture is placed away for 24h. For the settlement of the two components, the bucket is closed with a lid for the swelling of powder and water to be as good as possible. Before starting tests, the mixture is mixed for 2 minutes to ensure thoroughly mixed components. Both polymer and distillate water mixes are completed with the same steps and mixing time.

The amount of PAC is mixed with water at two different concentrations.

- 5 g PAC / 5L water.
- 10 g PAC / 5L Water

4

Results and Discussions

This chapter contains lab results of the experiments described in chapter 3. The calibration analysis, viscoelastic properties, oscillatory analysis, pressure drop, and FFT are presented in this chapter.

4.1 Calibration Analysis

Equipment calibrations are important and are an important basis for further testing. Results from this equipment calibration are given and calibration was done using distilled water.

4.1.1 Anton Paar - Density

In this section results from the density measurements are given. The methods are explained in section 3.1.5. It should be noted that Anton Paar density meter is precalibrated.

Water density

In table 4.1 the result from density measurement for water is presented. It could be seen that the density is not the same as the theoretical density.

Density	0,9983 g/cm^3
Density temperature	19,98 $°C$
Specific gravity	1,0001
Density condition	VALID

Table 4.1: Anton Paar Density meter - Water

PAC treated water density

1 wt% PAC and 2 wt% PAC are added to distilled water as viscosifier. The density of these two concentrations were measured and gave the same value, 0.9991 g/cm^3.

This means that a better densitometer with higher resolution is needed.

4.1.2 Ohaus mass balance weight

The following table and figure are from Ohaus scale calibration. The calibration is performed for two Ohaus mass balance scales. This has been made due to sporadic errors in Bluetooth performance of the first Ohaus scale. During the tests, the results from the actual weight in the table 4.2 are used in all tests. The weights used for calibration were from Mettler Toledo.

Table 4.2 are used in all weight measurements in this thesis, the figure 4.1 are from the set and actual weight when using new Ohaus scale. The R^2 number provides in-site into how well the trend line is for the values weighted and set. Trend-line for the new table is perfectly aligned. This is seen from the $R^2 = 1$ number.

Set weight	Actual weight
1	1
2	2
3	3
100	100,19
200	200,39
300	300,59
400	400,79

Table 4.2: Table of Set and Actual weight from the second Ohaus weight

The following table. **??** and figure. 4.2 are from the defected Ohaus mass scale. The first runs of calibration tests with water running through the system gave an error in the Bluetooth connection. The scale failed to send updated weight to the program, and all weight measurements were set as zero. The test was therefore

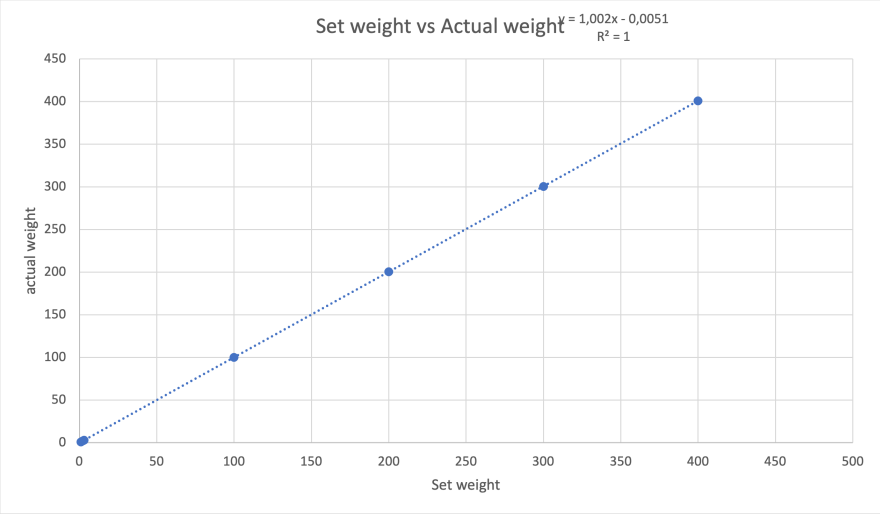

Figure 4.1: Graphics of set vs actual weight, Ohaus second weight, units in gram

visually seen and estimated when the measuring flask was 500ml filled with water. This way of measuring can lead to errors in time and volume of the test. Therefore, this scale was not used further.

Set weight	Actual weight
100	100,23
200	200,47
300	300,70
400	400,39

Table 4.3: Table of Set and Actual weight from the defect Ohaus scale

A perfect trendline of the relationship between the Ohaus weight and the Mettler weight is presented in figure 4.2. When the weight is placed on the Ohaus mass scale the measured weight is recorded in PASCO software. For mass measurements, a fast sampling rate is required.

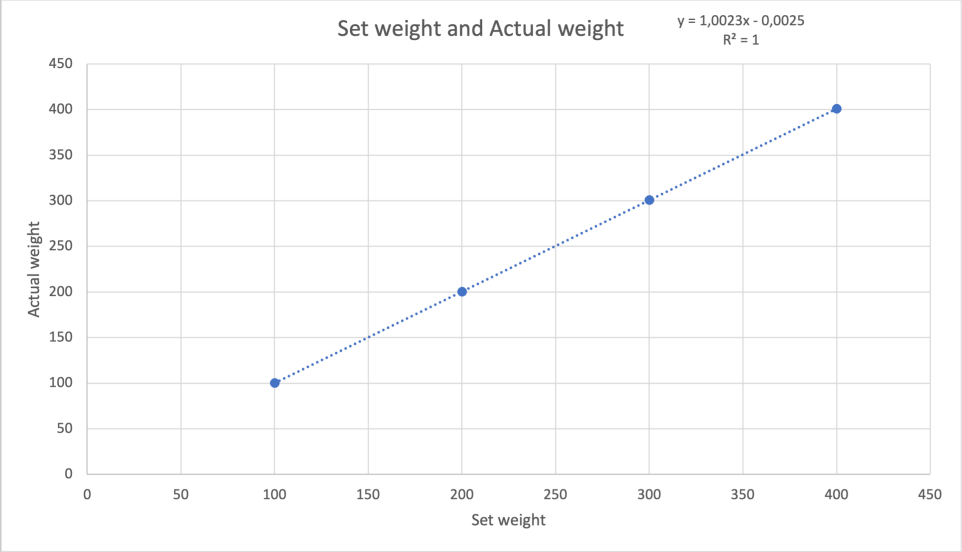

Figure 4.2: Graphics of set vs actual weight, Ohaus Defect

4.1.3 Calibration under constant flow rate

Calibration of the pump is performed to evaluate the volumetric flow rate of the peristaltic pump. In this section, multiple tests were performed. The first test was performed using the defected Ohaus mass scale and measured volumetric mass was made visually using a flask of 500 ml. The second and third tests contain the new Ohaus weight which can measure up to 420g. This gives the volume of water in the test to be lowered to 250 ml. All of the measurements were conducted under the same conditions as seen in figure 3.5

Test number two and three are performed three times each for a correct result, and all test results are placed in Appendix A, B, and C.

Test one : Water = 500 meter and defect Ohaus mass scale

The first test was performed in one round. There is no need to proceed with multiple tests when the test is performed with a lack of quality. Results in figure 4.3 show steady flow and all trendlines align with the measuring points by 99.8 %. Flow is approximately 6 cm^3/s when the pump is rotating at 100 rpm.

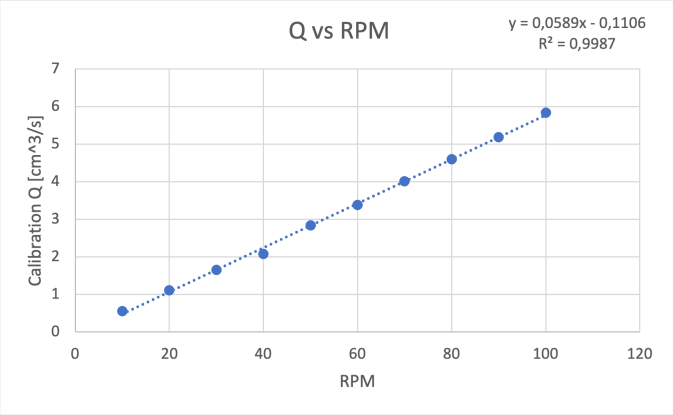

Figure 4.3: Calibration Q vs rpm, 500 ml, and defect Ohaus weight

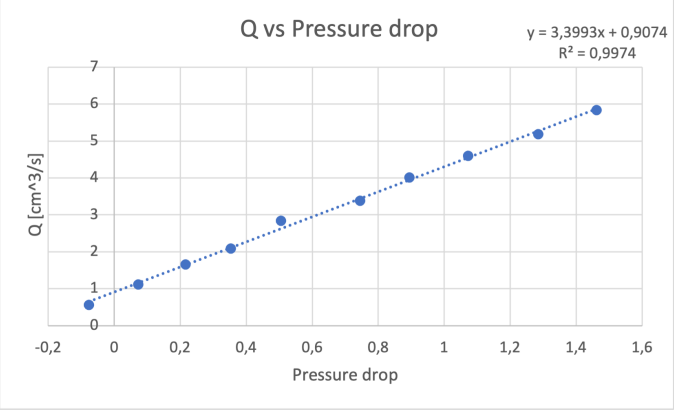

Figure 4.4: Calibration Q vs Pressure drop, 500 ml, and defect Ohaus weight

Figure 4.5 shows the result of Reynolds number vs flow rate. Reynolds number

is under 2000 for all points and this will correspond to laminar flow. The highest value is Reynolds number 1800 approximately and 5000 flow rate.

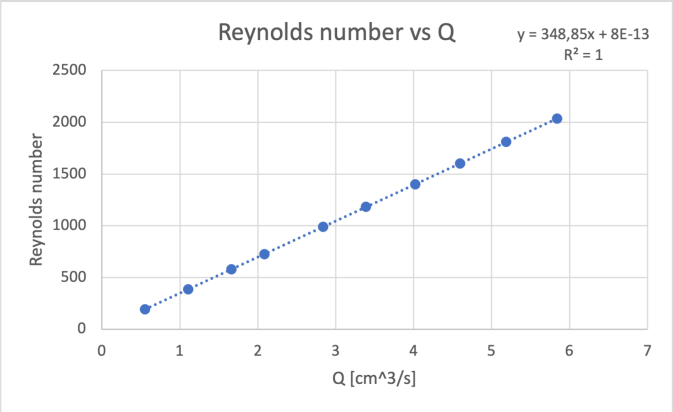

Figure 4.5: Calibration Q vs Reynolds number, 500ml, defect Ohaus weight

Test two : Water = 250 ml and weight under test section level

illustration are given in 3.5 b, in section 3.2.2 Tests are performed by measuring the time for 250 ml water to flow through the system, pump rotations, and rpm, which are increased for each measuring point. Starting the test, the peristaltic pump is set to 10 rpm, for every new measurement the rpm increases by 10 rpm. Tests are final at 100 rpm. Figure 4.6 shows the result from one of the three test runs, the rest of the tests are placed in Appendix B. Figure 4.6 has test run number three results. Subfigure 4.6a plots pump rpm on the x-axis and flow rate, Q, on Y-axis. The trendline aligns with the measured points in an almost perfect state, and the measuring points are almost a perfect straight increasing line. From subfigure 4.6b, Flow rate Q and pressure drop are shown. The pressure drop indicated on the graph is an average of the pressure drop measurements for one point. For the first measuring

point, where the pump is set to 10 rpm, the pressure increases and decreases with the time it takes for the water to fill the amount of water intended for the test. The pressure measures are taken and plotted as an average for each step of rpm and plotted with Q. Some of the measuring points in figure 4.6b don't align with the trendline, especially since the last point at Q=6 is off the trendline. When there are greater speeds on the peristaltic pump, the equipment tends to move, which can cause some irregularities whit regard to the pressure drop.

Figure 4.6c plots Q and Reynolds numbers; calculations are provided as an excel screen clipping in the appendix. Three points indicate laminar flow, where the value is under 2000 and has a blue color. From 2000 to 4000, there is a transition phase between the laminar and turbulent flow. Flow rate, Q, equals 4000, gives a Reynolds number equal to 4000, and the points with higher Q have turbulent flow. From the figure, all three stages of flow shown with Reynolds number are provided in the plot.

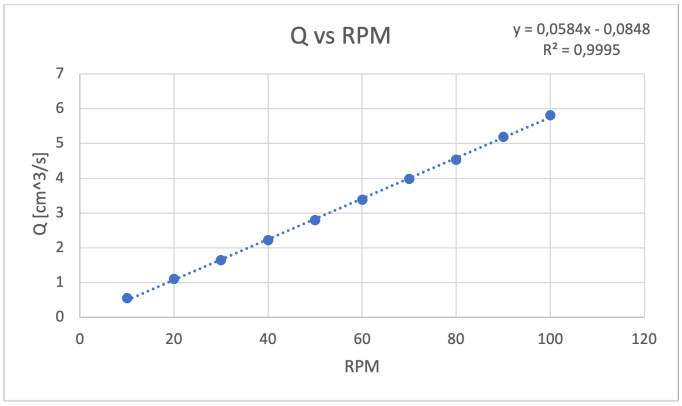

(a) fig:Q vs rpm - Test 2

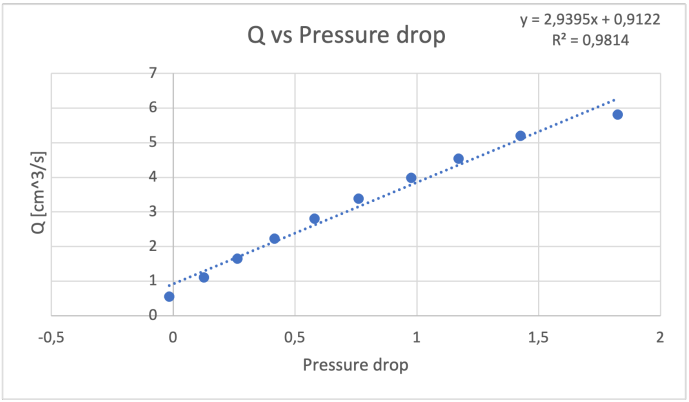

(b) Q vs Pressure drop - Test 2

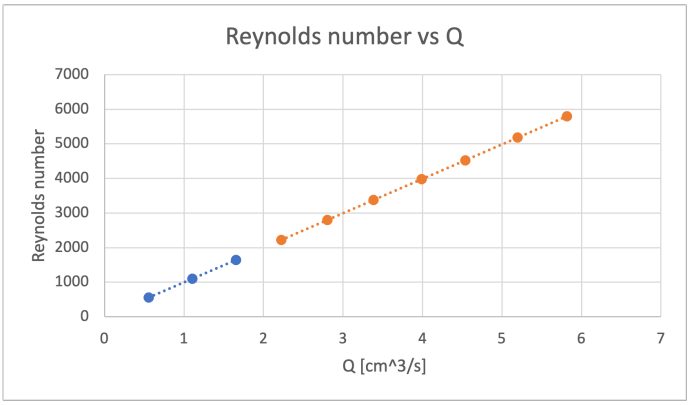

(c) Q vs Reynolds number - Test 2

Figure 4.6: Calibration under constant flow rate, Test two

Test three :Water = 250 ml and weight at test section level

In the third test, the tube and Ohaus weight are placed at the same height as the test section and the pump. An illustration of these tests is given in figure 3.5a, in section 3.2.2. The peristaltic pump rate is increased from 10-150 rpm. Thus, this will give more significant data for measuring points in the following graphs. The tests are performed three times and all results can be found in Appendix C. These tests are performed with the same procedure and should provide the same results. Figure 4.7 provides adequate information results regardless of test run number.

From figure 4.7a, plotting flow rate Q versus pump rate, the measurement results are linear when adding a trendline. This gives a 99% of linear regression constant. By comparing test three and figure 4.6a, both plots show the same tendency and have approximately the same flow for the corresponding pump rates. In figure 4.7b, is the flow rate, Q, and pressure drop plotted. Every single point are taken from an average of approximately 100 data points in figure 4.7b. A polynomial curve fitting was applied and gave a parabolic equation. The relationship between the measuring points and the trendline gave a linear regression of 98,59%. It could be seen that a difference in scales appears when comparing figures 4.6b and 4.7b. The flow rate has a maximum of 4,4 cm^3/s in figure 4.7 and 5.8 cm^3/s in figure 4.6. Thus, a change in the weight placement can be a determining factor for the pressure drop and flow rate curve outcome.

Figure 4.7c is a plot of flow rate, Q, versus Reynolds number. The plot indicates laminar flow for the first nine measuring points. The remaining points Shown in orange are in the transition phase. Figure 4.7c is not in the turbulent flow regime, as shown in plot 4.6. It has a higher flow rate.

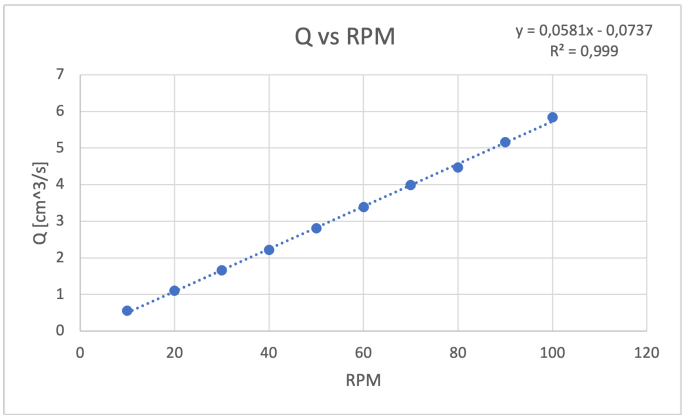

(a) Q vs rpm - Test 3

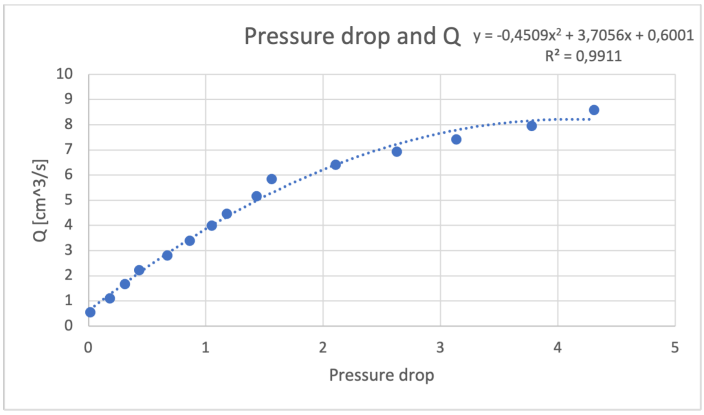

(b) Q vs Pressure drop - Test 3

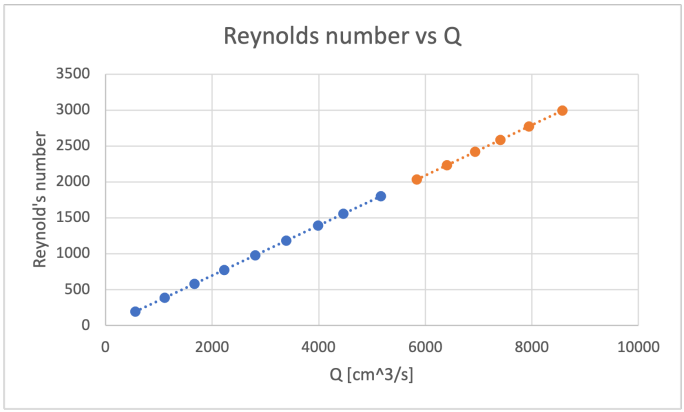

(c) Q vs Reynolds number - Test 3

Figure 4.7: Calibration under constant flow rate, Test three

Reynolds number vs. Flow rate, Q, are in subfigure 4.7c. Show a shift from laminar to transition phase when flow rate, Q, is over 5000 and Reynolds number is over 2000. Marked in the graph, the blue line indicates laminar flow and the Orange line indicates the transition phase to turbulent flow.

4.1.4 Calibration under constant pressure

Evaluation of tube diameter for the test section tube is provided in the following table 4.4. In each height,time was recorded for filling 1000ml of liquid. This will give the flow rate in table 4.4, from the equation 1000ml/time. According to the table, the flow rate versus height can be plotted and presented in figure 4.8.

The formula given from calibration results are

$$Q = 0,0589 * H + 5,4745 \tag{4.1}$$

$$Q = 1000/Time \tag{4.2}$$

The following table 4.4 is the result of the calibration under constant pressure.

Height [cm]	Time [sec]	Flow rate, Q [ml/s]	Ln ($\frac{175,5}{H}$)
175,5	63,9	15,65	0
163,5	65,75	12,21	0,0708
132,5	75,35	13,24	0,2810
104	84,45	11,84	0,5232
17,2	103,15	19,69	0,87444

Table 4.4: Table of measured weight for calibration during constant pressure

The corresponding graph is shown in figure 4.8. It can be seen when a linear

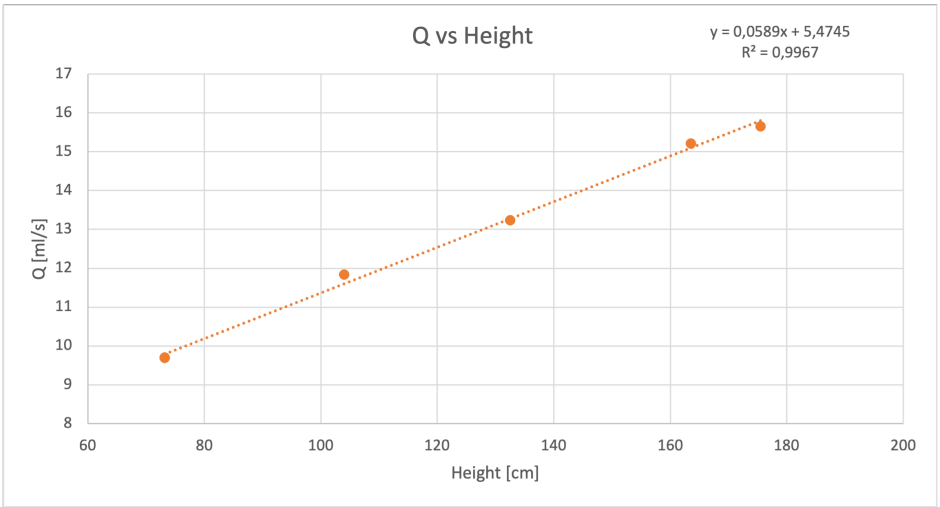

Figure 4.8: Q vs Height

trend between the data points is added, that the regression coefficient is 0,9967.

4.1.5 Calibration under variable pressure and flow rate

Data from table 4.4 were used in this test. The height of 175,5 cm was used as a reference height. By varying the heights as a function of time one can observe that the height and pressure are simultaneously decreasing. The results are given in the same table 4.4. Figure 4.9 shows $\ln(\frac{175,5}{H})$ versus time which is a plot of the results from this test.

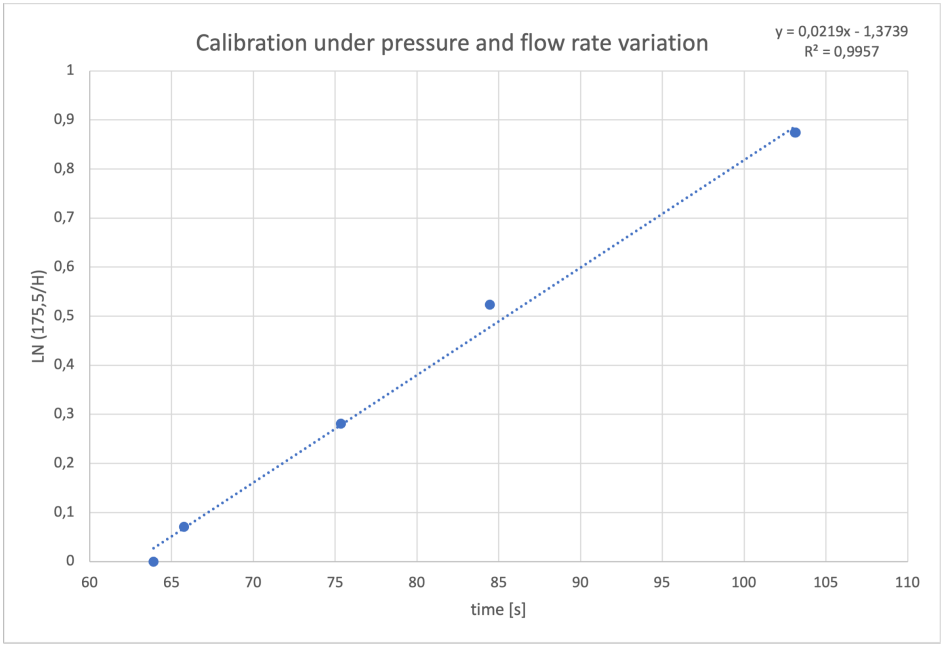

Figure 4.9: Logaritm vs time

4.2 Analysis of tests using water

Proceeding with tests, the formula from the calibration of the peristaltic pump is the basic equation to calculate the flow rate. Figure 4.7a provides the formula

$$Q = 0.0582 * rpm - 0.0738 \tag{4.3}$$

in this case, rpm corresponds to pump speed to evaluate flow rate. Equation 4.3 was used during all experiments.

4.2.1 Pressure drop Analysis

A preliminary measurement of pressure drop was taken at a sampling rate of 20 Hz. The sampling rate corresponds to the maximum sampling rate of Ohaus mass weight. As shown in figure 4.10, the result of the sampling rate, 20Hz, shows low sampling rates. Figure 4.10 and 4.11 were taken from the same pump rate (4 rpm) but, with different sampling rates which are 20 and 1000 Hz respectively. It should be mentioned that the graphs are differential pressure as a function of time. By looking at figures 4.10 and 4.11, there is a need to increase the sampling rate to the maximum allowable sampling rate for the pressure drop sensor which is 1 kHz. Figures 4.10 and 4.11 are equal on all points besides the sampling rate. The pump was set to 4 rpm which corresponds to 0,16 cm^3/s in flow rate. The trends for both lines are the same for the whole period, and graphs are made where the lines are easiest to evaluate.

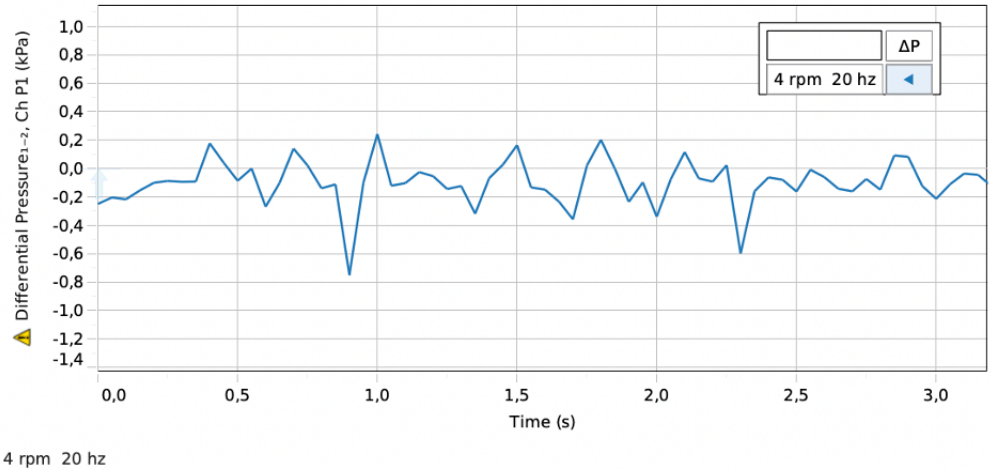

Figure 4.10: Flow rate = 0,16cm^3/s, 20 Hz sampling rate

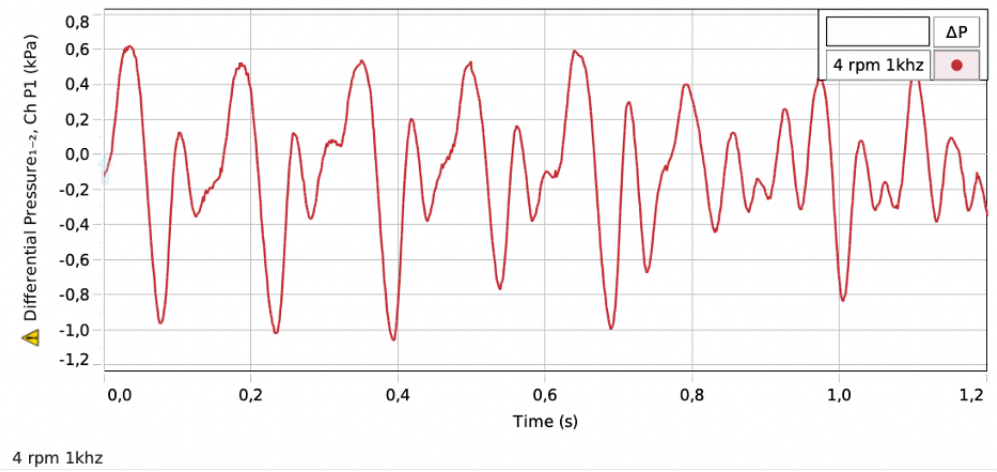

Figure 4.11: Flow rate = 0,16 cm^3/s, 1 kHz sampling rate

Figure 4.12 plots time and differential pressure when the peristaltic pump is pumping with 13 rpm, corresponding to 0,68 cm^3/s in flow rate. The visualized tendency in the plot can be from one of the three arms to the peristaltic pump. However, there is some difference in the signal shapes, and it can be estimated to be three different signals for the three arms in the pump. The estimated period can be from time 2,5 seconds to 4 seconds.

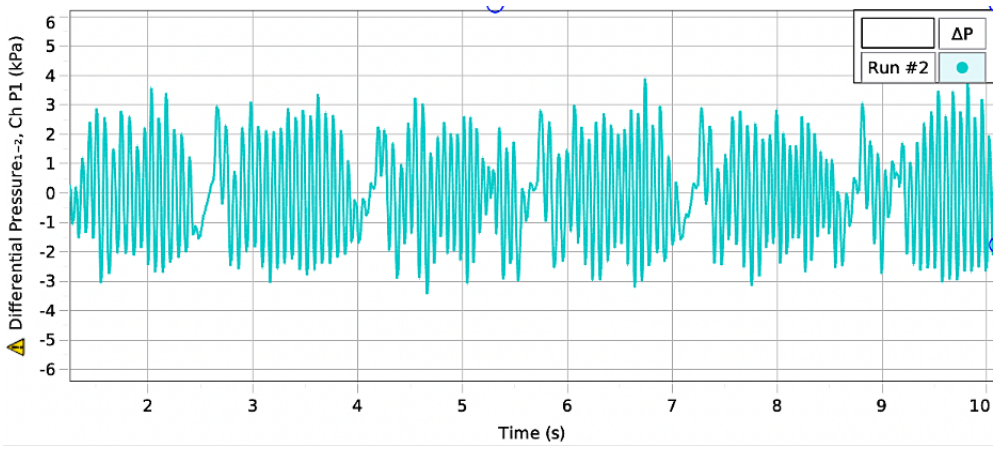

Figure 4.12: Sampling graph when flow rate =0,68 cm^3/s

Figure 4.13 plots the differential pressure versus time. The peristaltic pump is set to 81 rpm, providing a flow rate of 4,64 cm^3/s. It's noticeable that the fluctuations are more stable for a higher flow rate and show the same tendency as figure 4.12, regarding patterns of the three pump arms. The plot indicates a slightly increasing trend with a peak before a minimal pressure drop before growing again. After the third increase in pressure drop, the pressure will fall to the lowest point at approximately -11kPa. Before increasing to the same trend again, the maximum increase of differential pressure is 9kPa.

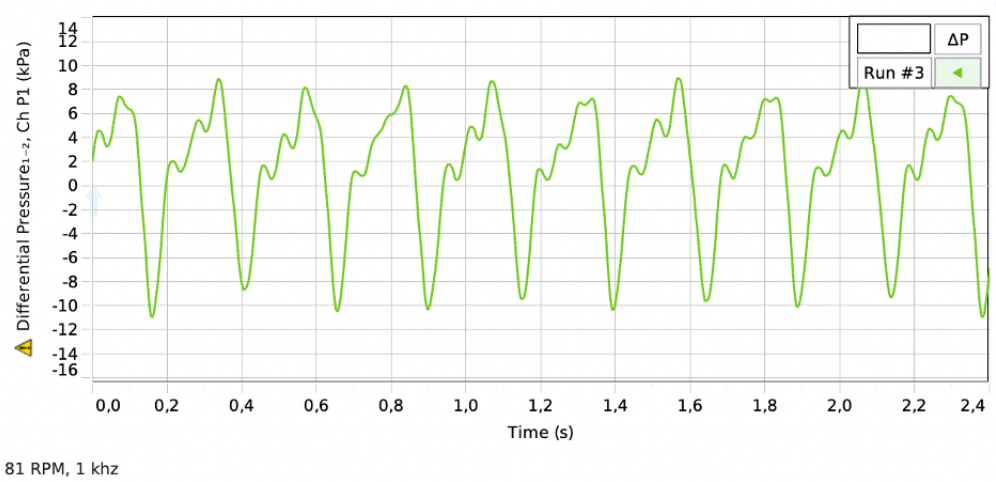

Figure 4.13: Sampling graph when flow rate =4,64 cm^3/s

Figure 4.14 has a higher rpm rate and is tested with 125 rpm providing a flow rate of 7,20 cm^3/s. Comparing figures 4.14 and 4.13, 4.12, differential pressure is clearly different when increasing pump speed. Figure 4.14 has the highest differential pressure and varies from 13 kPa to -12 kPa. More stability in differential pressure are visualized for higher flow rates. For flow rate 7,20 cm^3/s the pressure increases twice before decreasing to -12 kPa. Differential pressure of 13 kPa is reached multiple times and, from this point, drops to 4 kPa and -12 kPa every second time.

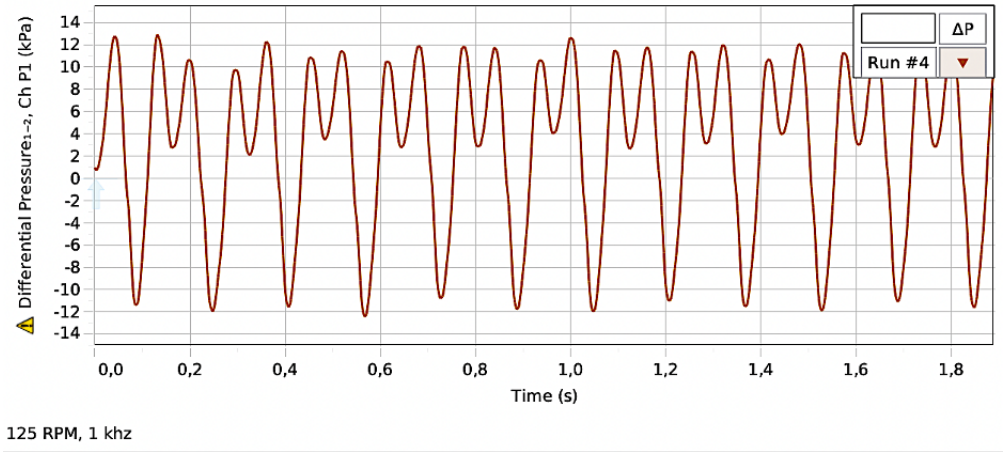

Figure 4.14: Sampling graph when flow rate =7,20 cm^3/s

4.2.2 FFT test

FFT tests show the unsteadiness of pressure reading in a frequency domain. Figures 4.15 and 4.16 have the same flow rate of 0,16 cm^3/s. Differences in the plot are the sampling rate. It is visualized a change from figure 4.15 with a sampling rate of 20 Hz and figures 4.16 with a sampling rate of 1 kHz. There is more unsteadiness for figure 4.15 with a lower sampling rate. There are many tops, and every top indicates an unsteady measurement. Figure 4.16 are more stable than figure 4.15, however, have many tops of frequency. The highest point for figure 4.15 is 6.387 Hz, and figure 4.16 has the highest top at a value of 4.883 Hz. The figures have the same tendency, although there is a lower frequency when the sampling rate is higher.

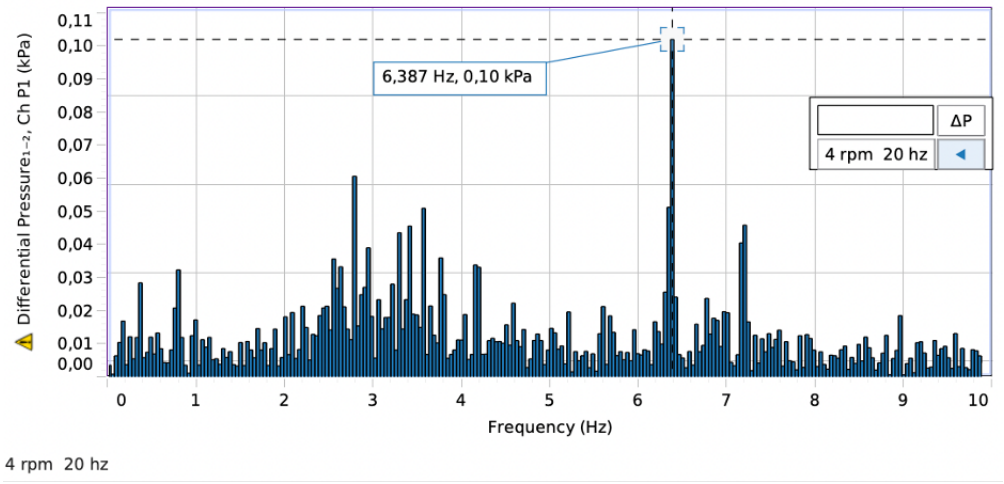

Figure 4.15: flow rate of 0,16 cm^3/s , FFT , 20 Hz sampling rate

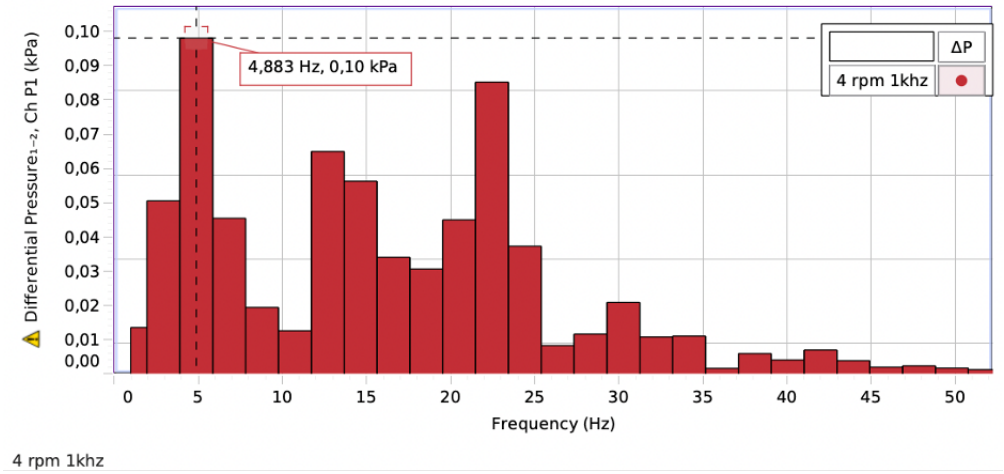

Figure 4.16: flow rate of 0,16 cm^3/s, FFT ,1 kHz sampling rate

Figure 4.17 plots the differential pressure and frequency domain for a flow rate equal to 0,68 cm^3/s. The frequency domain shows the highest top at 12.695 Hz. The flow rate of 0,68 cm^3/s gives the highest overall frequency domain compared to figure 4.15,4.16,4.18,4.19. Uncertainty is connected to the reasoning for a higher frequency domain for a flow rate of 0,68 cm^3/s. As the equipment used in differential pressure

analysis is susceptible to external noise it can affect the test. Thus, causing the high Hz.

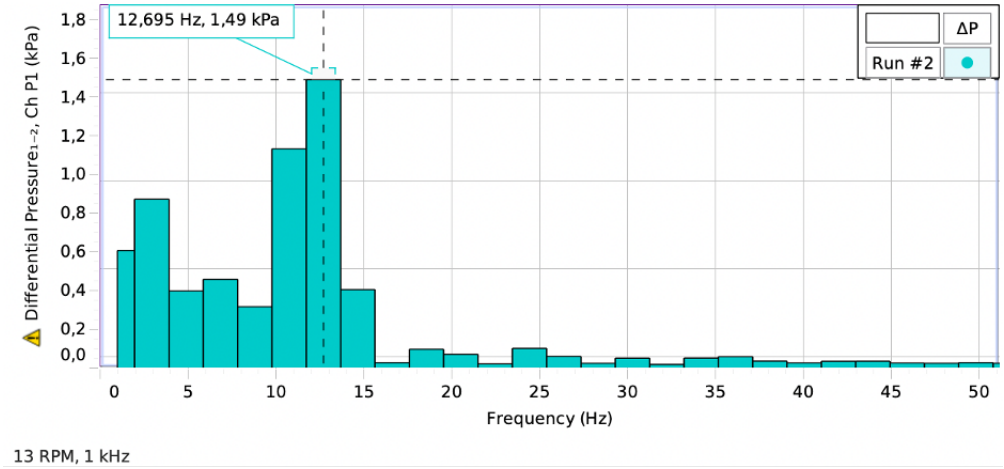

Figure 4.17: flow rate = 0,68 cm^3/s

Figure 4.18 plots the differential pressure and frequency domain for a flow rate equal to 4,64 cm^3/s. The highest frequency domain is 2.93 Hz when the differential pressure is 6,08 kPa.

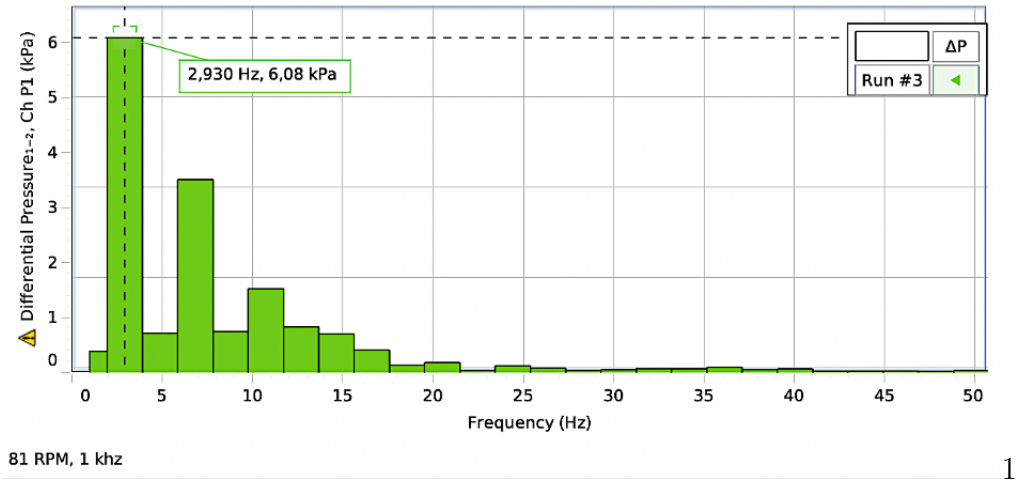

Figure 4.18: flow rate = 4,64 cm^3/s

Figure 4.19 plots the differential pressure and frequency domain for a flow rate equal to 7,20 cm^3/s. The highest frequency domain is 4,883 Hz when the differential pressure is 7,27 kPa.

All figures compared, figure 4.16 4.15,4.17,4.18 and 4.19. The highest frequency domain is for the figure 4.15, and the differential pressure increases with increased peristaltic pump rpm.

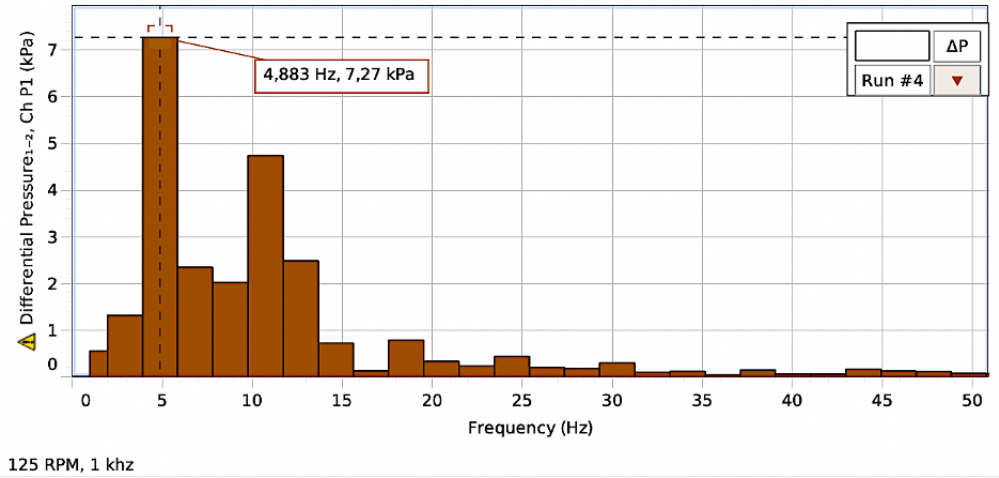

Figure 4.19: flow rate = 7,20 cm^3/s

4.3 Rigid vs Elastic pipe

This section evaluates the pressure drop difference when changing tubes around the test section, from the test section to the pressure sensor and at the exit of the test tube. There are five tests with elastic tubes and five tests with rigid tubes. Tests with the same rpm on the pump are plotted in the same plot. rpm refers to the rounds per minute the pump rotates, and the tree arms make the pattern shown in the plot. Pump speed rotations are 20 rpm, 80 rpm,140 rpm,200 rpm, and 260 rpm, correspondingly giving a flow rate of 1,09 cm^3/s , 4,58cm^3/s, 8,07cm^3/s, 11,57cm^3/s and 15,06cm^3/s.

Figure 4.20 has a purple indicator for the result using flexible pipes. From evaluating the scope, the plot area of differential pressure and time shows similarities for elastic and rigid pipes. However, the signal shifts according to time and some differences in pattern. One of the reasons might be that the three pump arms are recorded at different times. Differential pressure is approximately the same for both pipes when estimating the highest and lowest point of pressure.

Figure 4.21 has black colour for Elastic pipe differential pressure and blue for rigid pipe, the pump is set at 80 rpm giving a flow rate of 4,58cm^3/s. The two graphs are almost overlapping, however, the rigid tube has the lowest value in pressure drop, approximately -12 kPa, while the elastic pressure drop is a minimum at -10kPa.

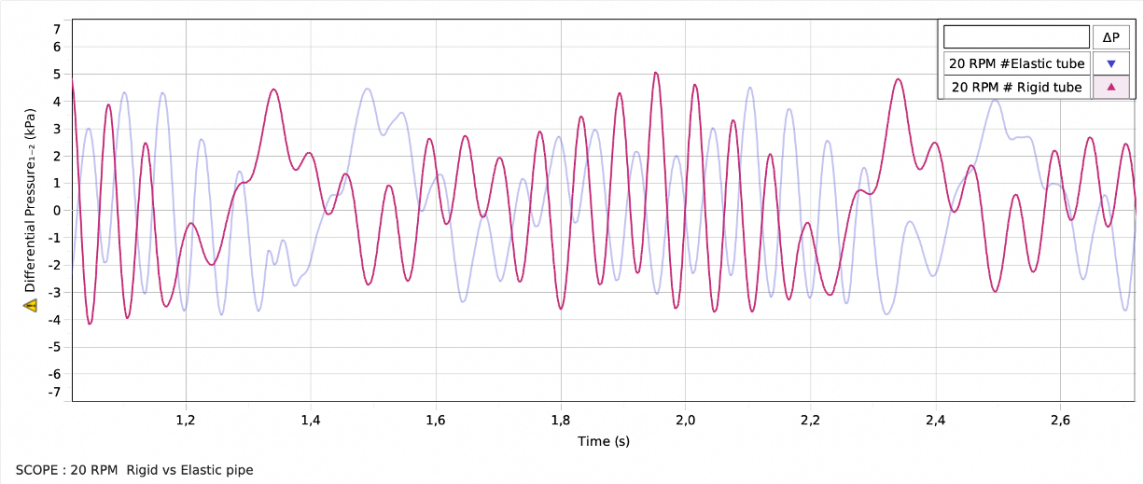

Figure 4.20: 20 rpm and flow rate = 1,09 cm^3/s, elastic vs rigid tube

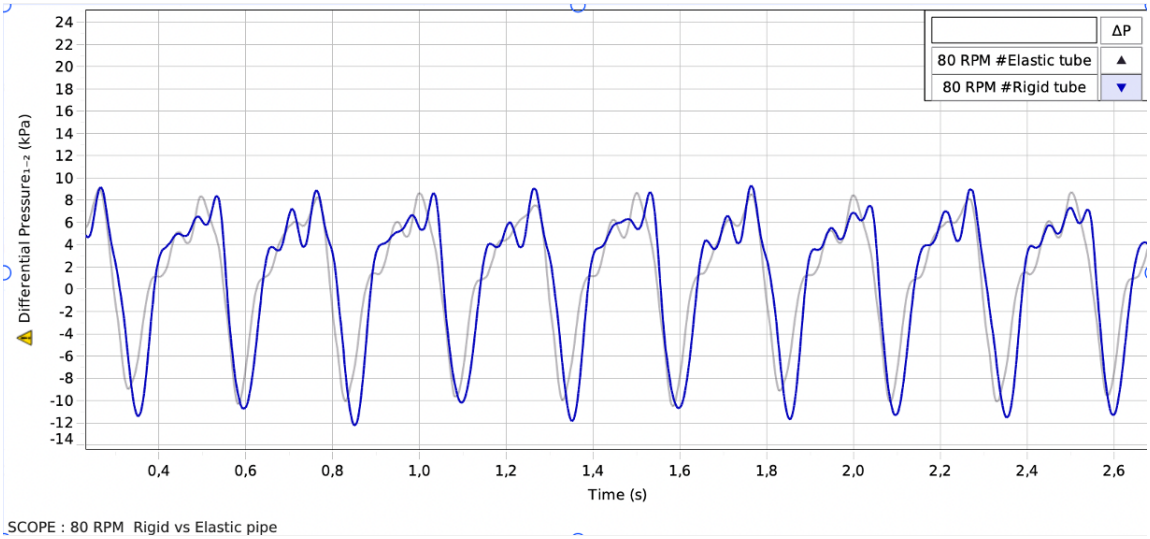

Figure 4.21: 80 rpm, flow rate =4,58cm^3/s, elastic vs rigid tube

Figure 4.22 indicates the elastic tube with purple color and rigid pipe with red color. The pump is set to 140 rpm giving a flow rate of 8,07cm^3/s, and the differential pressure increases from the previous figure 4.21. The stern tube has a differential pressure from 20 kPa to -20kPa. On the other hand, the elastic pipe has differen-

tial pressure values from 15kPa to -13KkPa. Therefore, concluding the differential pressure is greater for the rigid tube. The graph pattern is approximately the same for both tubes, where the tendency is a significant increase, followed by a tiny drop with about 10 kPa for the rigid tube and 5kPa for the elastic pipe. After the decrease in differential pressure, the value increases to the highest achieved value before decreasing to the minimum differential pressure.

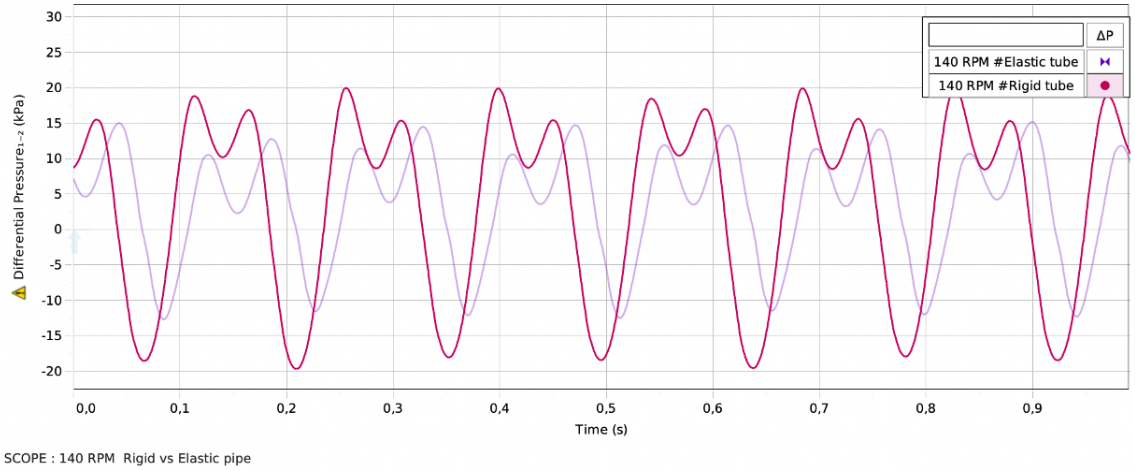

Figure 4.22: 140 rpm, flow rate =8,07cm^3/s, elastic vs rigid tube

Figure 4.23 shows the differential pressure drop and time for flow when the pump is set to rotate with 200 rpm giving a flow rate of 11,57cm^3/s. The elastic pipe is shown with green color, and the rigid pipe is shown as red. The rigid pipe gives a higher differential pressure and is in the value range between 24 kPa and -10 kPa. The differential pressure for the elastic pipe is between 15kPa and -4kPa. Patterns for the rigid tube have less noise and are close to a sinusoidal wave. Elastic curves have minor irregularities for the first decrease after reaching the highest differential pressure value.

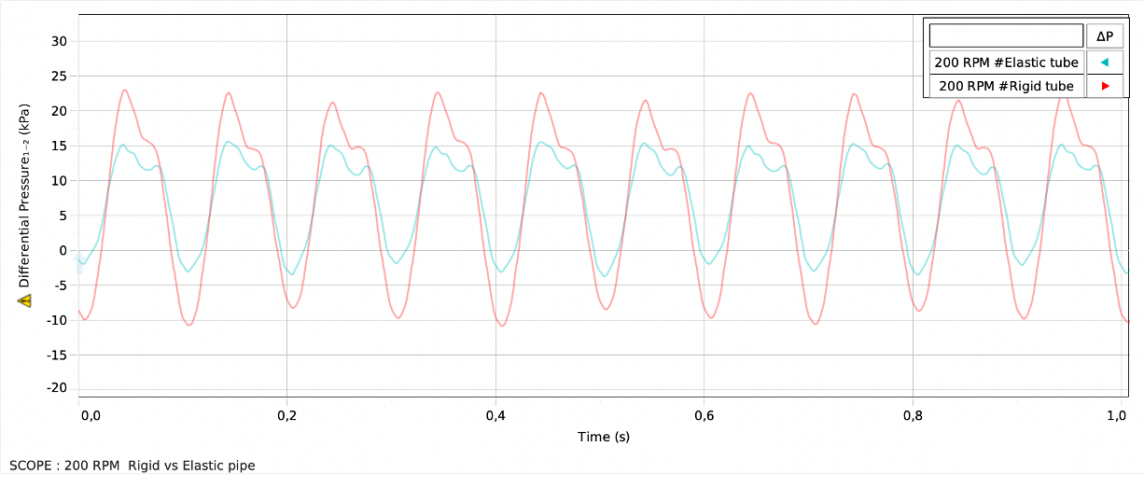

Figure 4.23: 200 rpm, flow rate =11,57cm^3/s, elastic vs rigid tube

Figure 4.24 shows the differential pressure drop and time for flow when the pump is set to rotate with 260 rpm giving a flow rate equal to 15,06cm^3/s. The elastic pipe is shown with green color, and the rigid tube is shown as red. The rigid tube's differential pressure is higher than the elastic tube. The rigid tube has differential pressure values between a maximum of 40 kPa, an average of 35kPa as the average highest point, and a minimum differential pressure of -15kPa. The elastic tube ranges from 30kPa to -10kPa. There is minor noise in the graphs, and curves for rigid and elastic tubes have the same pattern. The curve shows similarities to a sinusoidal wave and is increasing and decreasing in the differential pressure range whit no small drops in between.

Comparing all figures reveals higher differential pressure values for the rigid tube graphs for all pump rotations greater than 80 rpm and flow higher than 4,58 cm^3/s. The plot scopes give similar plots for rigid and elastic tubes, but with a shift with regard to time on some of the figures.

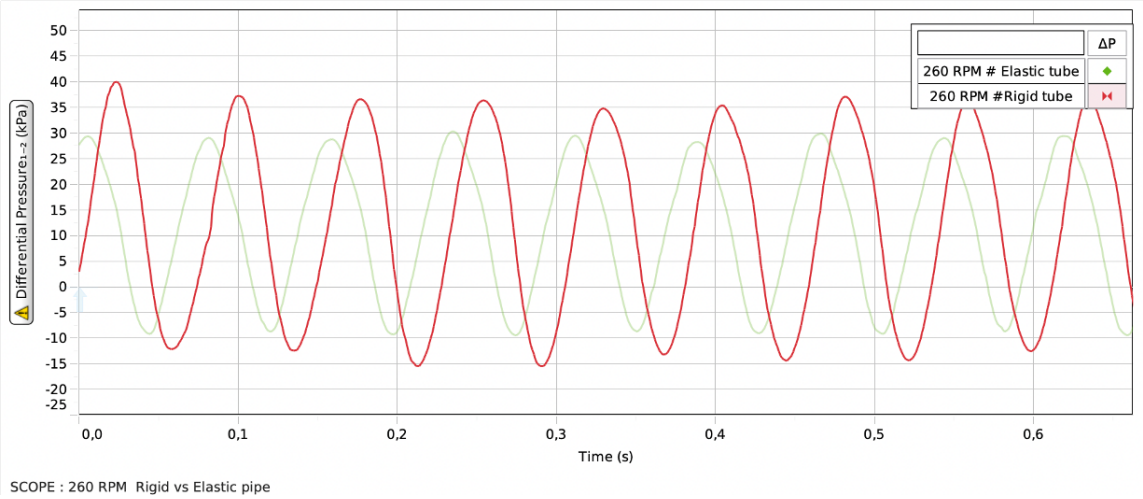

Figure 4.24: 260 rpm, flow rate = 15,06cm^3/s, elastic vs rigid tube

There might be a difference in the time the three arms are operating. Thus, making a shift regarding the time in the pressure drop analysis. The differential pressure sensor is placed differently for the elastic tube and rigid tube tests. To ensure the elastic is not to be contracted or extracted, the DP sensor is placed higher than the test section at a height where the tubes hang freely. For the rigid tubes, there is no consideration for elongations and contractions, and the DP sensor is placed in the center of the test section and at the same height, contributing to a triangle shape.

Pressure drops are in the main scope of the thesis and proceeding to tests with PAC-treated water, rigid tubes will be used.

4.4 Polymer results

4.4.1 Amplitude and hysteresis test

The amplitude sweep test is taken before and after a PASCO oscillating test. The reasoning is to evaluate if the flooding through the rigid tubes in the oscillating test will impact the fluid properties. Amplitude sweep tests are performed for two batches, one batch with water treated with 5g PAC and the other with 10 g PAC. This will be 1% PAC and 2% PAC, respectively.

Rheological tests for water with 1 % PAC are performed two times. The test is performed two times as the time for starting up the test and as the amplitude sweep test was performed after a viscoelastic test. The viscoelastic test could impact the test results, and a new batch was made to ensure a quality test and to perform the test again for different concentrations of PAC.

Figure 4.25 displays the curves of Storage and loss modulus plotted with shear stress. Marked in the test with blue and black are the same batch. The sample is plotted two times in the graph as the sample where tested two times. The black and blue curves are taken after the viscoelastic and PASCO oscillating test. Colored green is a sample with water and 5g PAC that have been still for 24h and are not endured in any other test before the amplitude sweep test. There are fluctuation in the start for the three lines for values below shear stress values of 0,0001 Pa. for blue and black lines, storage modulus and loss modulus have a crossing point at approximately 0,004 Pa. this indicates the fluid have viscoelastic properties. For green line there is no crossing and the fluid will be liquid.

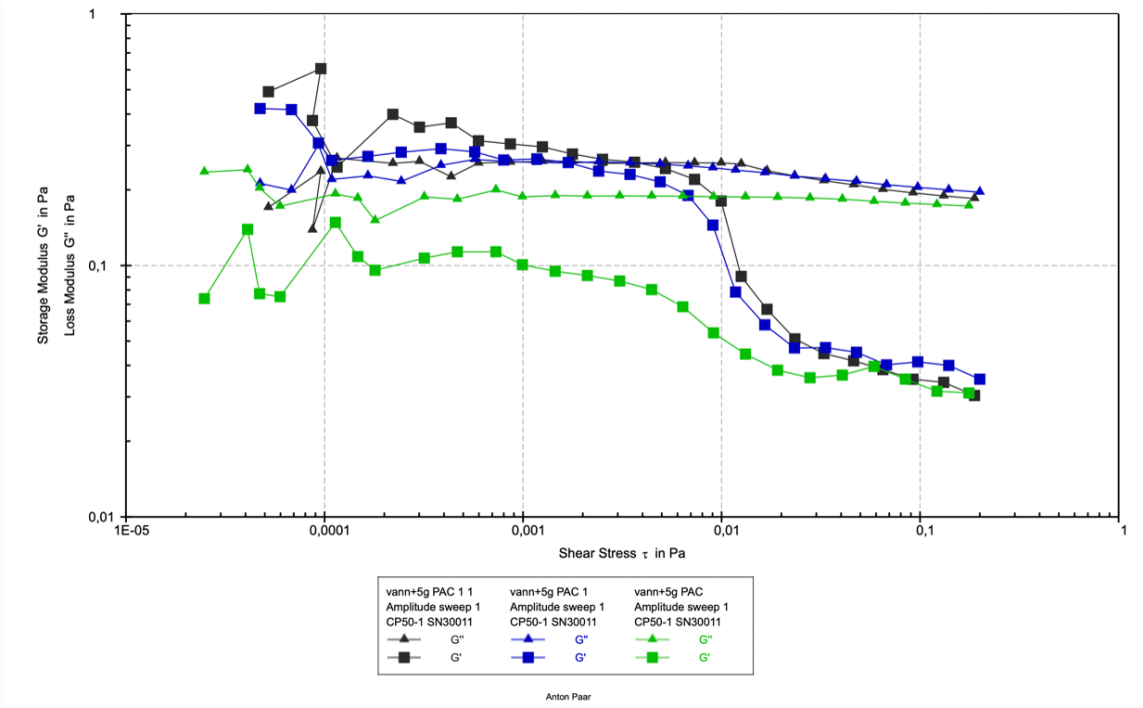

Figure 4.25: Anton Paar first test

Figure 4.26 Shows 5g(1%) PAC treated water. Before performing the PASCO Oscillating test plotted lines are shown in black and after the test are shown with the color red.

From the start of graph, there are unstable fluctuations. The red graph has a plateau from 0.001 to approximately 0.004 shear stress. From 0.004 shear stress the red graph has a crossing point between G' and G", after the crossing, G" smooths out and decays towards the value 0.05 storage modulus.

The G' curve drops for value 0.004 and to 0.01 before the structure smooths out. The drops indicate gradual breakdown of the structure for the given amount of shear stress applied. G" describes the amount of deformation energy lost during shearing, energy is lost due to internal friction. G' indicates the gel strength of the sample in

the LVE region.

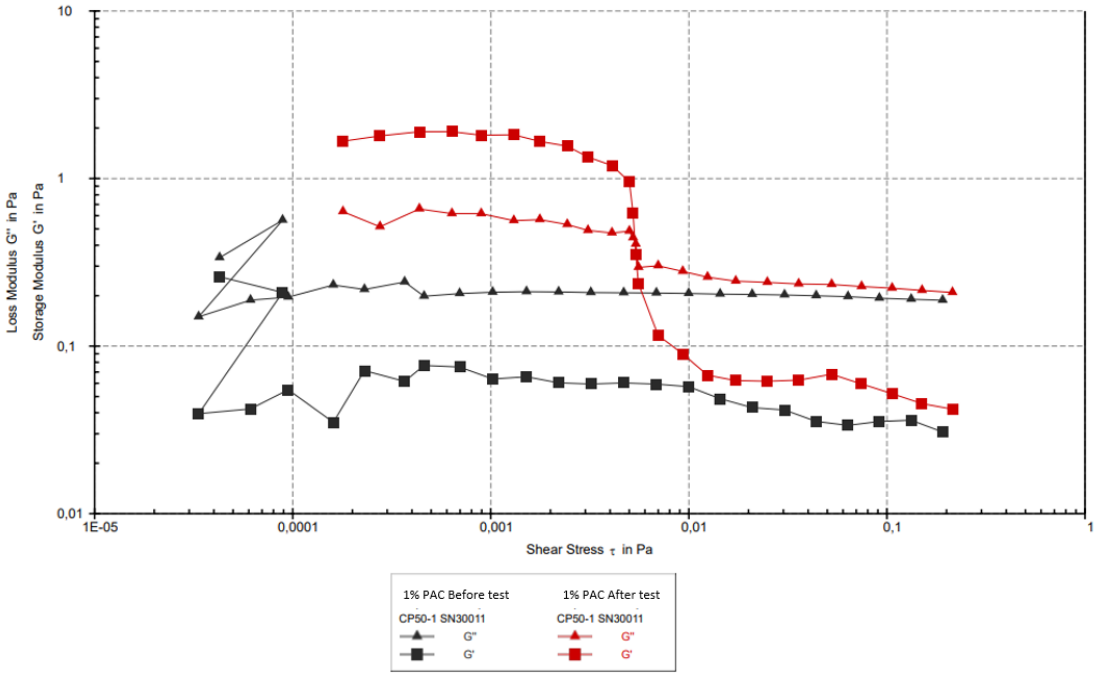

Figure 4.26: Amplitude sweep test, Before and after PASCO Oscillation test, 5g PAC (1%)

Figure 4.27 show 2% PAC treated water. Indicated on the graph are red lines for the test after the sample has flown through PASCO oscillatory test section tube. Before flowing through the oscillatory test section, the sample is marked with a black indicator. The results are different from what is predicted. The results indicate no viscoelastic behavior. Comparing the results of figure 4.26 and 4.27, the prediction would be to have viscoelastic behavior as there is a higher concentration of PAC in the sample. There can be an error with conducting the test, and the test section can be too short whit respect to shear stress.

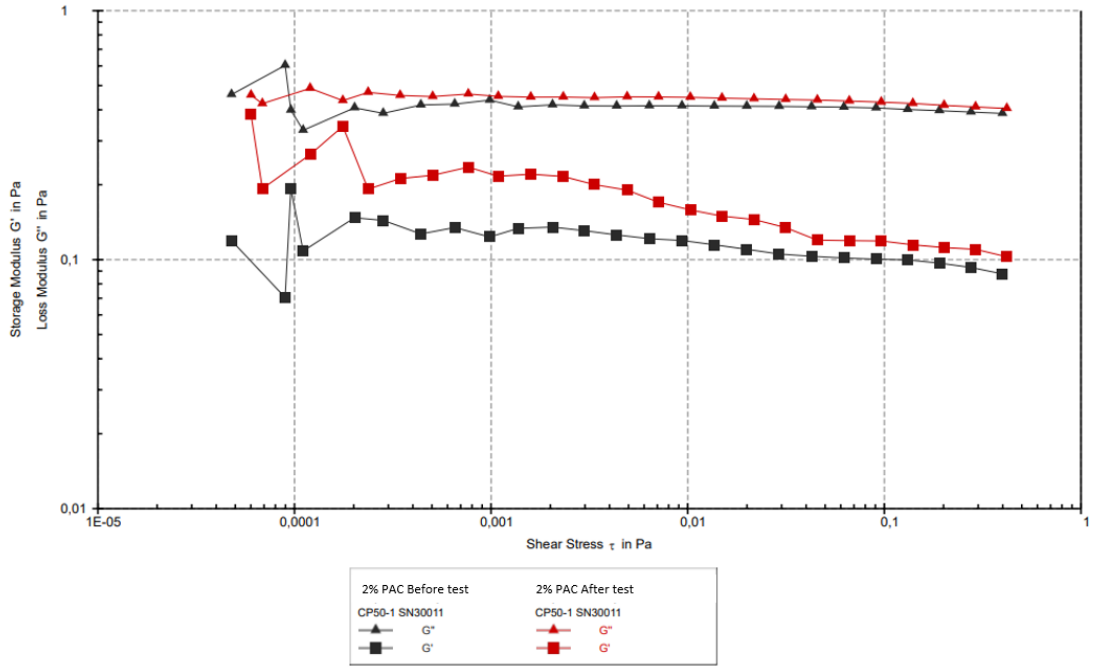

Figure 4.27: Amplitude sweep test, Before and after PASCO Oscillation test, 10g PAC (2%)

4.4.2 Hysteresis results

Hysteresis results are plotted for 1%, and 2% PAC treated water.

Figure 4.28 plotted shear stress and shear rate for 1% PAC treated water before the solution has flown through PASCO oscillatory test. The graph shows hysteresis and is seen from a lowered graph when the test goes from 130 γ^* and is reduced to 5 γ^*. The Red line makes the increasing values of the shear rate, and the grey line shows when decreasing shear stress. Hysteresis result gives Viscosity for the first point when the shear rate is 5 γ^*, equal to 25,33 $mPa * s$. The Viscosity for the last point is 13,75 $mPa * s$. The hysteresis area is A=4,4881 Pa/s.

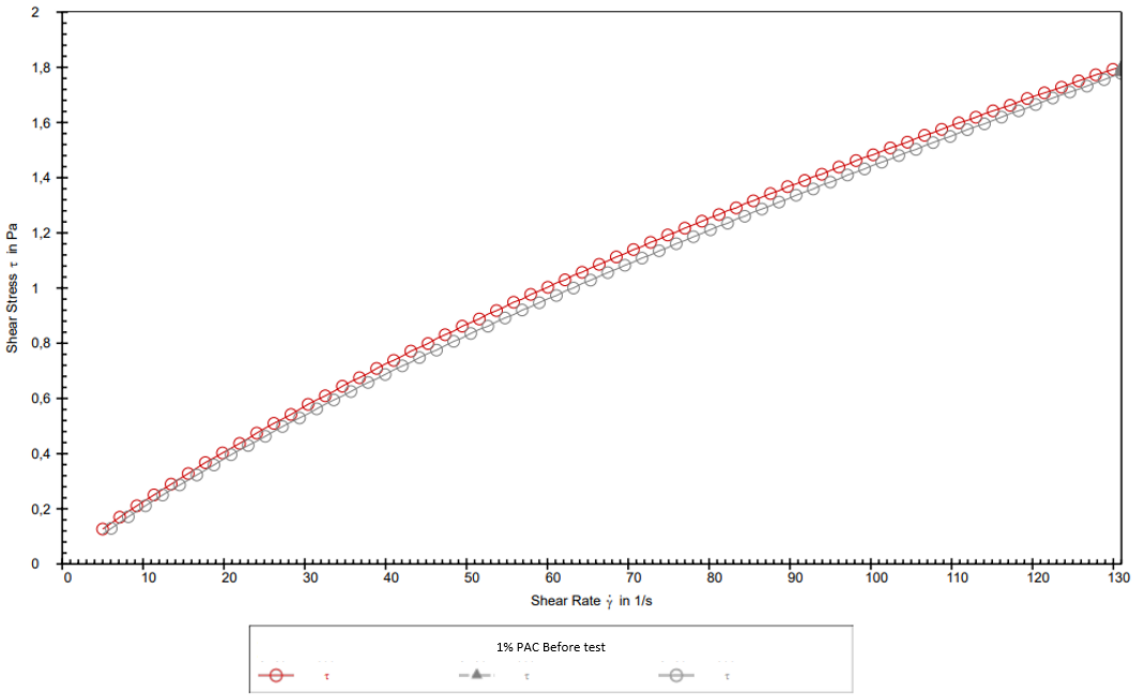

Figure 4.28: Hysteresis , 5g PAC (1%) Before test

Figure 4.29 plotted shear stress and shear rate for 1% PAC treated water after

the solution has flown through PASCO oscillatory test. Increasing and decreasing shear rates are plotted with a black indicator. The top line increases shear stress, and the lower line reduces shear stress. Figure 4.28 and 4.29 have the same viscosity and hysteresis values.

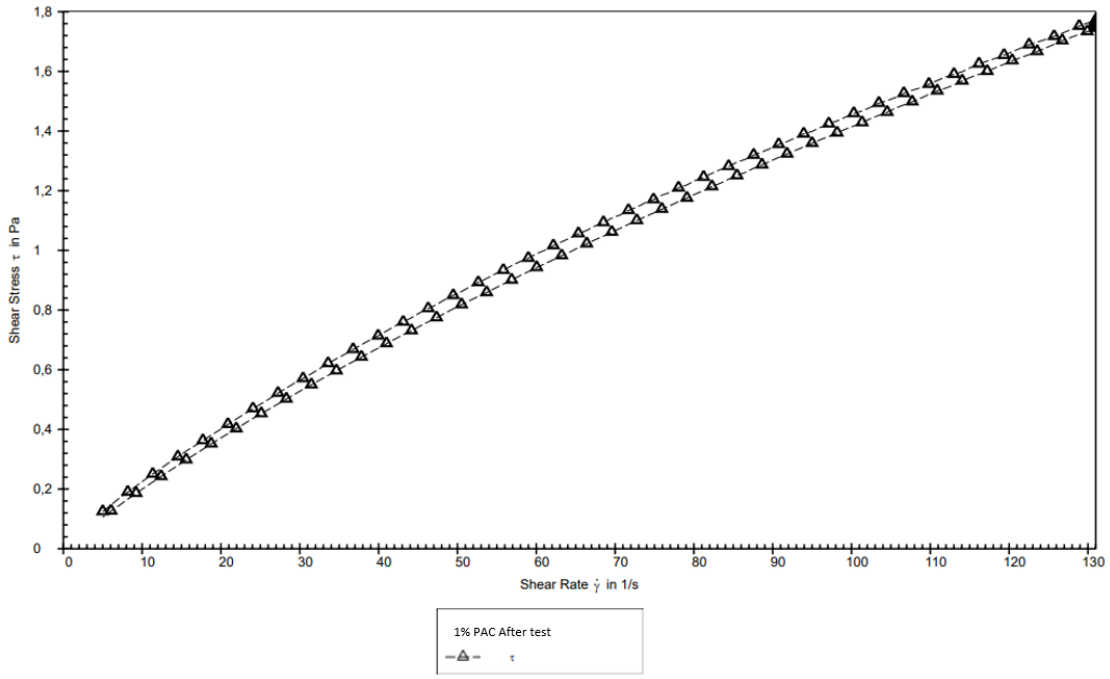

Figure 4.29: Hysteresis , 5g PAC (1%) After test

Figure 4.30, is a graph of hysteresis for 2% PAC treated water before flowing through the test section of PASCO oscillatory test tubes. Increasing share rates are indicated with a blue line, and decreasing shear rates are plotted with a black line. There is a hysteresis tendency between the sample as the lines don't overlap.

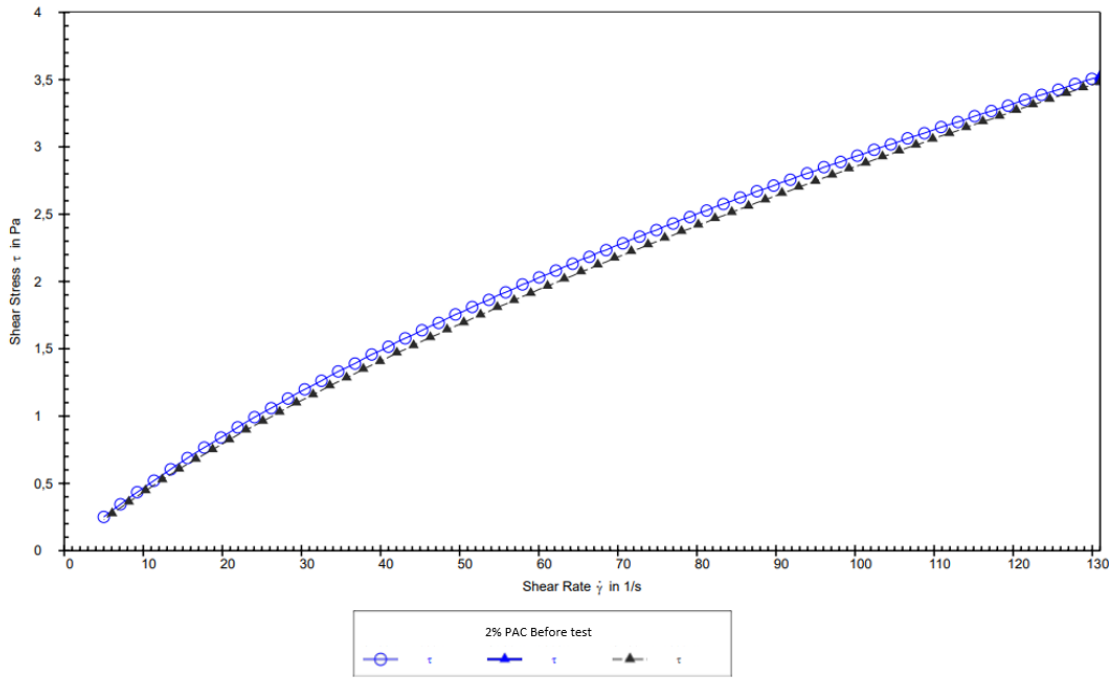

Figure 4.30: Hysteresis , 10g PAC (2%) Before test

Figure 4.31 are performed after PASCO oscillating test and have an overlying line for increasing shear rate values and a lower line for decreasing shear rate. Plotted are 2% PAC treated water and have a viscosity at the first and last points are respectively 50,1 mPa*S and 26,9 mPA*S. The hysteresis area is given as A= 8,8909 Pa/s.

There is hysteresis for PAC-treated water both before and after PASCO oscillatory test, and no noticeable difference between hysteresis for the before and after flow through the oscillatory test section. However, the hysteresis area is increasing by 98,10 % from 1% PAC treatment to 2% PAC treatment. The trend shows the amount of PAC in water affects the hysteresis area of samples.

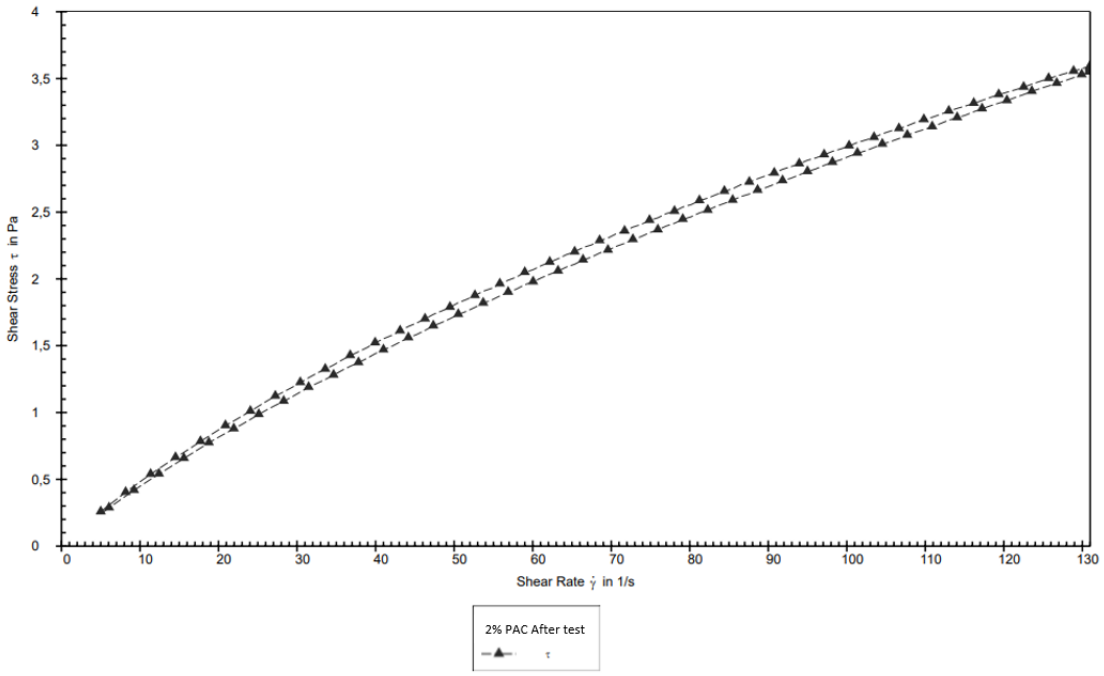

Figure 4.31: Hysteresis , 10g PAC (2%) After test

Viscosity for the first point has increased by 97,79 % from 1% PAC treatment to 2% PAC treatment.

4.4.3 PASCO Oscillating test,scope, water+1 percent and 2 percent PAC

Figure 4.32 shows the pressure drop time series for water (pink), 5g PAC (Green), and 10g PAC (purple). Differential pressure is, on average, at higher values for PAC-treated water, and there is an increase when an increasing amount of PAC. 2% PAC treated water ranges from a differential pressure between the highest value of 14 kPa and the lowest value of -3 kPa. The signal is between 4 kPa and to 12kPa, and between the bulk signals, the differential pressure drops to -3kPa. Pump arm rotations can cause the effect. Figure scope 20 rpm has a flow rate of 1,09 cm^3/s. It is much noise in the plot, and the trend of noisy results is shown for all graphs in the thesis when the flow rate is 1,09 cm^3/s. Overall curvature outcomes are the same, with a shift concerning the pressure drop and, to some extent, time. The pink graph corresponding to water has lower differential pressure and ranges between 4 kPa to -4 kPa. 1% PAC treated water is in the differential pressure range of 6 kPa to -1kPa.

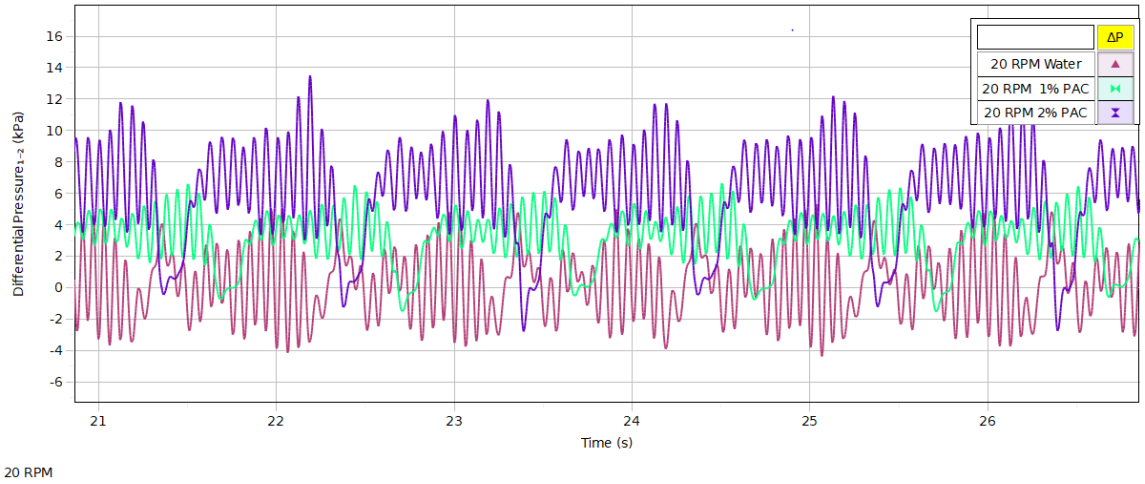

Figure 4.32: scope, 20 rpm , water , (1%) and (2%) PAC

From the figure 4.33 differential pressure and time for flow rate equal to 4,58 cm^3/s is plotted. The pressure drop for water is lower than the pressure drop for 2% PAC. Water is plotted with a blue indicator with differential pressure variations between 9 kPa and -10 kPa. 1% PAC treated water indicated with pink color has differential pressure values between 15kPa and -5kPa. The visualization graph of water and 1% PAC have the same tendencies and three drops at around the highest differential pressure values before decreasing to the lowest range value. 2% PAC treated water has greater ranges of differential pressure and ranges from 30kPa to -23kPa. Visualized in the graph is one significant increase from the lowest differential point before reaching the top point. After that, the graph dropped and increased two times before reaching the lowest differential pressure. For flowrate 4,58 cm^3/s, there is a more significant difference both in differential pressure and visualization between 2% PAC treatment and water.

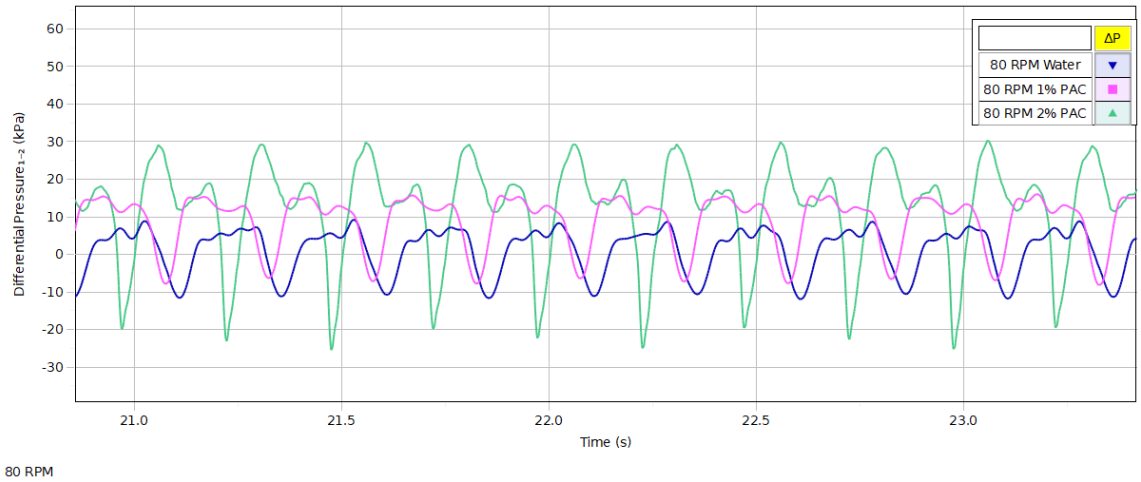

Figure 4.33: scope, 80 rpm , water , (1%) and (2%) PAC

Figure 4.34 have flow rate equal to 8,07 cm^3/s when using a pump speed of 140 rpm. Water is shown with purple color, 1% PAC treated water is in orange color, and 2% PAC treated water has a blue color. Water has fewer differential pressure variations, ranging from 20 kPa to -20kPa. 1% PAC goes from 30kPa to -12 kPa, and 2% PAC treated water from 45 kPa to -22 kPa. All three graphs have the same visual outlook and differ in differential pressure values. The graphs increase from the lowest differential pressure to the maximum value, with a tiny drop before a new increase occurs. From the second increase, the differential pressure drops to the lowest values. This tendency is seen for all three graphs. Differential pressure variations are highest for 2% PAC treated water, and a trend for more significant differential pressure variation and higher values are seen for all flow rates.

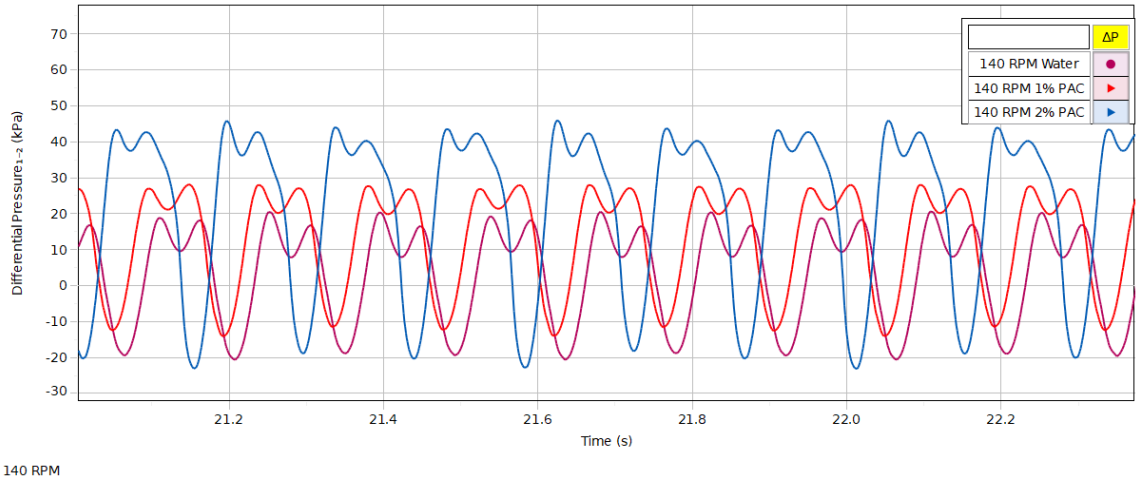

Figure 4.34: scope, 140 rpm , water , (1%) and (2%) PAC

Figure 4.35, shows the impact of PAC treated water and distillate water with a flow rate of 11.5562 cm^3/s.Differential pressure variates from 20kPa to -10kPa, 39kPa to -10kPa, and 62 kPa to -30kPa for water, 1% PAC, and 2% PAC, respectively. The differential pressure increase in variation when increasing PAC concentration. 2% PAC treatment shows a more steady graphing with the same tendency for flow rate,8,07 m^2/s. The water graph has one increase and a minor bump before decreasing to the lower range of differential pressure for flowrate 11,57 cm^3/s, thus, smoothing out the last bump that can be seen for water with 8,07 cm^3/s flow rate. Increasing the flow rate provides a more significant differential pressure for all samples.

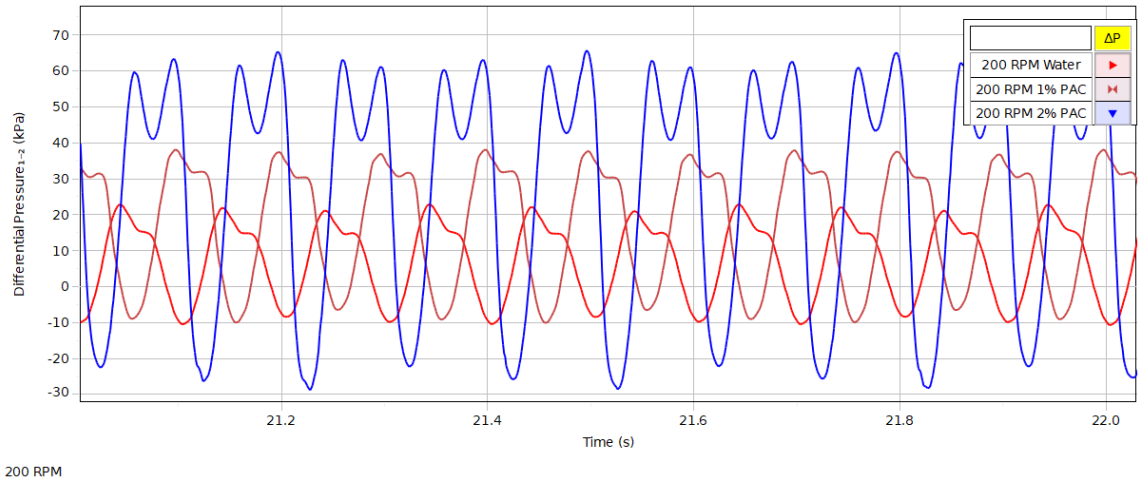

Figure 4.35: scope, 200 rpm , water , (1%) and (2%) PAC

Figure 4.36 have a flow rate of 15,06 cm^3/s, water is plotted with a red indicator, 1% PAC with a blue indicator, and 2%PAC with a green indicator. Differential pressure varies from 40 kPa to -19 kPa, 150kPa to -59 kPa, and 99kPa to -30kPa for water, 1% PAC, and 2% PAC, respectively. The tendency for the graph has a shift for the flow rate of 15.0582 cm^3/s. For this flow rate, the sample with considerable differential pressure variation is for 1% PAC treated sample. 1% PAC sample varies between the highest and lowest differential pressure with no drop in between. The graph shows the differential pressure values are some seconds longer at the bottom of the value scale compared to the higher value. 2% PAC treated sample increases and has a slight decrease and growth between the highest and lowest differential pressure value. The water graph shows the same trend as the 1% PAC sample, on the other hand, with a much lower range concerning differential pressure.

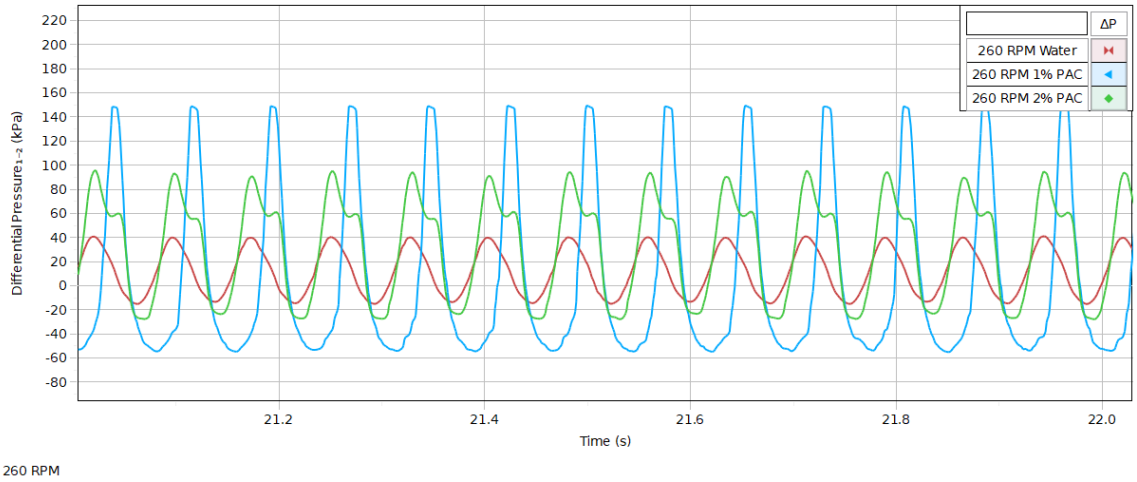

Figure 4.36: scope, 260 rpm , water , (1%) and (2%) PAC

The higher flow rate provides more apparent graphs and eases the stability in the pressure fluctuations for the inlet and outlet of the test section.

Evaluating the time for one period for water, 1% PAC, and 2% PAC to establish if the period is different with higher concentrations of PAC. In figure 4.36, water has a period of 20,985s and a differential pressure of -14.81kPa. The next differential pressure low point is at time 21,063s and -15,27kPa. For 1% PAC, one phase can be between 21,155s at -54,05kPa and 21,236s at -53,20kPa. 2% PAC have a phase between 21,144s at -23,65kPa and 21,223s at -27,23kPa. Evaluating the differences in time for the three phases, the water have a total phase of 0,078s, 1% PAC uses 0,081s, and 2% PAC uses 0,079s to complete one phase. Thus, the period for the samples is approximately the same. Appendix D has time for all flow rates and periods indicated on the respective graphs. The result are approximately equal for all flow rates.

4.4.4 FFT

FFT graphs are plotted in one graph for results with the same rpm and corresponding flow rate. Water, 1% PAC and 2% PAC are given in all graphs. The X-axis is Frequency, and Y-axis is the differential pressure. A table of relevant numbering is provided below the figures as a courtesy and for easier reading for all FFT graphs.

Figure 4.37 have a flow rate of 1,09 cm^3/s. The 1% PAC treated sample has the highest differential pressure value, and a sheared frequency value as 2% PAC treated sample. 2% PAC treated sample have differential pressure of 1.90 kPa while 1% PAC treated sample has a differential pressure value of 2,07 kPa. Water has differential pressure unsteadiness when the differential pressure is 1.67 kPa at 14.648 Hz.

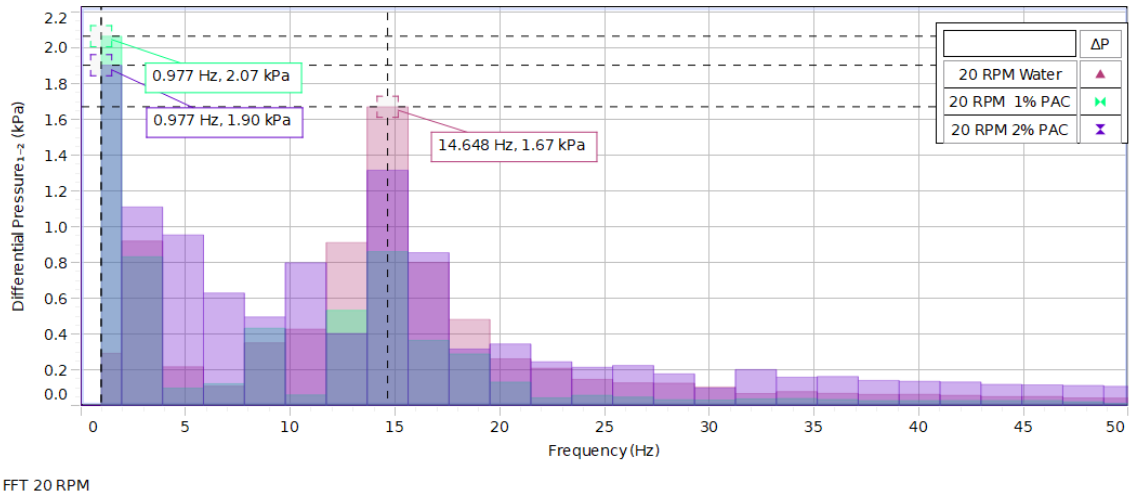

Figure 4.37: FFT, 20 rpm , water , (1%) and (2%) PAC

The table 4.5 provides the given values in figure 4.37 for water , 1% PAC and 2% PAC sample.

Frequency values [Hz]	Differential pressure values[kPa]	Water (Pink)	1% PAC (Green)	2% PAC (purple)
0-50	0-2.1	14.648 [Hz] & 1.67 [kPa]	0.977 [Hz] & 2.07 [kPa]	0.977 [Hz] & 1.90 [kPa]

Table 4.5: Table of FFT values. 20 rpm , water , (1%) and (2%) PAC

Figure 4.38 and corresponding table 4.6 provides result for water, 1% PAC and 2% PAC treated solutions when flow corresponds to 4,5882 cm^3/s. FFT graph shows water in blue, 1% PAC with pink, and 2%. PAC in green. The figure shows unsteadiness for differential pressure with the highest amount for 2% PAC and has the value of 2,930 Hz at 13,40 kPa. 1% PAC and water have the same frequency domain as 2% PAC and correspond to 2,930 Hz. 1% PAC has the frequency domain when differential pressure is 8,13 kPa and water at 7,17 kPa. Thus, the differential pressure unsteadiness increases with the amount of PAC in the water.

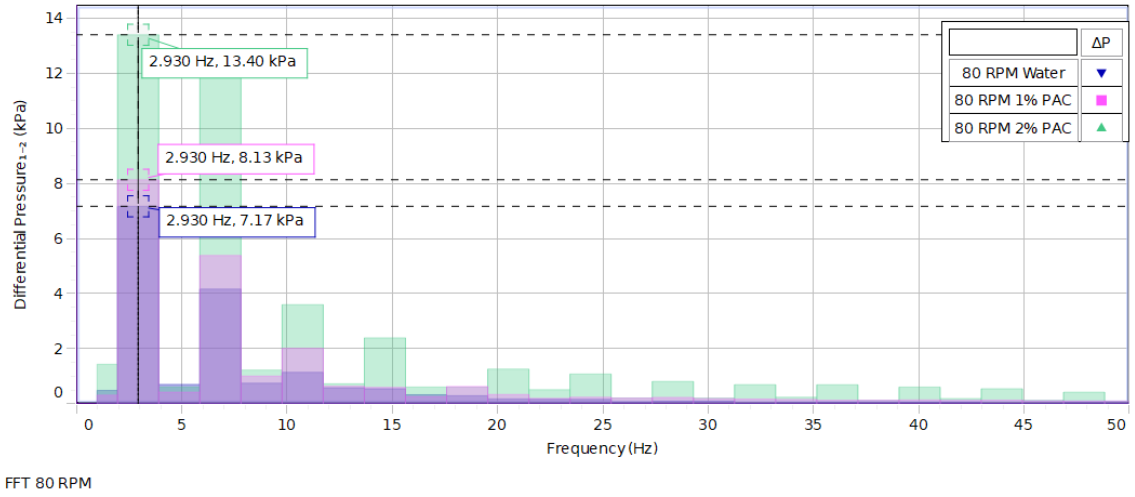

Figure 4.38: FFT, 80 rpm , water , (1%) and (2%) PAC

Frequency values [Hz]	Differential pressure values[kPa]	Water (Blue)	1% PAC (Pink)	2% PAC (Green)
0-42	0-13	2.930 [Hz] & 7.17 [kPa]	2.930 [Hz] & 8.13 [kPa]	2.930 [Hz] & 13.40 [kPa]

Table 4.6: Table of FFT values. 80 rpm , water , (1%) and (2%) PAC

Figure 4.39 and table 4.7 have values for flow rate 8,07 cm^3/s. Water has the lowest differential pressure drop value and 12,46 kPa with a frequency of 6,836 Hz. However, PAC-treated samples have the same frequency domain of 6,836 Hz at 12,90 kPa and 21,42 kPa for the corresponding concentrations of 1% PAC and 2% PAC. Therefore, water is shown at the bottom fields in purple, 1% PAC is indicated with orange, and 2% PAC in blue.

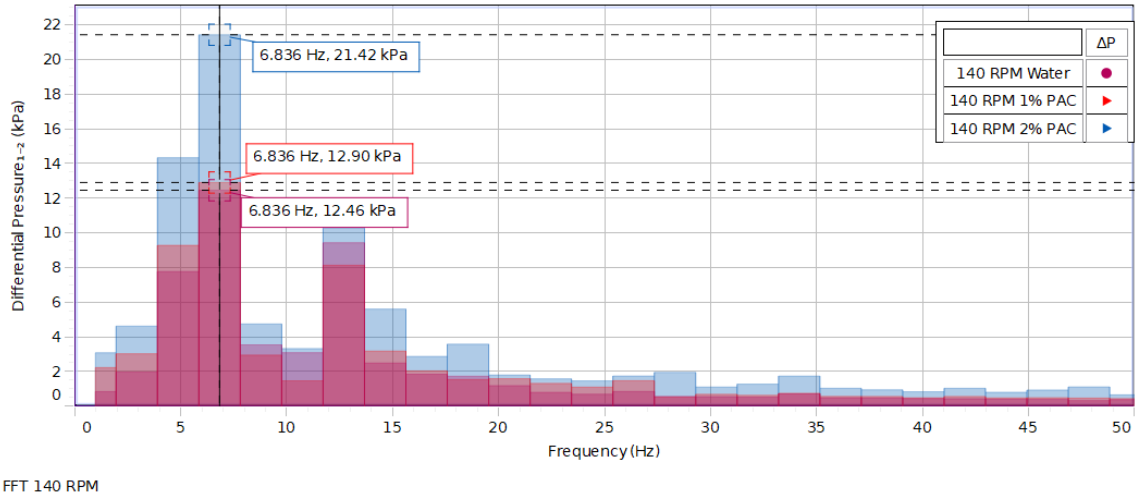

Figure 4.39: FFT, 140 rpm , water , (1%) and (2%) PAC

Frequency values [Hz]	Differential pressure values[kPa]	Water (Purple)	1% PAC (Orange)	2% PAC (Blue)
0-48	0-22	6.836 [Hz] & 12.46 [kPa]	6.836 [Hz] & 12.90 [kPa]	6.836 [Hz] & 21.42 [kPa]

Table 4.7: Table of FFT values. 140 rpm , water , (1%) and (2%) PAC

Figure 4.40 and table 4.8 show the FFT test result when the flow rate is increased to 11,5562 cm^3/s.The frequency spectrum from FFT analysis shows instability in the pressure domain that increases with PAC treatment. Starting at the lowest values, Water has differential pressure with the highest frequency at 14,22 kPa and 8,789 Hz, 1% PAC at 21.79 kPa and 8,789 Hz, and 2% PAC at 37,75 kPa at 8,789 Hz. Water is indicated with orange, 1% PAC is indicated with purple, and 2% PAC is marked with blue.

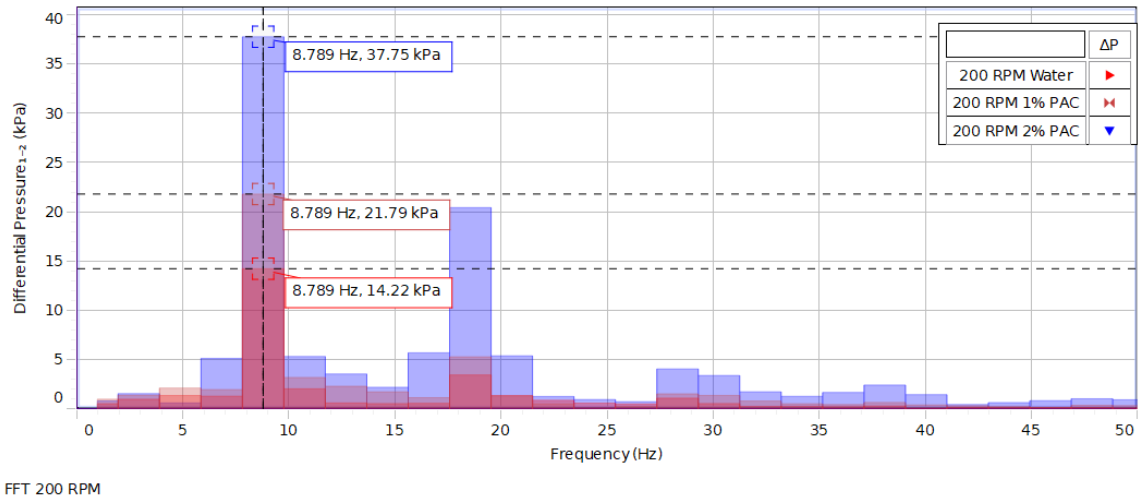

Figure 4.40: FFT, 200 rpm , water , (1%) and (2%) PAC

Frequency values [Hz]	Differential pressure values[kPa]	Water (Red)	1% PAC (Pink)	2% PAC (Blue)
0-50	0-38	68.789 [Hz] & 14.22 [kPa]	8.789 [Hz] & 21.79 [kPa]	8.789 [Hz] & 37.75 [kPa]

Table 4.8: Table of FFT values. 200 rpm , water , (1%) and (2%) PAC

Figure 4.41 and corresponding table 4.9 shows frequency domain for a flow rate of 15,06 cm^3/s. Indicated with orange is water, blue is 1% PAC, and green is 2% PAC. The frequency domain is for the three samples equal and has a value of 12,695 Hz, and water has the lower differential pressure value of 22,34 kPa. PAC-treated samples show a more considerable differential pressure reading unsteadiness for 1% PAC sample and correspond to 74,48 kPa. 2% PAC treated water is in the mid specter and has a differential pressure value equal to 47,51 kPa.

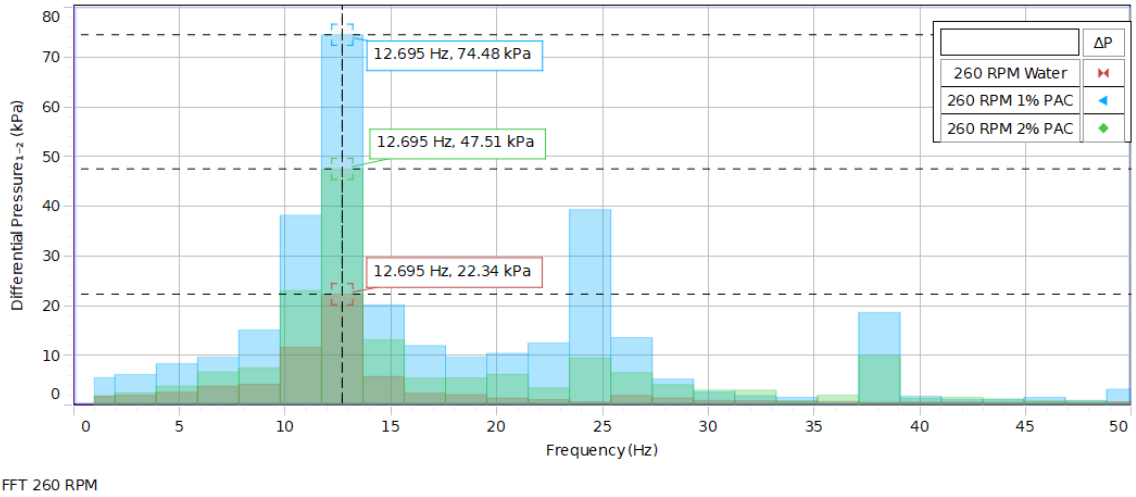

Figure 4.41: FFT, 260 rpm , water , (1%) and (2%) PAC

Frequency values [Hz]	Differential pressure values[kPa]	Water (Orange)	1% PAC (Blue)	2% PAC (Green)
0-50	0-75	12.695 [Hz] & 22.34 [kPa]	12.695 [Hz] & 47.51 [kPa]	12.695 [Hz] & 74.48 [kPa]

Table 4.9: Table of FFT values. 260 rpm , water , (1%) and (2%) PAC

Comparing FFT for all flow rates, there is a visible change for the flow rates of 1,09 cm^3/s and 15,06 cm^3/s. For the two flow rates, the 1% PAC treated solutions have a higher differential pressure unsteadiness while comparing the other flow rates, and the 2% PAC treated solutions show the highest differential pressure unsteadiness.

5

Conclusion

Oscillating flow and pressure drop in horizontal pipes have been evaluated whit multiple tests. Calibration using water are performed to ensure a basis for experiments and are used for flow calculations. Water and two concentrations of PAC treated water are evaluated to see the impact of polymers and viscosity have on the oscillations and pressure drop. Further, some of the main findings are listed below.

Calibrations

- The flow are stable for calibration with constant pressure and calibration with constant flow show fluctuations.
- Comparing results form figure 4.6 and 4.7 shows a change in graphs and the placement of Ohaus mass scale that can show a small impact of the result form where the weight is placed. This can come from the tube leading from test section and to the end water container placed on Ohaus weight, the tube will be in a slightly downwards or straight position.

Rheology testing

- Testing viscoelasticity gives unforseen results as 2% PAC treated water shows no sign of viscoelasticity. On the other hand, for 1% PAC sample there is viscoelastic behavior. It would be expected to see the same tendencyes for both PAC consentrations. Extending the test of viscoelastic behavior can lead to a better understanding of the results. Lager testing span can show improved results and a anton paar rheometer with lower shear rates and more accuracy can have an improvement base.
- For 1% PAC and 2% PAC consentrations show hystereses both before and after PASCO oscillation test. Comparing the hysteresis from before and after PASCO test provides the same hysteresis area and viscosity. Taking hysteresis test before or after therefore don't seem to have an impact on hysteresis outcome.

PASCO oscillation test

- Needs high sampling rate for better evaluation of oscillations, prefered sampling rate are 1kHz
- Differential pressure increases with higher concentration of PAC in the sample. This can be caused by viscoelastic behavior, but are not conformed by rheology test show unexpected results.
- Evaluating the periods for all concentrations and flow rates indicates no significant changes in time for different periods. For more viscous samples, there might be differences in periods due to a gel-like structure in the flow, causing the selection to flow slower.
- Increasing the flow rate stabilizes differential fluctuations in differential pressure.

The experiment can symbolize how big pumps offshore react to fluid injection and how the pressure drop reacts to fluid infusion. Furthermore, how the mass flow rate and oscillation change with the change of pump rpm. Understanding oscillatory flow and pressure drop in pipes can be used to choose a fluid mixture when pumping at any platform.

References

[1] P. D. M. M. Amaratunga, R. W. Time, and R. H. Rabenjafimanantsoa, *Particle settling in shear thinning non-newtonian drilling fluids : Effect of oscillatory motion*, Generic, 2020.

[2] O. Skjeggestad, *Boreslamteknologi : teori og praksis*, nob. Bergen: Alma Mater, 1989, ISBN: 8241900104.

[3] D. X. M. Dr. Xiuhua Zheng, *Drilling fluids*, 1st edition. 29 Xueyuan Road Beijing, 100083, China: School of Engineering and Technology China University of Geosciences (Beijing), 2010. [Online]. Available: `https://www.scribd.com/doc/119810740/DRILLING-FLUIDS-Manual-Important`.

[4] A. Saasen and J. D. Ytrehus, "Viscosity models for drilling fluids-herschel-bulkley parameters and their use," eng, *Energies (Basel)*, vol. 13, no. 20, p. 5271, 2020, ISSN: 1996-1073.

[5] B. Brunone, B. W. Karney, M. Mecarelli, and M. Ferrante, "Velocity profiles and unsteady pipe friction in transient flow," *Journal of water resources plan-*

ning and management, vol. 126, no. 4, pp. 236–244, 2000, ISSN: 0733-9496. DOI: 10.1061/(ASCE)0733-9496(2000)126:4(236).

[6] M. Manna, A. Vacca, and R. Verzicco, "Pulsating pipe flow with large-amplitude oscillations in the very high frequency regime. part 1. time-averaged analysis," eng, *Journal of fluid mechanics*, vol. 700, pp. 246–282, 2012, ISSN: 0022-1120.

[7] R. W. Time, "Two-phase flow in pipelines, pet505 compendium,"

[8] J.-h. ZHANG, C.-q. YAN, and P.-z. GAO, "Characteristics of pressure drop and correlation of friction factors for single-phase flow in rolling horizontal pipe," eng, vol. 21, no. 5, pp. 614–621, 2009, ISSN: 1001-6058.

[9] P. M. Quinn, J. A. Cherry, and B. L. Parker, "Relationship between the critical reynolds number and aperture for flow through single fractures; evidence from published laboratory studies," *Journal of hydrology (Amsterdam)*, vol. 581, p. 124 384, 2020, ISSN: 0022-1694. DOI: 10.1016/j.jhydrol.2019.124384.

[10] F. i. pipes, *Chapter 8, flow in pipes*, Web Page. [Online]. Available: https://www.kau.edu.sa/Files/0057863/Subjects/Chapter%208.pdf.

[11] G. scientific, "The importance of calibration," [Online]. Available: https://www.gemscientific.co.uk/blog/importance-of-calibration/.

[12] Henderson-biomedical, "Laboratory equipment calibration," [Online]. Available: https://henderson-biomedical.co.uk/laboratory-equipment-calibration/?v=79cba1185463.

[13] T. G. Mezger, *Applied Rheology, with Joe Fow on rheology road*, 1st edition. Anton-Paar-Str.20 8054 Graz, Austria: anton-paar gmbh, 2015, ISBN: 978-3-9504016-0-8.

[14] M. V. OCHOA, "Analysis of drilling fluid rheology and tool joint effect to reduce errors in hydraulics calculations," p. 191, [Online]. Available: https://oaktrust.library.tamu.edu/bitstream/handle/1969.1/4334/etd-tamu-2006B-PETE-viloria.pdf?sequence=1&isAllowed=y.

[15] T. Mezger, *The rheology handbook : For users of rotational and oscillatory rheometers*, eng, Hannover, 2020.

[16] a. s. Binh bui, jason maxey, mehmet e ozbayoglu, stefan z miska, menghiao yu, and nicholas e takach, "Viscoelastic properties of oil-based drilling fluids," [Online]. Available: http://www.etrustin.com/product_detail_en/id/263.html.

[17] M. I. Worldwide., "A basic introduction to rheology," [Online]. Available: https://cdn.technologynetworks.com/TN/Resources/PDF/WP160620BasicIntroRheology.pdf.

[18] T. G. Mezger, *The rheology handbook : for users of rotational and oscillatory rheometers*, 3rd rev., ser. European coatings tech files. Hannover: Vincentz, 2011, ISBN: 9783866308640,3866308647.

[19] T. chemical, "Pac(polyanionic cellulose)," p. 1, [Online]. Available: http://www.etrustin.com/product_detail_en/id/263.html.

[20] A. Busch, V. Myrseth, M. Khatibi, P. Skjetne, S. Hovda, and S. T. Johansen, "Rheological characterization of polyanionic cellulose solutions with application to drilling fluids and cuttings transport modeling," eng, 2018, ISSN: 1430-6395. [Online]. Available: http://hdl.handle.net/11250/2634344.

[21] N. audio, "Fast fourier transformation fft, basics," [Online]. Available: https://www.nti-audio.com/en/support/know-how/fast-fourier-transform-fft.

[22] f. t. s. Watson marlow, "Peristaltic pumps - how do they work?," [Online]. Available: https://www.wmfts.com/en/support/pump-principles/how-do-peristaltic-pumps-work/.

[23] G. F. R. R. F. S. K. P. F. Villecco, "Fluid–structure interaction modeling applied to peristaltic pump flow simulations," [Online]. Available: https://www.mdpi.com/2075-1702/7/3/50/pdf.

[24] Avantor, "Peristaltic pumps pp 3300 and pp 3400," [Online]. Available: https://no.vwr.com/store/product/20660477/peristaltic-pumps-pp-3300-and-pp-3400.

[25] Pasco, "Pasport dual pressure sensor manual," p. 3, 6/2018. [Online]. Available: https://www.pasco.com/products/sensors/pressure/ps-2181#documents-panel.

[26] P. 8. U. I. M. No.UI-5000, "Pasco 850 universal interface model no.ui-5000," p. 26, [Online]. Available: https://www.pasco.com/products/interfaces-and-dataloggers/ui-5000#documents-panel.

[27] A. P. d. meter, "Anton paar density," 2022. [Online]. Available: https://www.anton-paar.com/kr-en/products/details/benchtop-density-meter-dma-4100-m/.

[28] G. lab sustainable equipment, "Silverson l2r ultra turrax," [Online]. Available: https://www.geminibv.com/labware/silverson-l2r-ultra-turrax/.

[29] E. Dellali, S.Begot, F. Lanzetta, and E. Gavignet, "Pressure drop analysis of oscillating flows through a miniature porous regenerator under isothermal and nonisothermal conditions," 2019. [Online]. Available: https://www.researchgate.net/publication/330571580_Pressure_drop_analysis_of_oscillating_flows_through_a_miniature_porous_regenerator_under_isothermal_and_nonisothermal_conditions.

[30] H. Fujioka, K. Oka, and K. Tanishita, "Oscillatory flow and gas transport through a symmetrical bifurcation," *J Biomech Eng*, vol. 123, no. 2, pp. 145–153, 2001, ISSN: 0148-0731. DOI: 10.1115/1.1352735.

[31] A. Tsimpoukis, S. Naris, and D. Valougeorgis, "Oscillatory pressure-driven rarefied binary gas mixture flow between parallel plates," *Phys Rev E*, vol. 103, no. 3-1, pp. 033 103–033 103, 2021, ISSN: 2470-0045. DOI: 10.1103/PhysRevE.103.033103.

[32] G. Formato, R. Romano, A. Formato, *et al.*, "Fluid-structure interaction modeling applied to peristaltic pump flow simulations," *Machines (Basel)*, vol. 7, no. 3, p. 50, 2019, ISSN: 2075-1702. DOI: 10.3390/machines7030050.

[33] F. Jiang, P. Zhao, G. Qi, *et al.*, "Pressure drop in horizontal multi-tube liquid–solid circulating fluidized bed," *Powder technology*, vol. 333, pp. 60–70, 2018, ISSN: 0032-5910. DOI: 10.1016/j.powtec.2018.04.003.

[34] A. Saasen and J. D. Ytrehus, "Viscosity models for drilling fluids-herschel-bulkley parameters and their use," *Energies (Basel)*, vol. 13, no. 20, 2020, ISSN: 1996-1073.

6

Appendix

Appendix A

All plots with defect Bluetooth signals from Ohaus mass scale weight.

V= Qt			10 RPM	20 RPM	30 RPM	40 RPM	50 RPM	60 RPM	70 RPM	80 RPM	90 RPM	100 RPM
V=m/t		ml	500	500	500	500	500	500	500	500	500	500
Q= V/t		sec	901,05	451	301,3	240	176,2	147,6	124,45	108,8	96,4	85,65

RPM	Q[m^3/s]	g->kg		Reynolds number	
10	0,554908163	554,9081627		0,0193578	193,577962
20	1,10864745	1108,64745		0,03867482	386,748165
30	1,659475606	1659,475606		0,05789028	578,902829
40	2,083333333	2083,333333		0,07267643	726,764261
50	2,837684449	2837,684449		0,09899173	989,917267
60	3,387533875	3387,533875		0,11817305	1181,7305
70	4,017677782	4017,677782		0,14015542	1401,55422
80	4,595588235	4595,588235		0,16031565	1603,15646
90	5,186721992	5186,721992		0,18093716	1809,3716
100	5,837711617	5837,711617		0,20364673	2036,46728

Using V=m/rho to get m^3 for Q		
	0,9983	g/cm^3
	998,3	kg/m^3

Viscosity		
	1,0016	mPa
	10016000	kPa

Pressure drop average		
10	average =	-0,0773685
20		0,07216949
30		0,216165
40		0,35353625
50		0,50531631
60		0,74461043
70		0,8948413
80		1,07270096
90		1,28528527
100		1,46214702

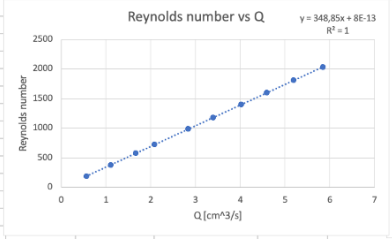

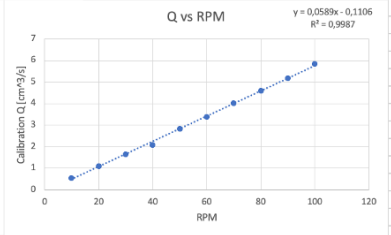

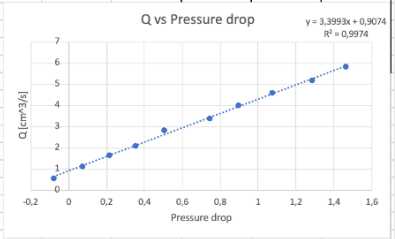

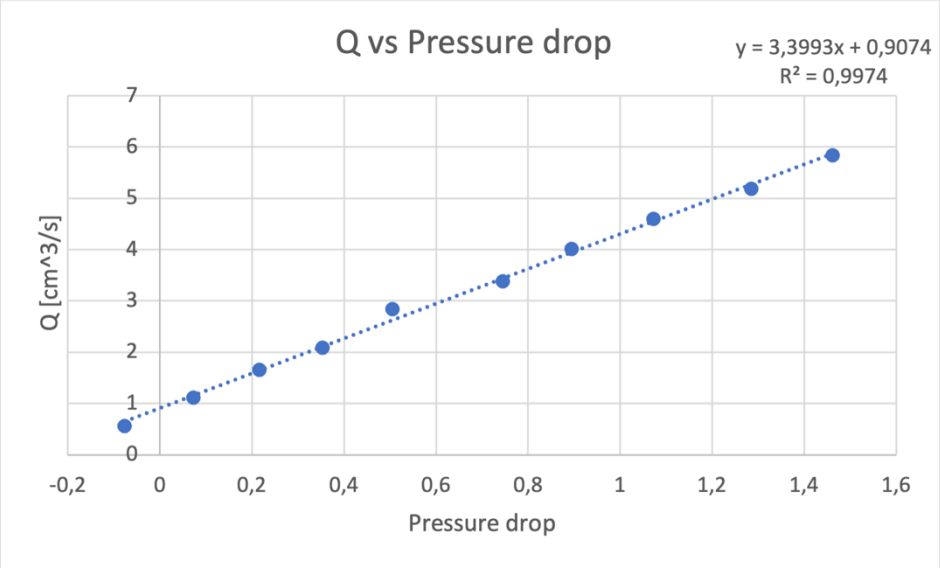
Q vs Pressure drop
y = 3,3993x + 0,9074
R² = 0,9974
Q [cm^3/s]
Pressure drop
7
6
5
4
3
2
1
0
-0,2
0
0,2
0,4
0,6
0,8
1
1,2
1,4
1,6

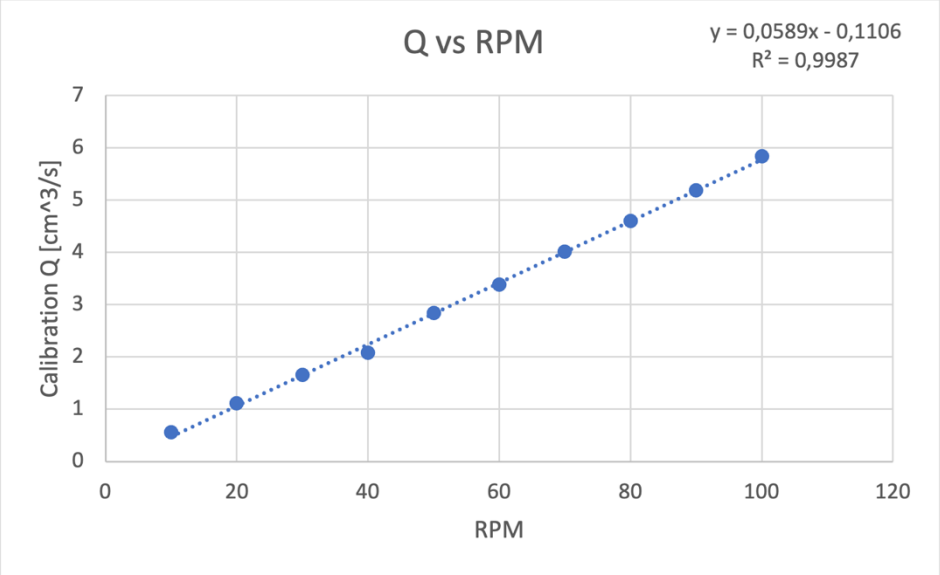
Q vs RPM
y = 0,0589x - 0,1106
R² = 0,9987
Calibration Q [cm^3/s]
RPM
7
6
5
4
3
2
1
0
0
20
40
60
80
100
120

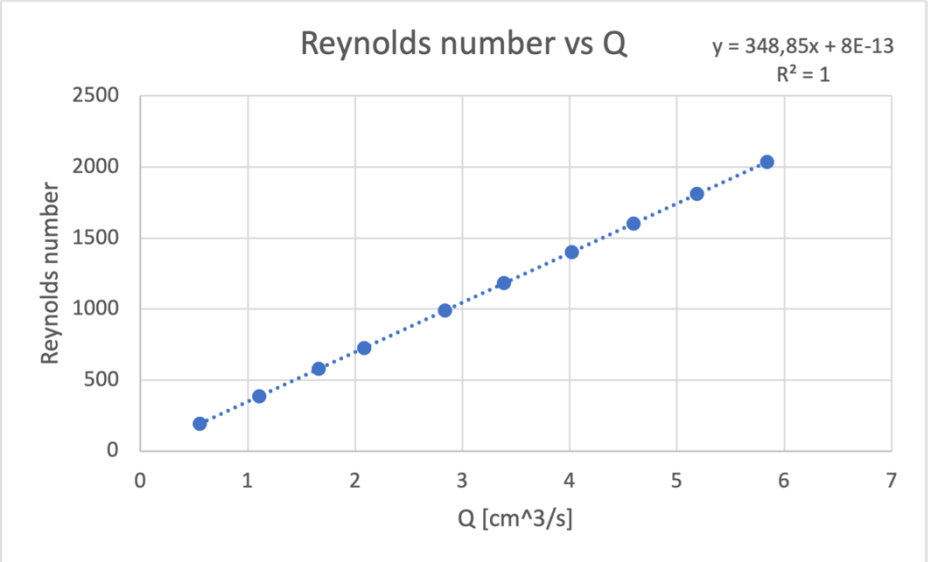
Reynolds number vs Q
y = 348,85x + 8E-13
R² = 1
Reynolds number
Q [cm^3/s]
2500
2000
1500
1000
500
0
0
1
2
3
4
5
6
7

Appendix B

A New Ohaus mass scale weight was used and placed under the table. The amount of water used is 250 ml.

Round 1

V= Qt			1	2	3	4	5	6	7	8	9	10
V=m/t		ml	250,23	249,85	249,71	250,9	249,85	250,27	249,1	251,87	251,31	248,26
Q= V/t		sec	451	226	151	114	89,5	74	62	56	50	43

RPM	Q[cm^3/s]
10	0,5548337
20	1,105531
30	1,6537086
40	2,2008772
50	2,7916201
60	3,382027
70	4,0177419
80	4,4976786
90	5,0262
100	5,7734884

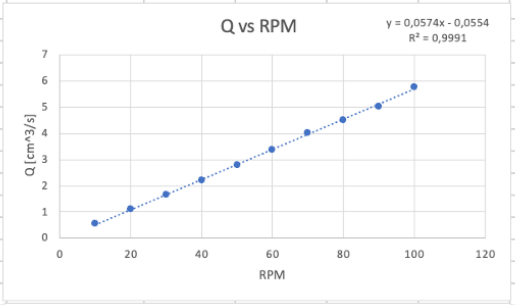

Q	Pressure drop
0,5548337	-0,0322766
1,105531	0,1076599
1,6537086	0,2690256
2,2008772	0,4110798
2,7916201	0,3745647
3,382027	0,8052362
4,0177419	0,9743192
4,4976786	1,1641703
5,0262	1,3805746
5,7734884	1,6621444

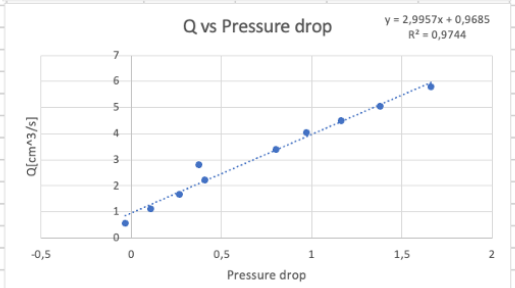

Q	Reynolds number	
0,5548337	0,0193552	193,5519868
1,105531	0,0385661	385,6609922
1,6537086	0,0576891	576,891031
2,2008772	0,0767769	767,7690651
2,7916201	0,0973848	973,8478685
3,382027	0,1179809	1179,809458
4,0177419	0,1401577	1401,576598
4,4976786	0,1569001	1569,00098
5,0262	0,1753374	1753,374013
5,7734884	0,2014063	2014,063204

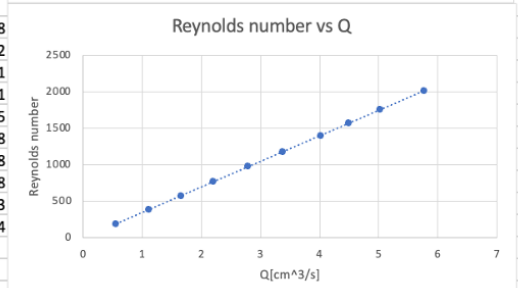

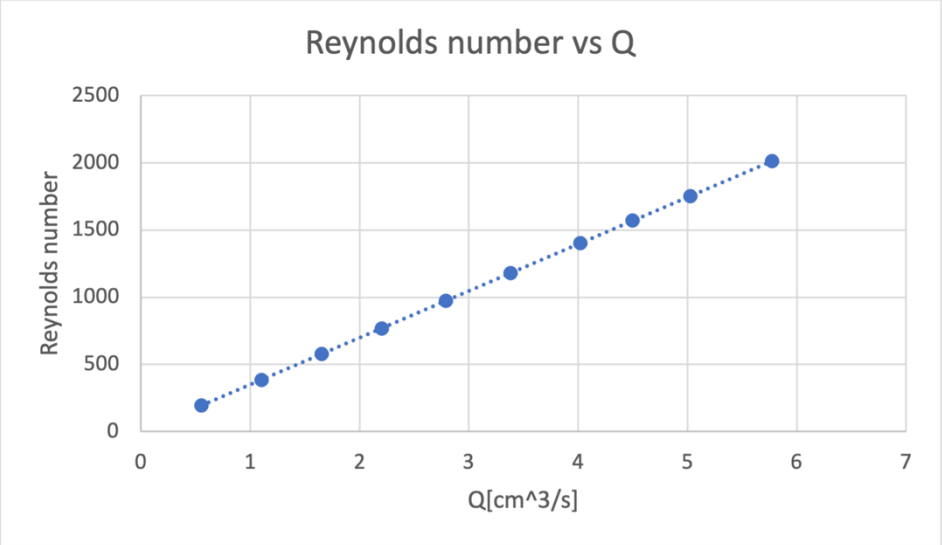
Reynolds number vs Q
Reynolds number
2500
2000
1500
1000
500
0
0
1
2
3
4
5
6
7
Q[cm^3/s]

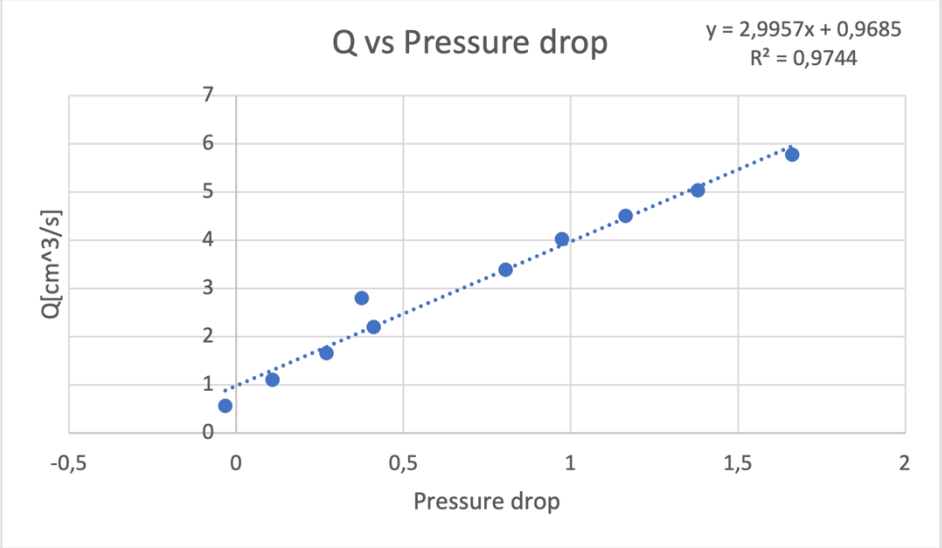
Q vs Pressure drop
y = 2,9957x + 0,9685
R² = 0,9744
Q[cm^3/s]
7
6
5
4
3
2
1
0
-0,5
0
0,5
1
1,5
2
Pressure drop

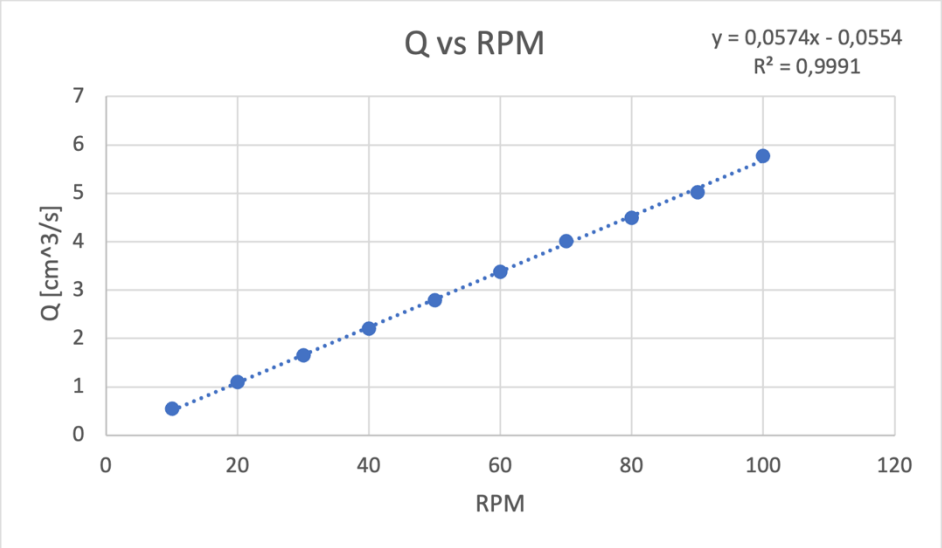
Q vs RPM
y = 0,0574x - 0,0554
R² = 0,9991
Q [cm^3/s]
7
6
5
4
3
2
1
0
0
20
40
60
80
100
120
RPM

Round 2

V= Qt		10 RPM	20 RPM	30 RPM	40 RPM	50 RPM	60 RPM	70 RPM	80 RPM	90 RPM	100 RPM
V=m/t	ml	250,04	250,41	250,7	250,8	250,045	249,07	250,49	249,8	250,29	250,48
Q= V/t	sec	450	226	152	113	89,5	74	63	56	49	44

	RPM	Q
	10	0,555644
	20	1,108009
	30	1,649342
	40	2,219469
	50	2,793799
	60	3,365811
	70	3,976032
	80	4,460714
	90	5,107959
	100	5,692727

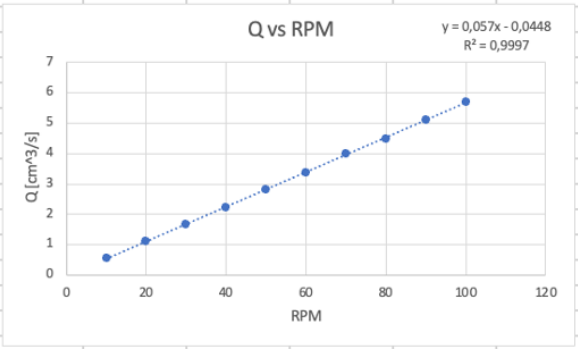

density =kg /	998,3	
Viscosity	1,0016	kPa

	Q	Pressure drop
	0,555644	-0,026284
	1,108009	0,107024
	1,649342	0,263959
	2,219469	0,434603
	2,793799	0,47696
	3,365811	0,788847
	3,976032	0,954031
	4,460714	1,11972
	5,107959	1,357113
	5,692727	1,500525

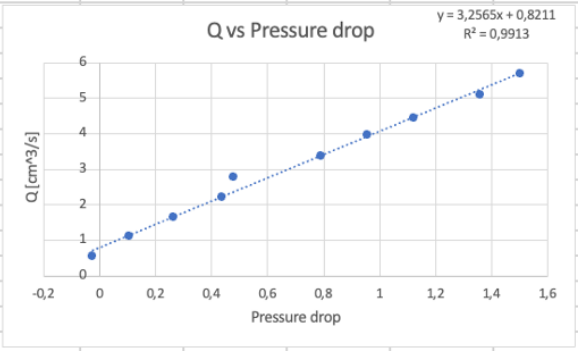

		Reynold
	0,555644	553,8137
	1,108009	1104,358
	1,649342	1643,908
	2,219469	2212,156
	2,793799	2784,594
	3,365811	3354,721
	3,976032	3962,932
	4,460714	4446,017
	5,107959	5091,13
	5,692727	5673,971

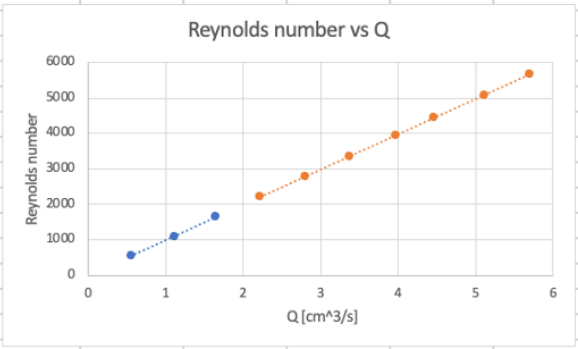

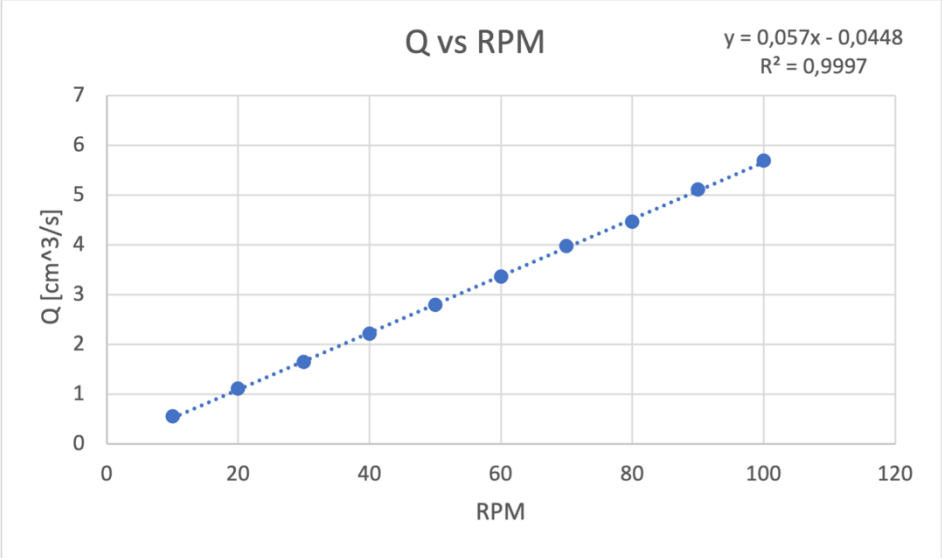
Q vs RPM
y = 0,057x - 0,0448
R² = 0,9997
Q [cm^3/s]
RPM
0
1
2
3
4
5
6
7
0
20
40
60
80
100
120

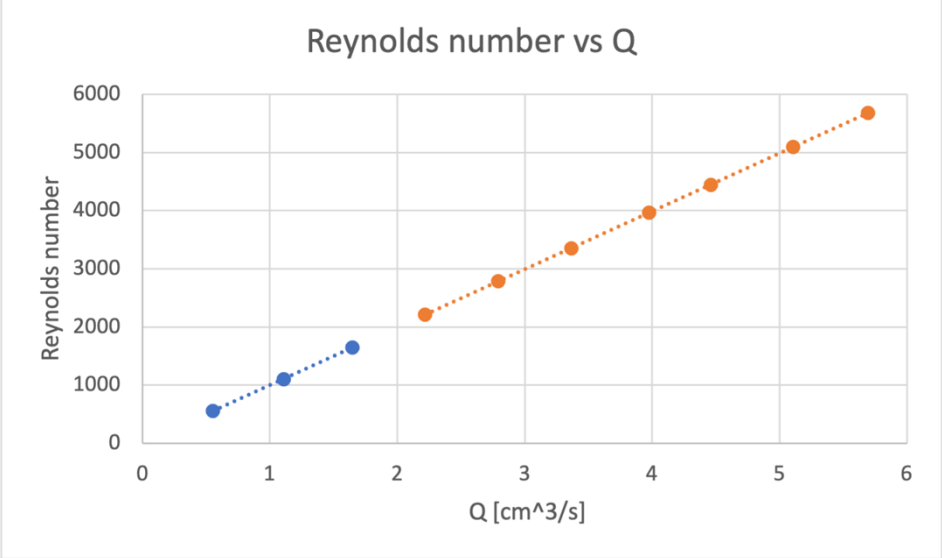
Reynolds number vs Q
Reynolds number
Q [cm^3/s]
0
1000
2000
3000
4000
5000
6000
0
1
2
3
4
5
6

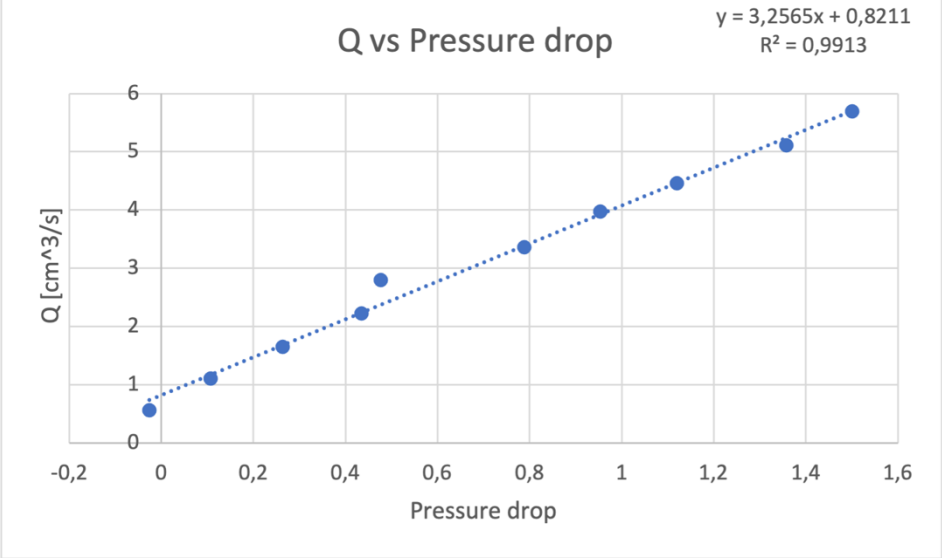
Q vs Pressure drop
y = 3,2565x + 0,8211
R² = 0,9913
Q [cm^3/s]
Pressure drop
0
1
2
3
4
5
6
-0,2
0
0,2
0,4
0,6
0,8
1
1,2
1,4
1,6

Round 3

V= Qt		1	2	3	4	5	6	7	8	9	10
V=m/t	ml	249,81	249,72	249,53	250,06	249,37	250,25	249,285	249,63	150,61	250,13
Q= V/t	sec	452	226	151	112,5	89	74	62,5	55	29	43

	RPM	Q
	10	0,552677
	20	1,104956
	30	1,652517
	40	2,222756
	50	2,80191
	60	3,381757
	70	3,98856
	80	4,538727
	90	5,193448
	100	5,816977

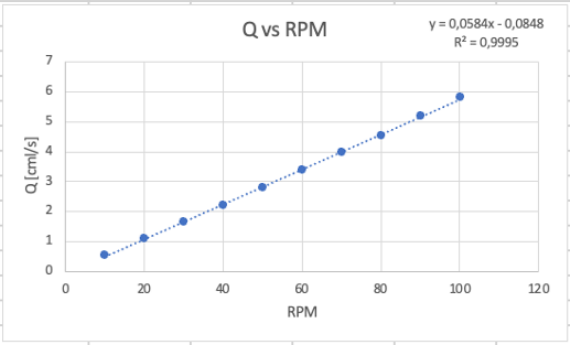

density =kg /	998,3	
Viscosity	1,0016	kPa

	Q	Pressure drop
	0,55267699	-0,015568
	1,10495575	0,1261
	1,65251656	0,263949
	2,22275556	0,415233
	2,80191011	0,580365
	3,38175676	0,760682
	3,98856	0,976475
	4,53872727	1,170954
	5,19344828	1,426334
	5,81697674	1,824901

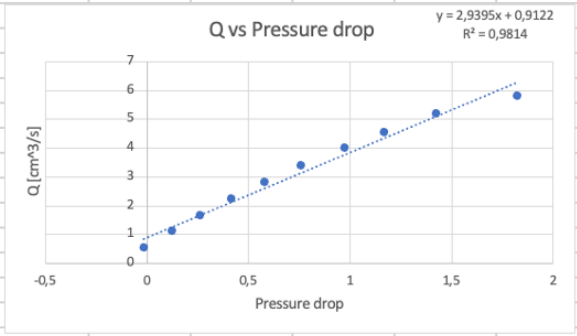

		Reynold
	0,55267699	550,8561
	1,10495575	1101,315
	1,65251656	1647,072
	2,22275556	2215,432
	2,80191011	2792,679
	3,38175676	3370,615
	3,98856	3975,419
	4,53872727	4523,773
	5,19344828	5176,337
	5,81697674	5797,811

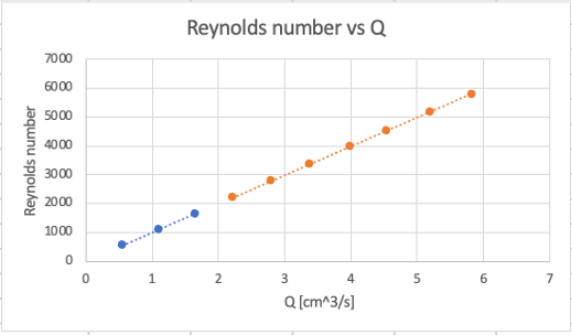

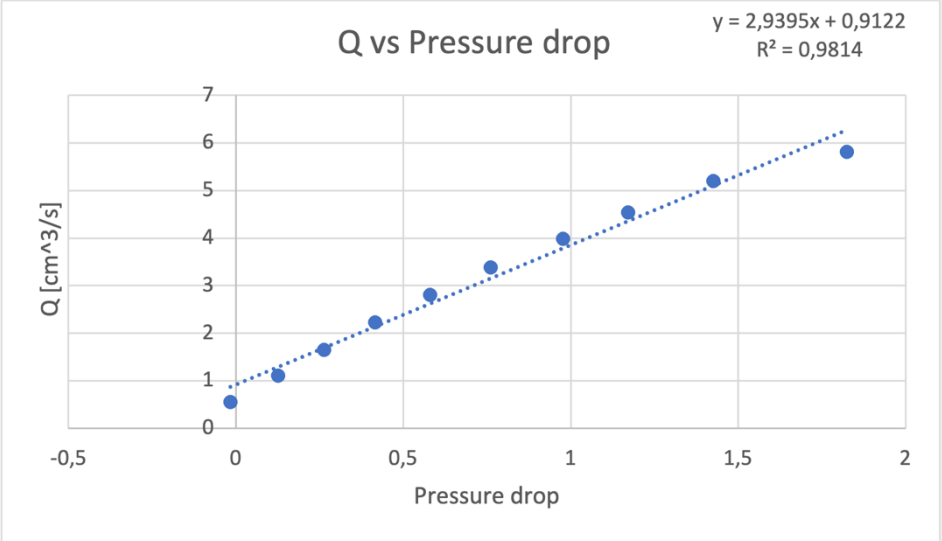
Q vs Pressure drop
y = 2,9395x + 0,9122
R² = 0,9814
Q [cm^3/s]
Pressure drop
7
6
5
4
3
2
1
0
-0,5
0
0,5
1
1,5
2

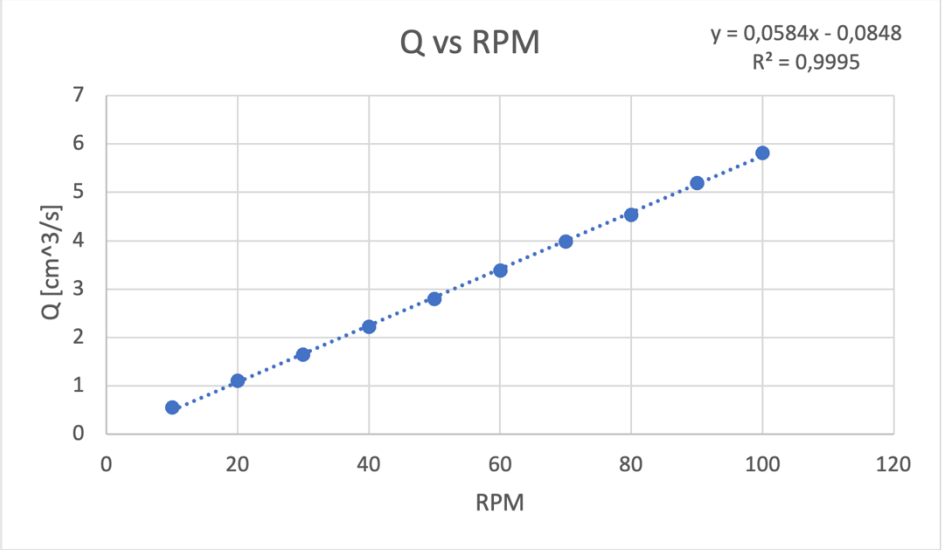
Q vs RPM
y = 0,0584x - 0,0848
R² = 0,9995
Q [cm^3/s]
RPM
7
6
5
4
3
2
1
0
0
20
40
60
80
100
120

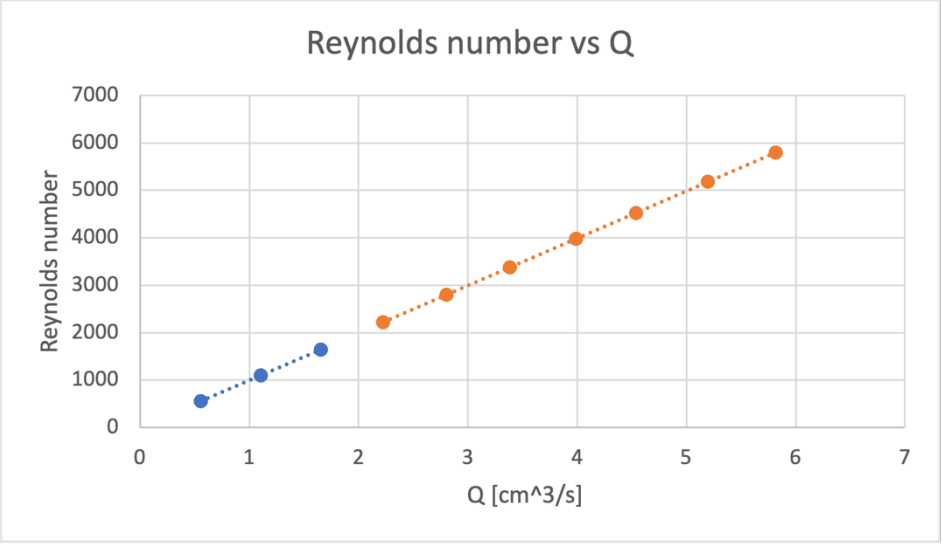
Reynolds number vs Q
Reynolds number
Q [cm^3/s]
7000
6000
5000
4000
3000
2000
1000
0
0
1
2
3
4
5
6
7

Appendix C

Ohaus mass scale weights are placed at the same level as the test section tube, causing the water to stream continuously at the same level while in a tube. The amount of water used is 250 ml.

Round 1

V= Qt			10 RPM	20 RPM	30 RPM	40 RPM	50 RPM	60 RPM	70 RPM	80 RPM	90 RPM	100 RPM	110 RPM	120 RPM	130 RPM	140 RPM	150 RPM
V=m/t			250,21	249,73	250,35	249,45	251,42	250,48	250,3	249,9	252,17	250,61	249,96	249,24	247,93	248,92	247,54
Q= V/t			453	228	152	112	90	74	63	55	49	43	40	36	37	31	29

RPM	Q[m^3/s]	g->kg		Reynolds number	
10	0,55328053	552,3399558		0,0192682	192,68205
20	1,09717221	1095,307018		0,0382094	382,0944
30	1,64984421	1647,039474		0,0574565	574,56452
40	2,23102489	2227,232143		0,0776963	776,96291
50	2,79831269	2793,555556		0,0974523	974,52304
60	3,39062893	3384,864865		0,1180799	1180,7994
70	3,9797815	3973,015873		0,1385974	1385,9741
80	4,5513737	4543,636364		0,1585033	1585,0332
90	5,15509018	5146,326531		0,179528	1795,2798
100	5,83806424	5828,139535		0,2033128	2033,1281
110	6,25964139	6249		0,2179944	2179,9439
120	6,93512304	6923,333333		0,2415183	2415,183
130	6,71222159	6700,810811		0,2337557	2337,5567
140	8,04335112	8029,677419		0,2801128	2801,1276
150	8,55039775	8535,862069		0,2977709	2977,7086

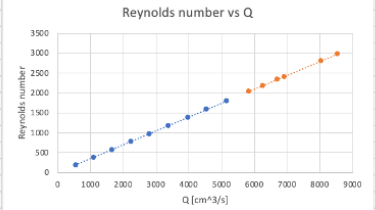

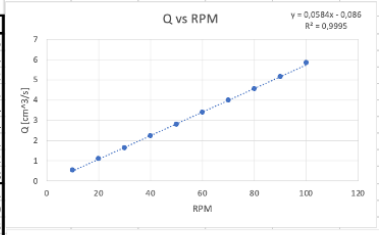

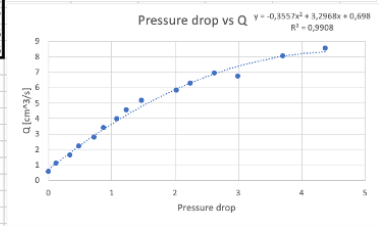

Using V=m/rho for å finne m^3 for Q		
0,9983	g/cm^3	
998,3	kg/m^3	

Pressure drop average		
10	average =	0,0071173
20		0,1248863
30		0,3480862
40		0,4861776
50		0,7238928
60		0,8742416
70		1,0867804
80		1,2300439
90		1,4782111
100		2,0197553
110		2,2430807
120		2,6214505
130		2,9906472
140		3,701401
150		4,3724613

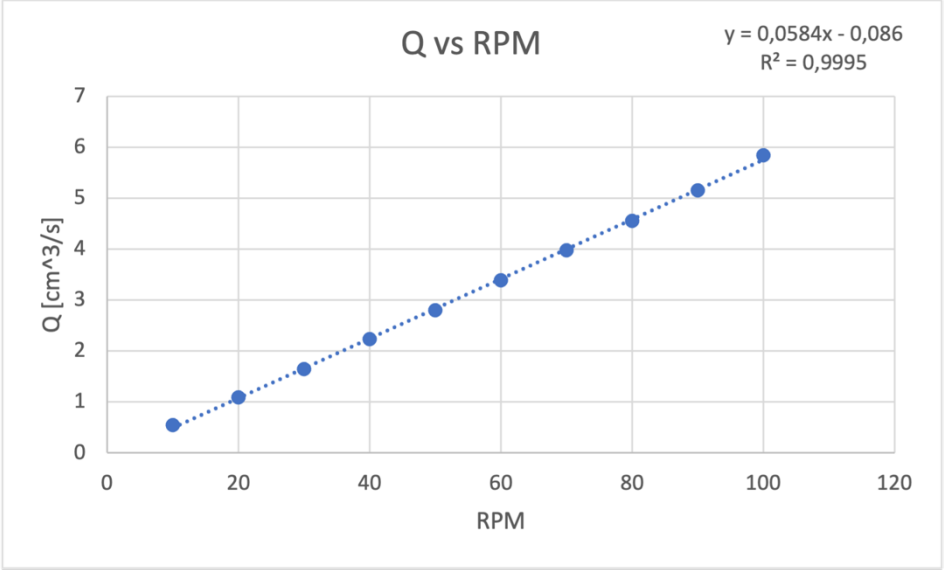
Q vs RPM
y = 0,0584x - 0,086
R² = 0,9995
Q [cm^3/s]
RPM
0
1
2
3
4
5
6
7
0
20
40
60
80
100
120

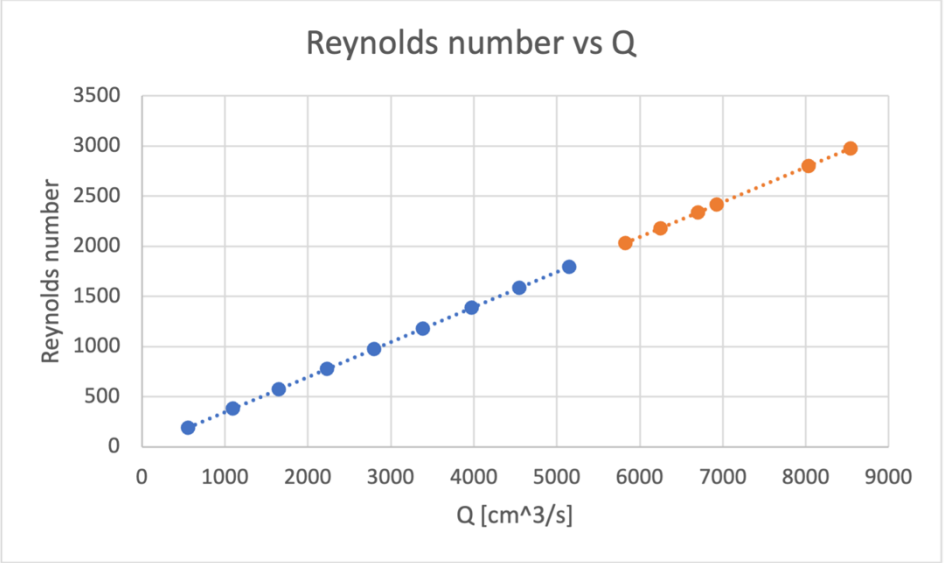
Reynolds number vs Q
Reynolds number
Q [cm^3/s]
0
500
1000
1500
2000
2500
3000
3500
0
1000
2000
3000
4000
5000
6000
7000
8000
9000

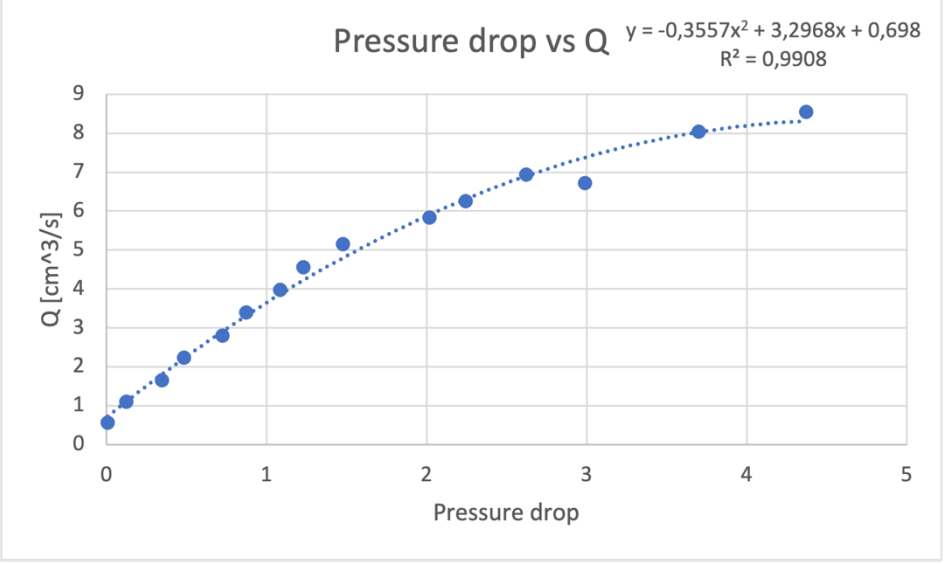
Pressure drop vs Q
y = -0,3557x² + 3,2968x + 0,698
R² = 0,9908
Q [cm^3/s]
Pressure drop
0
1
2
3
4
5
6
7
8
9
0
1
2
3
4
5

X

Round 2

V= Qt			10 RPM	20 RPM	30 RPM	40 RPM	50 RPM	60 RPM	70 RPM	80 RPM	90 RPM	100 RPM	110 RPM	120 RPM	130 RPM	140 RPM	150 RPM
V=m/t			250,44	250,29	250,55	249,64	249,83	251,35	250,9	248,91	250,155	251,27	249,77	249,47	248,18	250,39	251,95
Q= V/t			451	225	151	112	89	75	63	55	48,5	44	39	36	34,5	31,5	29,5

RPM	Q[m^3/s]	g->kg		Reynolds number	
10	0,55624495	555,2993348		0,019371	193,7144
20	1,1142943	1112,4		0,038806	388,0572
30	1,66209709	1659,271523		0,057883	578,8316
40	2,2327242	2228,928571		0,077755	777,5547
50	2,81185881	2807,078652		0,097924	979,2405
60	3,3570403	3351,333333		0,11691	1169,102
70	3,98932153	3982,539683		0,13893	1389,296
80	4,53334305	4525,636364		0,157875	1578,754
90	5,1666183	5157,835052		0,179929	1799,294
100	5,72040651	5710,681818		0,199215	1992,153
110	6,41526492	6404,358974		0,223414	2234,14
120	6,94152281	6929,722222		0,241741	2417,412
130	7,20587317	7193,623188		0,250947	2509,473
140	7,96242501	7948,888889		0,277294	2772,945
150	8,55522184	8540,677966		0,297939	2979,389

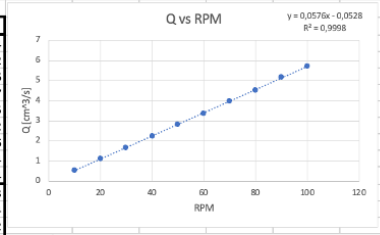

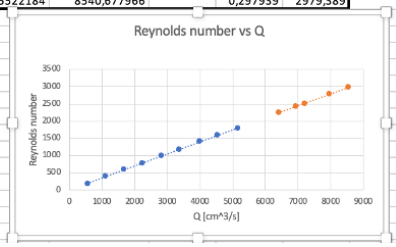

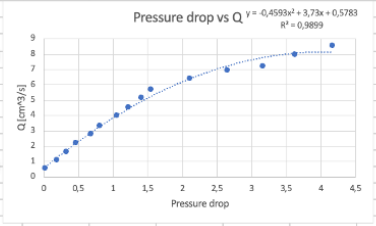

Using V=m/rho for å finne m^3 for Q

0,9983	g/cm^3
998,3	kg/m^3

Pressure drop average

10	average =	0,02103
20		0,184641
30		0,320983
40		0,463668
50		0,673262
60		0,809676
70		1,049025
80		1,223451
90		1,411143
100		1,540568
110		2,103188
120		2,642483
130		3,154182
140		3,620935
150		4,160034

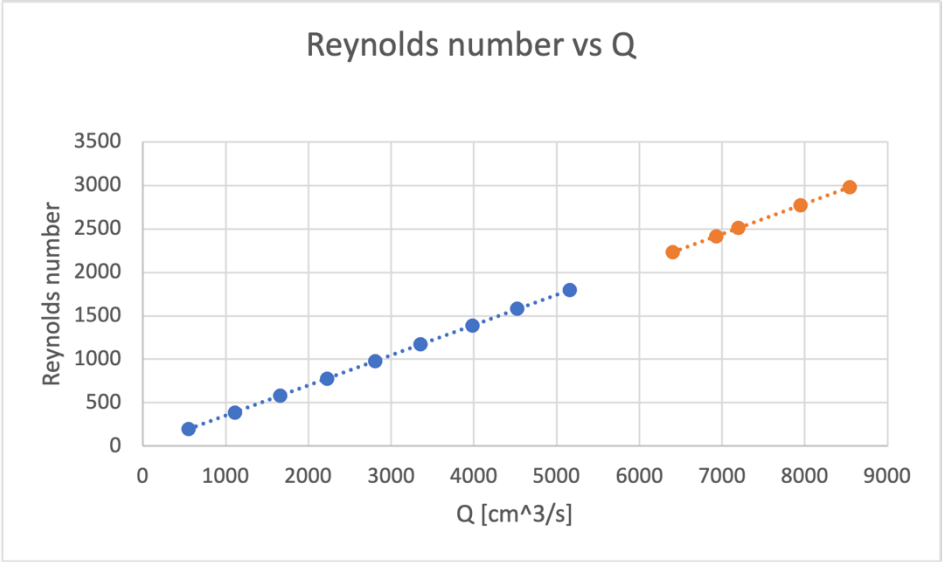
Reynolds number vs Q
Reynolds number
3500
3000
2500
2000
1500
1000
500
0
0
1000
2000
3000
4000
5000
6000
7000
8000
9000
Q [cm^3/s]

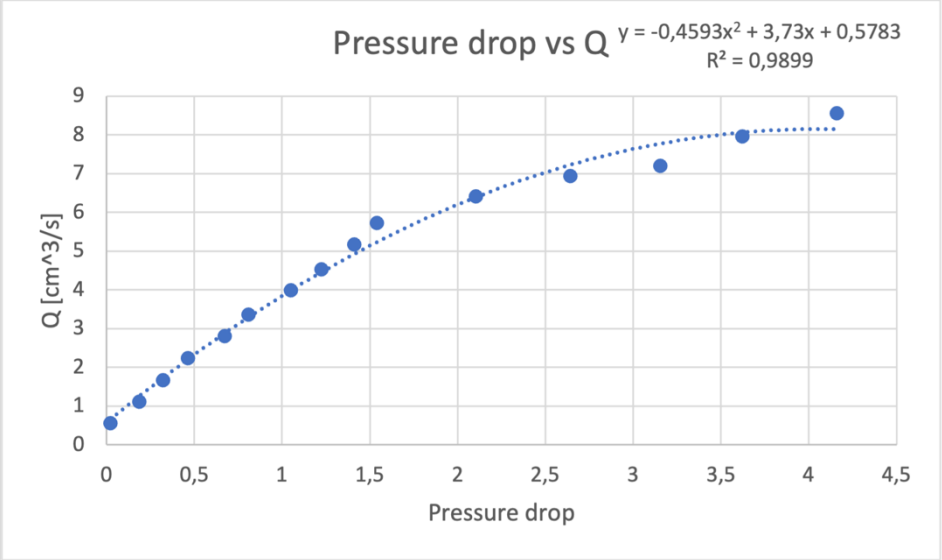
Pressure drop vs Q
y = -0,4593x² + 3,73x + 0,5783
R² = 0,9899
Q [cm^3/s]
9
8
7
6
5
4
3
2
1
0
0
0,5
1
1,5
2
2,5
3
3,5
4
4,5
Pressure drop

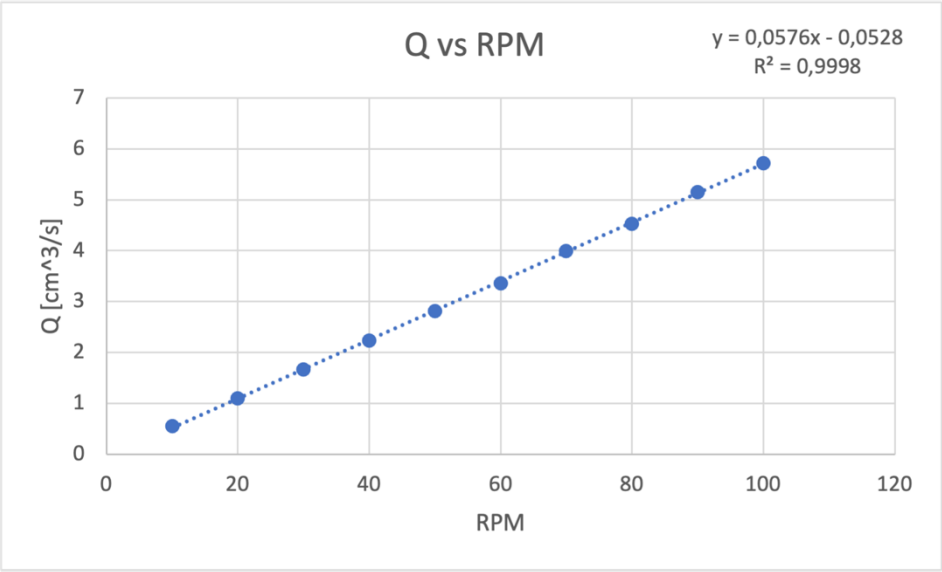
Q vs RPM
y = 0,0576x - 0,0528
R² = 0,9998
Q [cm^3/s]
7
6
5
4
3
2
1
0
0
20
40
60
80
100
120
RPM

Round 3

V= Qt			10 RPM	20 RPM	30 RPM	40 RPM	50 RPM	60 RPM	70 RPM	80 RPM	90 RPM	100 RPM	110 RPM	120 RPM	130 RPM	140 RPM	150 RPM
V=m/t		ml	250,34	250,91	249,77	249,06	249,94	250,66	251,06	250,01	250,425	251,04	249,7	249,64	251,9	250,265	248,7
Q= V/t		s	450	227	150	112	89	74	63	56	48,5	43	39	36	34	31,5	29

RPM	Q[cm^3/s]	g->kg		Reynolds number
10	0,55631111	556,3111111		0,019407 194,0674
20	1,1053304	1105,330396		0,038559 385,591
30	1,66513333	1665,133333		0,058088 580,8765
40	2,22375	2223,75		0,077575 775,7482
50	2,80831461	2808,314607		0,097967 979,6717
60	3,3872973	3387,297297		0,118165 1181,648
70	3,98507937	3985,079365		0,139018 1390,182
80	4,46446429	4464,464286		0,155741 1557,414
90	5,16340206	5163,402062		0,180124 1801,237
100	5,83813953	5838,139535		0,203662 2036,617
110	6,4025641	6402,564103		0,223351 2233,514
120	6,93444444	6934,444444		0,241906 2419,059
130	7,40882353	7408,823529		0,258454 2584,545
140	7,94492063	7944,920635		0,277156 2771,56
150	8,57586207	8575,862069		0,299166 2991,662

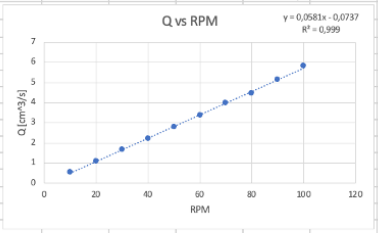

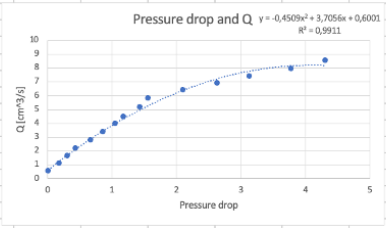

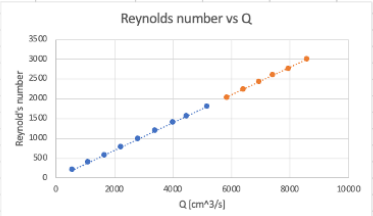

Using V=m/rho for å finne m^3 for Q		
0,9983	g/cm^3	
998,3	kg/m^3	

Pressure drop average		
10	average =	0,013922
20		0,181936
30		0,308887
40		0,432932
50		0,670803
60		0,86341
70		1,0518
80		1,179114
90		1,433378
100		1,559895
110		2,106031
120		2,628294
130		3,134611
140		3,776577
150		4,306781

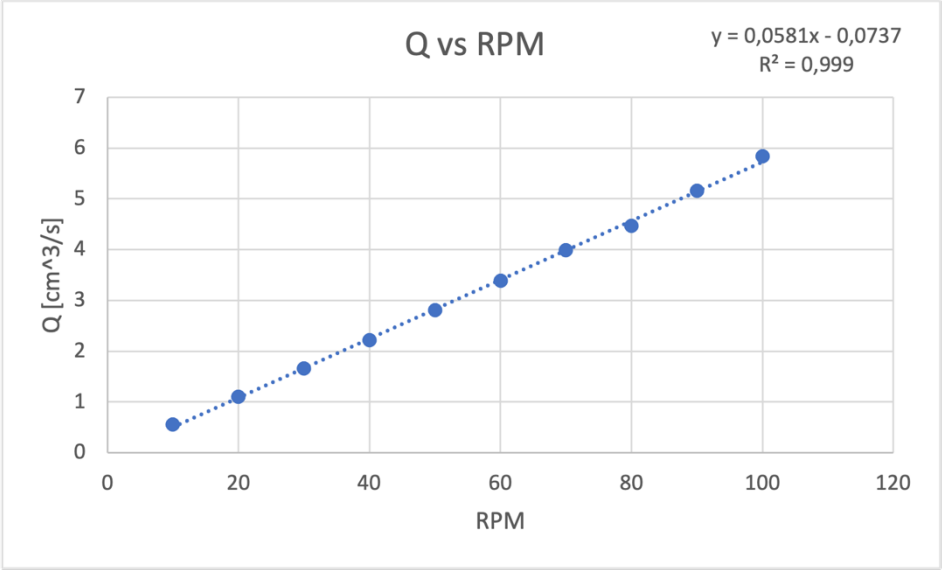
Q vs RPM
y = 0,0581x - 0,0737
R² = 0,999
Q [cm^3/s]
RPM
0
1
2
3
4
5
6
7
0
20
40
60
80
100
120

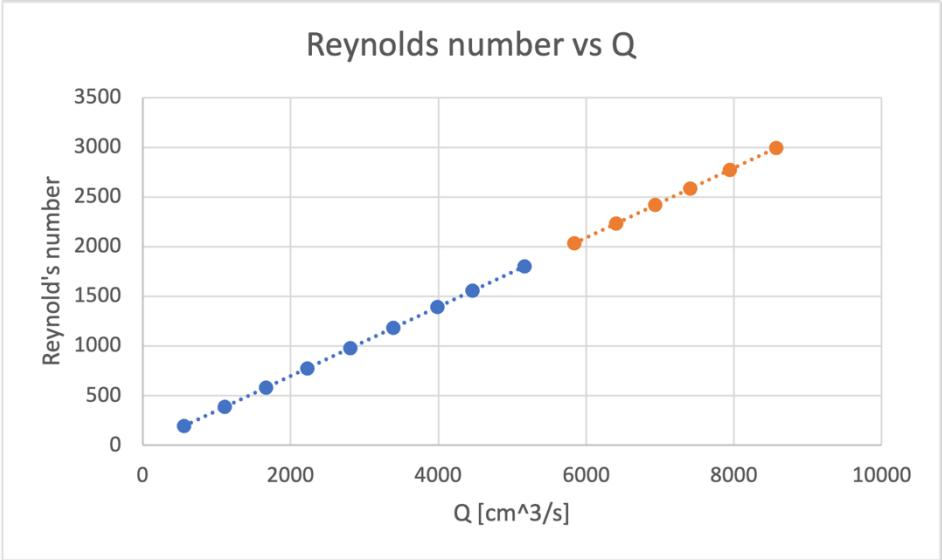
Reynolds number vs Q
Reynold's number
Q [cm^3/s]
0
500
1000
1500
2000
2500
3000
3500
0
2000
4000
6000
8000
10000

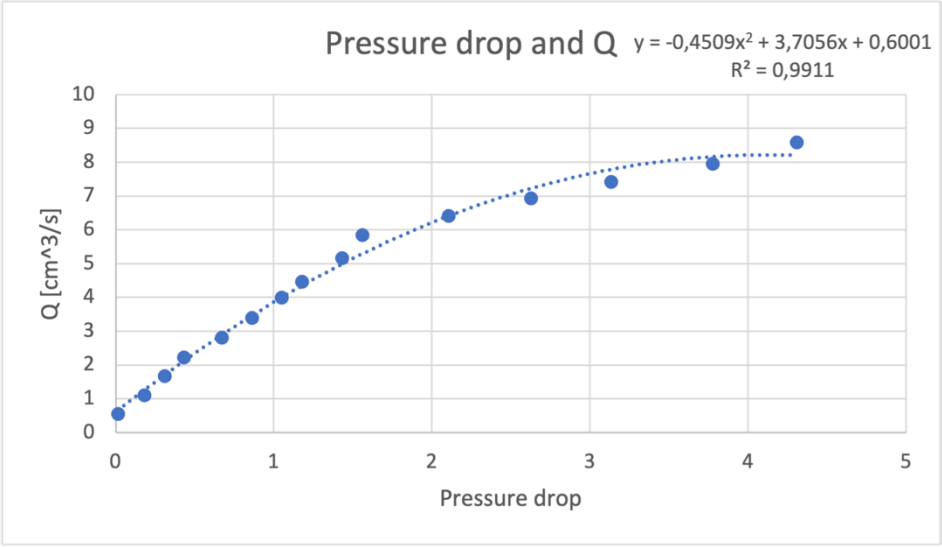
Pressure drop and Q
y = -0,4509x² + 3,7056x + 0,6001
R² = 0,9911
Q [cm^3/s]
Pressure drop
0
1
2
3
4
5
6
7
8
9
10
0
1
2
3
4
5

Appendix D

Time difference from water, 1% PAC treated water and 2% PAC treated water.
It was taken at the lowest point for each period.

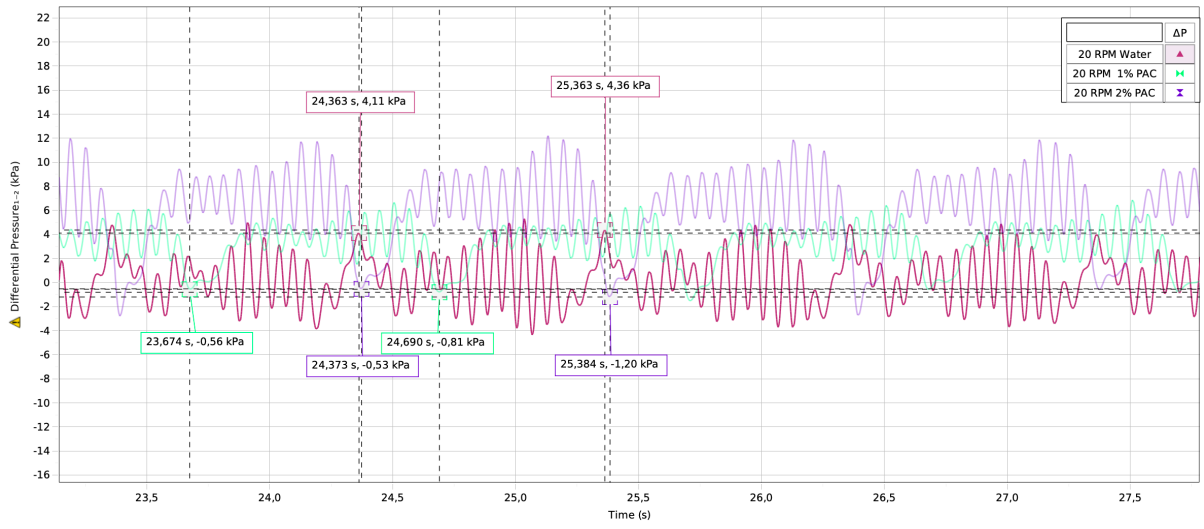

20 RPM

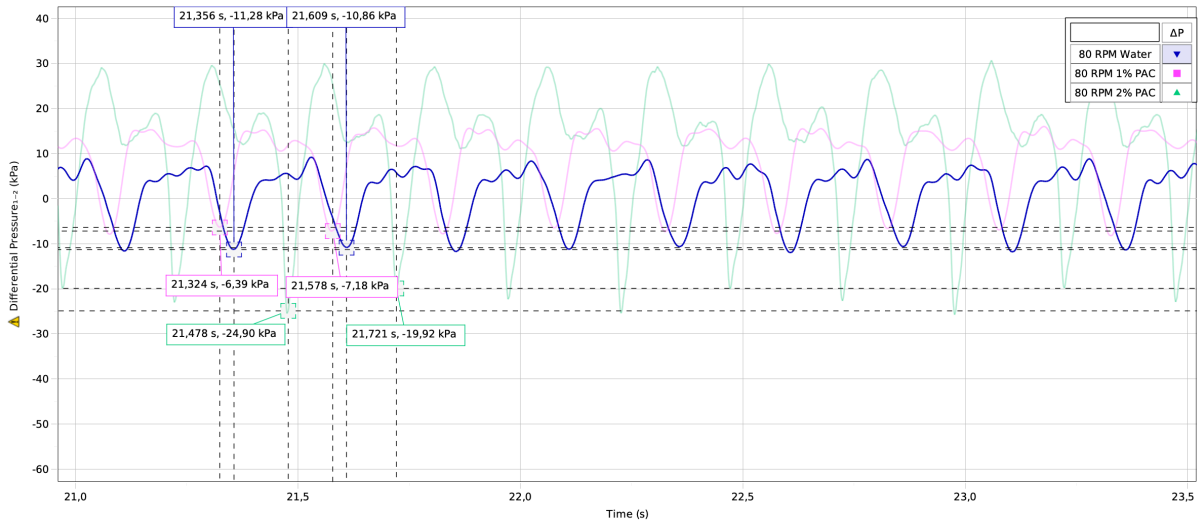

80 RPM

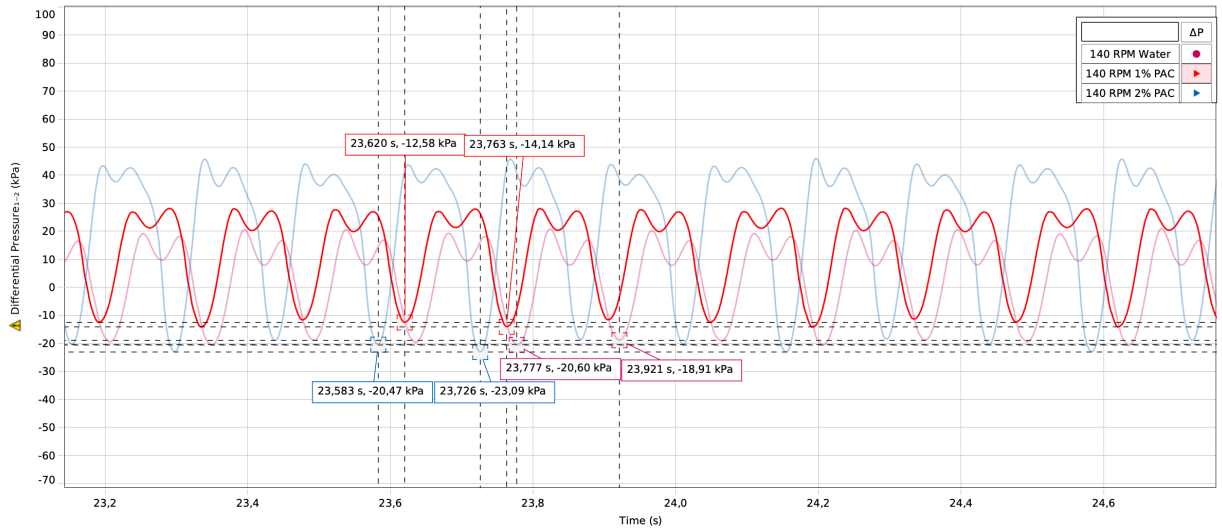

140 RPM

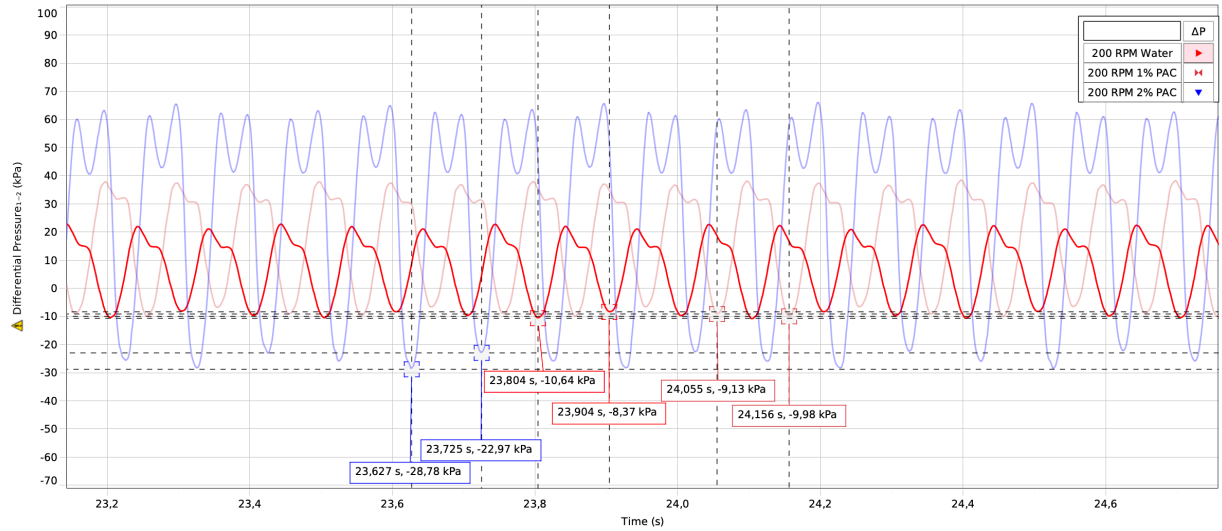

200 RPM

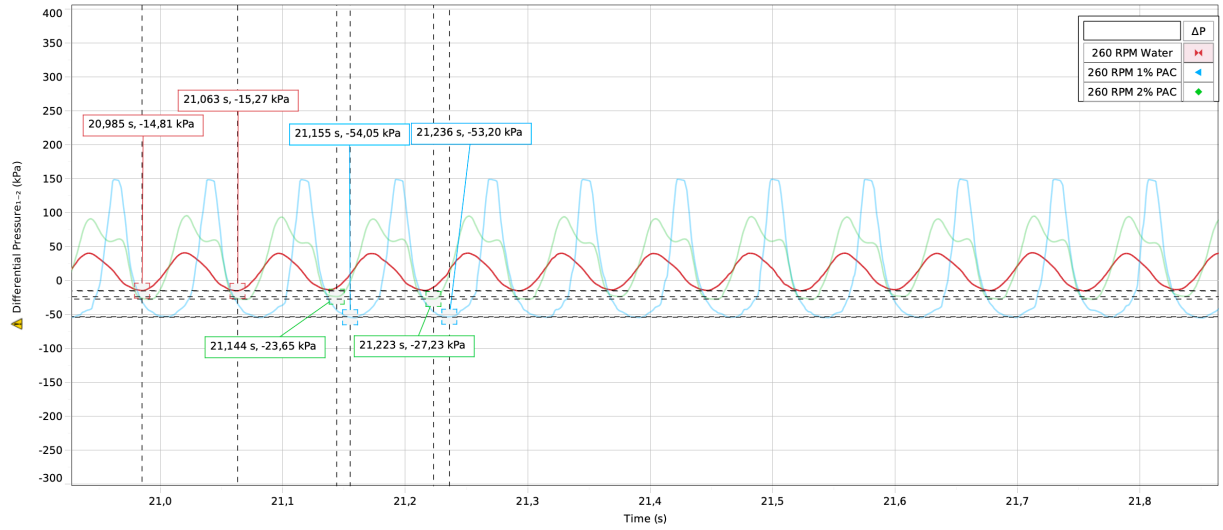

260 RPM

Appendix E

Photos are taken from the laboratory.

Mettler Toledo was used to calibrate Ohaus's mass weight.

Measured diameter of test section tube, Inner diameter

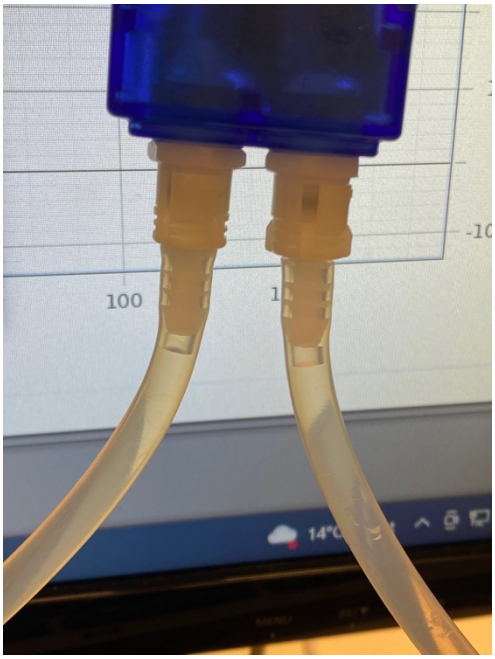

Air in the tube from the test section up to the differential pressure sensor

Cone/Plate used with Amplitude sweep test and Hysteresis test.

Mettler Toledo weighs 5g PAC to make 1% PAC solution in 5l water.

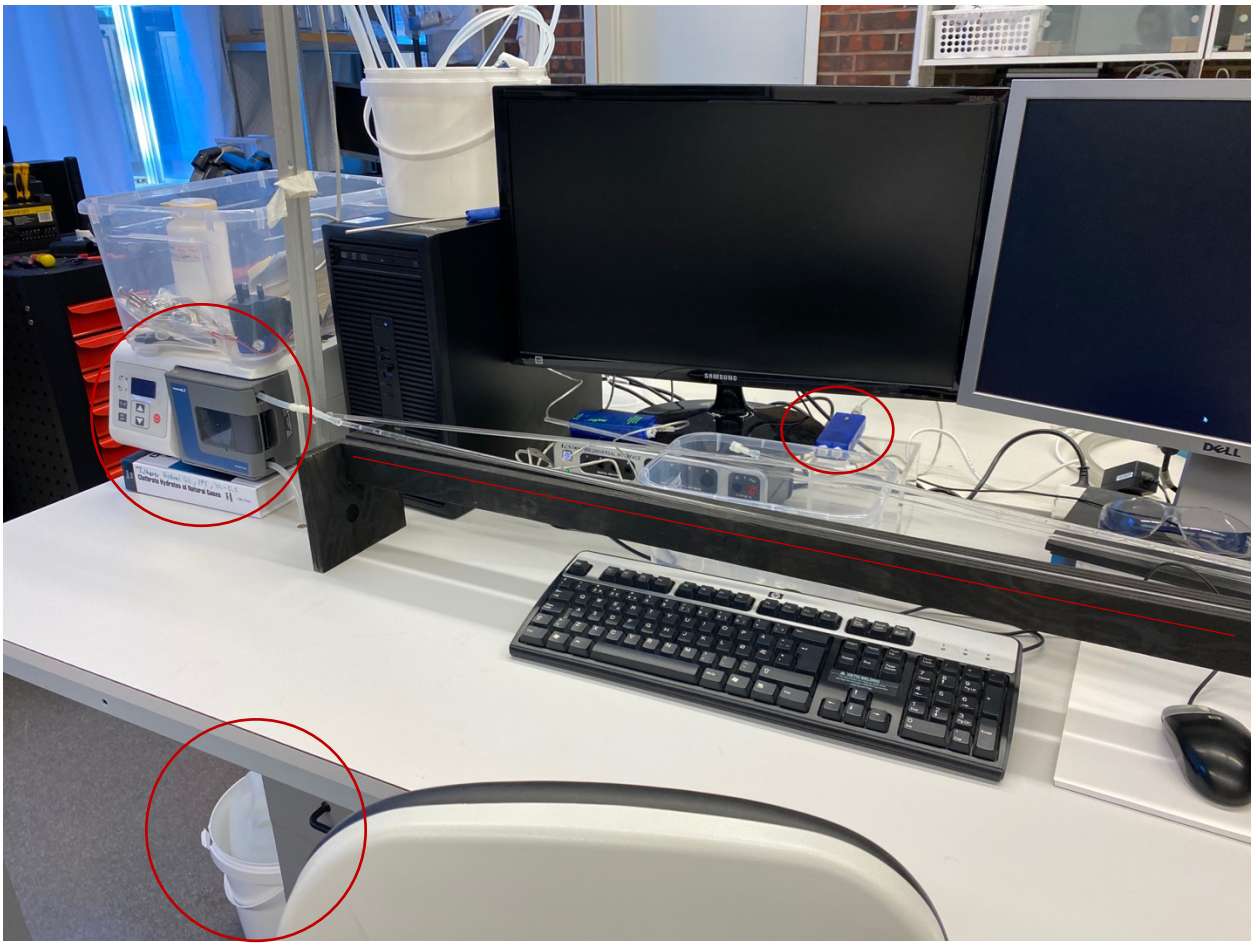

Experimental setup for PASCO tests and calibration. The peristaltic pump, computer, test section support, test section tube, and differential pressure sensor are shown in the photo. Ohaus's weight is placed on the right-hand side of the picture. The peristaltic pump receives water and PAC solution from the bucket demonstrated on the floor.

Coupling from test section tube to outlet and differential pressure tube. The setup is not in use at the time photo was taken.